Determination of Cemented Rockfill Strength with Large Scale UCS Tests under In-Situ Conditions

Isaac Vennes

Department of Mining and Materials Engineering

McGill University, Montreal, Quebec, Canada

July, 2014

A thesis submitted to McGill University in partial fulfillment of the requirements of the degree of

Master of Engineering

Abstract

Birchtree Mine is an underground nickel mine operated by Vale and located near Thompson, Manitoba. The mining method is sub-level stoping with delayed backfill, with cemented rockfill (CRF) employed as backfill. CRF is composed of sized or un-sized aggregate combined with binder slurry. With proper practice and quality control, CRF offers high strength and stiffness, yielding a stable fill exposure and reducing fill dilution. However, the backfill needs to be economically viable. It is therefore important to adjust and optimize the fill recipe to reduce cost while still attaining the fill strength requirement.

The primary goal of the study is to test current CRF practice at Birchtree Mine. The secondary goal is to test adjustments to the current backfill practice to reduce backfill cost. The third goal is to set up a permanent laboratory for the mine to conduct further custom tests as part of a quality control program. To achieve this, the experiment itself needs to be evaluated. Suggestions to improve the experiment, as well as recommendations for future testing, are included in this thesis. The general procedure of the study is described as follows. A literature review was conducted to determine the factors affecting CRF strength. A UCS experiment was then designed based on the literature review. A UCS was designed to conduct the UCS experiment for large scale specimens underground. The experiment was conducted, and the test results analyzed. Finally the experiment itself was evaluated.

The factors investigated are cement content, CRF mixing quality, water quality, and aggregate particle size distribution. 27 large scale specimens were prepared and cured under field conditions and tested in the underground lab. The effect of added binder, mixing quality, and grading were determined with respect to the current mine practice taking into account the variation of specimen density. Results for the effect of water quality on CRF strength were inconclusive.

An important hurdle the program is the manual preparation of uniform specimens in an underground environment. Consequently, a major shortcoming of the experimental procedure is that specimen particle size distribution (PSD) and moisture were monitored instead of controlled, and specimen uniformity was not achieved with respect to PSD and density. Nonetheless, future tests are recommended, and the laboratory is suitable for the conduct of custom tests. The effects of water content, curing time, and slurry mixing, needs to be determined to complete the study. In addition, two-way interactions between moisture content, binder content, and fines content, can be evaluated to optimize the fill recipe.

Keywords

Underground Mining, mine backfill, cemented rockfill, experimental work, rock mechanics.

Résumé

La mine Birchtree est une mine de Nickel souterraine opérée par Vale, située près de Thompson au Manitoba. La mine emploie la méthode d'abattage de chantiers ouverts avec remblayage. Le remblai utilisé est le remblai rocheux cimenté, composé d'agrégat dimensionné ou non-dimensionné recouvert de boue cimentée. Avec un bon contrôle de qualité, le remblai rocheux cimenté offre une grande résistance en compression ainsi qu'une grande rigidité, ce qui augmente la stabilité du remblai et réduit la dilution. Par contre, le remblai doit être économiquement viable. Il est donc important d'ajuster ou même d'optimiser la formule du CRF pour réduire le cout tout en atteignant la force requise du remblai.

Le but primaire de cette étude est de mettre à l'épreuve la pratique courante du remblai cimenté à Birchtree. Le but secondaire est de mettre à l'essai des ajustements à la pratique courante pour réduire le cout du remblai. Finalement, le but tertiaire est de mettre sur pied un laboratoire souterrain permanent pour mener des essais en compression uni-axial qui feront parti d'un programme de contrôle de qualité. Pour atteindre cet objectif, la procédure expérimentale doit être évaluée. Des suggestions pour améliorer l'essai, ainsi que des suggestions pour des essais futurs, sont présentées dans cette thèse. Les étapes de l'étude se résument comme suit. Une étude de la documentation a été conduite sur les facteurs qui affectent la résistance du remblai rocheux cimenté. Ensuite, l'essai en compression uni-axiale a été conçu basé sur l'étude de documentation. Un appareil pour effectuer l'essai en compression uni-axiale du remblai dans un laboratoire souterrain à été fabriqué, pour ensuite procéder à l'essai. Finalement, les résultats de l'essai ont été analysés et l'expérience a été évaluée.

Les facteurs mis à l'essai sont la teneure en ciment, la qualité du mélange, la qualité de l'eau, et la réparation des tailles des particules de l'agrégat. 27 spécimens à grande échelle ont été préparés et mis à l'essai dans le laboratoire souterrain. L'effet d'une addition de ciment, de la qualité du mélange, et de la répartition des tailles des particules, sur la résistance du remblai a été déterminé expérimentalement. Par contre, l'essai sur la qualité de l'eau n'a pas été concluant.

Un obstacle majeur présenté par cette étude est la préparation manuelle de spécimens dans un environnement souterrain. Par conséquence, un default de la procédure expérimentale est que la répartition des tailles des particules et la teneure en eau des spécimens sont suivis mais pas contrôlés. Les spécimens n'ont donc pas une densité uniforme. Néanmoins, des essais futurs sont recommandés, et le laboratoire est adéquat pour l'exécution de programmes d'essai répondant aux besoins de la mine. De plus, l'effet de la teneure en eau, de la durée de la période de séchage, et de la qualité du mélange de la boue cimentée doit être évalué pour compléter l'étude. Finalement, les interactions à deux facteurs entre la teneure en eau, la teneure en ciment, et la répartition des tailles des particules, doivent être évaluées pour optimiser la recette du remblai rocheux cimenté.

Mots Clés

Mine souterraine, remblai minier, remblai cimenté rocheux, travaux expérimentaux, mécanique de roche

Acknowledgments

I would like to thank first and foremost Dr. Hani Mitri, my thesis supervisor. I am grateful to him for his technical guidance, his professional advice, strategic planning skills, and his thoughtful encouragement which allowed me to complete this degree. Special thanks to him as well for having given me the opportunity of being part of the Mine Design Lab group. The financial support provided by Vale and by the National Sciences and Engineering Research Council of Canada (NSERC) fund that I was beneficiary of under his supervision is equally appreciated.

I would also like to thank Birchtree Mine Technical Services, notably Cecile Kelly, Tomasz Bak, Michael Grossman, Shane Ghouralal, for their time devoted to setting up the experiment and laboratory, and for all the help with the experiment. In addition, Elliott Hyska and Dean Collins also deserve thanks for their technical guidance and for providing the mill facilities required for the experiment. Birchtree mine operations also deserve thanks for providing the materials and manpower necessary for the experiment.

Finally, special thanks to all and each one of my fellow graduate students at the Mine Design Lab: Shahe, Wael, Zaka, Atsushi, Luc, Nick, Raju, Jenyfer, Jian, Chen, Zhang, and Guillaume for their help, technical advice, and friendship.

Table of Contents

List of Figures

List of Tables

Chapter 1

Introduction

1.1 UCS Experiment Overview

Backfill is an engineered material employed in underground mines to fill voids created by the extraction of ore. It provides passive support and limits ground movements [1]. Backfill has also been proven to reduce dilution from the footwall and hanging wall slough [2]. Use of backfill also maximizes ore recovery. Currently, high density fill systems, such as paste fill and cemented rockfill, are the norm [1]. The subject of this thesis is cemented rockfill (CRF), which is composed of sized or un-sized aggregate and cement slurry. In general, CRF behaves similarly to weak concrete. See below for typical recipes and strengths of CRF employed in North America.

Table 1: CRF recipes of North-American Mines [3, 4]

Mine	Aggregate Top Size (in)*	Binder Coarse/fines**	% Binder	UCS (PSI)
Deep Post	3.5	70/30	6.75	800
Carlin East	3.0	70/30	6.10	700
Deep Star	3.0	75/25	6.10	700
Rodeo	3.5	87/13	8.00	700
Meikle	2.0	60/40	6.00	800
Bullfrog	3.0	70/30	7.20	650
Turuoise Ridge	3.0	70/30	7.50	700
Kidd Creek	6.0	67/33	5.00	880
Bousquet	6.0	-	5.00	750
Birchtree	8.0	75/25***	4.00	-

*1′ = 2.54cm, **Fines defined as particles smaller than 3/8″ (1cm), ***Target fines of 25-40%,

Stable fill openings are a vital for the economical extraction of ore. With a proper recipe, placement, and quality control, CRF provides high strength and stiffness, increasing stability and enabling greater fill exposures. CRF is currently employed at Birchtree Mine, and the in-situ strength of the CRF was assessed with a large scale UCS experiment. The UCS experiment conducted at Birchtree Mine has three goals. These are:

- Test current CRF practice at Birchtree mine

- Test adjustments to current practice to reduce CRF cost or improve formula if strength is lacking
- Set up permanent laboratory for the mine to conduct custom tests

The specimens are large scale, prepared under in-situ conditions, with materials taken as-is from the mine level. The rationale is to simulate in-situ CRF material as much as possible.

1.2 Specimens

Cylindrical, large scale CRF specimens were prepared to estimate the in-situ strength of the backfill with a UCS test. The specimens are 15″ diameter (37.5cm) by 30″ (75cm) height. The specimens are prepared underground with material taken as-is from the mine level.

1.3 Experiment parameters

The factors investigated are water quality, cement content, CRF mixing quality, and aggregate particle size distribution. The rationale behind this selection is that these parameters can be readily adjusted if the mine practice yields inadequate CRF strength or if there is the potential to reduce CRF cost.

The water quality tests use mine effluent water to prepare the binder slurry. If the specimens prepared with mine effluent water have sufficient strength, using mine effluent water at the mine has the potential to reduce CRF cost.

The mixing quality tests investigate the effect of poor mixing on CRF strength. The poorly mixed specimens are prepared by simulating the mine practice ("bucket method" and "sump method"). The goal is to estimate the in-situ strength of poorly mixed CRF with respect to well mixed CRF, but also to determine if the sump method gives a sufficient strength increase over the bucket method.

The graded specimens are prepared to determine if grading the aggregate to match 5″ (12.7cm) or 3″ (7.6cm) Talbot graded curve to decrease CRF void ratio is an alternative to increasing the binder content. Finally, well graded but poorly mixed specimens are prepared to discern if grading can compensate for poor mixing.

In all, the specimens prepared and tested as part of the experimental program serve to test the current practice and test adjustments to the current practice. However, there are insufficient specimens to conduct recipe optimization. Important parameters, such as the water to cement ratio, are not varied. This experiment is nonetheless a first step to optimize the CRF formula with large scale specimens.

1.4 Experiment location

The experiment will be conducted underground for two reasons. The first reason is the easy procurement of CRF materials. Overall, this facilitates the preparation of custom tests as part of an ongoing program to improve the CRF recipe. The second reason is to facilitate the simulation of in-situ CRF, through the combination of large scale specimens and the use of aggregate and binder as-is from the mine level.

1.5 Uniaxial compression test

The strength of the CRF is tested in uni-axial compression. It is a relatively simple test to conduct, and result of a UCS test is easy to apply as the mine fill strength requirement (FSR) is a UCS value. The FSR of the CRF at Birchtree is 0.6MPa with a factor of safety of 1.5.

1.6 Thesis Structure

1.6.1 Literature review

The study is initiated with a literature Review on factors affecting CRF strength. The literature review is presented in this thesis. The factors investigated are:

- Aggregate grading
- Binder content
- Binder type
- Water to cement ratio
- Aggregate moisture content
- Aggregate strength
- Impact damage
- Water quality
- Placement and mixing

These factors were taken into account when performing the experiment or are part of the tested parameters. The literature review also served as the basis for the results analysis.

1.6.2 Birchtree Mine and current CRF practice

The current backfill practice at Birchtree is described. The mixing practice is simulated as part of the experiment. The current Birchtree CRF recipe serves as the base case set.

1.6.3 UCS Rig

The design and use of the UCS rig for the experiment is described. The UCS rig is built around a 200 ton (181.4 tonnes) hydraulic jack connected to a 10000PSI (68.95MPa) electric pump. The rig designed for use underground and the rig and specimens are handled with a forklift.

1.6.4 Experimental Procedure

The experimental procedure is described. Overall, several issues with the experiment were raised during the preparation of the specimens. Main issues described are the control of the ungraded specimen PSD and the control of specimen moisture.

1.6.5 Results

Results of the experiment are presented. Stress-strain curves were obtained for all specimens. Information taken from the tests are modulus of deformation, modulus of elasticity, and UCS.

1.6.6 Analysis of results and experiment

The results are analyzed taking into account the shortcomings of the experimental procedure and the parameters affecting CRF strength described in the literature review.

1.6.7 Conclusion

The conclusion consists of three parts:

- Recommendations to mine CRF practice
- Recommendations for future testing
- Recommended adjustments to the experiment

Chapter 2

Literature Review

2.1 Introduction

The purpose of this literature review is to determine the factors that affect the quality of cemented rockfill, and the methods used to optimize the quality of the fill taking into account these factors. The context of this review is a preparation for the UCS experiment to be conducted at Birchtree mine. The factors affecting the quality of cemented rockfill that are reviewed are cement content, the water to cement ratio, the particle size distribution, the mixing water quality, the placement of the fill (segregation), the mixing method of the fill, the strength of the aggregate, and finally moisture content of the aggregate.

2.2 Factors affecting CRF strength

2.2.1 Binder Content

The relation between CRF strength to binder content curve is not linear [5]. Incremental increases in binder content at high binder contents (ie. 15%) yields higher strength increases than at low binder contents. However, there is no universal empirical correlation as the relationship is specific to other factors such as water to binder ratio and aggregate grading [5]. At Kidd Creek mines, the observed relationship is [6]:

$$q_u = 1.5e^{0.25C} \tag{2-1}$$

where,

$q_u = Uniaxial\ compressive\ strength$

$C = portland\ cement\ content\ with\ respect\ to\ weight\ of - 4cm\ aggragate$

A statistical model for strength estimation was built at Birchtree Mine [7]. An increase of binder content from 4 to 5% was reported to increase strength by 15%. However, the strongest two way interaction for CRF strength is reported to be between the fines content (1cm particles and less) of the aggregate and the binder content. An incremental addition of binder has the greatest effect on CRF strength the higher the fines content of the aggregate [7].

Since binder is the most expensive component of a cemented rockfill program, it is of prime importance to minimize cement usage to attain the required backfill strength. This can be done by controlling other factors such as aggregate PSD and moisture.

2.2.2 Binder Type

There are 4 common binder used for cemented rockfill: ordinary Portland cement (OPC), fly ash, blast furnace slag (BFS), and non-ferrous slag [6].

Portland cement is a hydraulic cement, produced by pulverizing clinker consisting of hydraulic calcium silicates. In presence of water, calcium silicate hydrates form a gel that hardens. Fly ash is a by-product from combustion of pulverized coal. There are two types of commercial fly ash: C and F. Type F fly ash has a low lime content and little cementitious value. However with Portland cement, its combination with calcium hydroxide released during OPC hydration forms other cementing compounds. Type C fly ash on the other hand has high lime content, will react with water, and cement on its own. Blast furnace slag is a by-product of the steel industry. It results from fusion of calcium from the limestone with siliceous and aluminous residues from the iron ore in blast furnace. The physical state of the BFS is fundamental to its cementitious properties. Non-ferrous slags are from sulphide concentrates. These slags are produced at 3 different stages of smelting: roasting, smelting, and converting.

Studies to determine binder alternatives to OPC were conducted at Kidd Creek due to the relatively high cost of OPC [6]. At Kidd creek mines, large mortar cubes were poured and tested with a Schmidt hammer for relative dynamic strength determination, and small cylinders were poured and tested for UCS for static strength determination.

Conclusions of the studies conducted as Kidd Creek mines were that ground blast furnace slag can be used to replace up to 50% of the OPC without loss of strength. However, the curing time increased to three months. Nonetheless, some stopes did have three months of curing time available before adjacent pillar recovery and ground blast furnace slag was implemented with satisfactory results [6]. Use of blast furnace slags also results in a more fluid mix at the same water content than OPC [5]. Therefore, in longhole stopes where more fluid slurry is required (see section below); the required water content to obtain a fluid slurry can be reduced if BFS is used. In addition, blast furnace slags require an alkaline environment for hydration; an 85:15 mix of slag and lime is about 20% stronger than an equivalent weight of OPC after 50 days [5].

Type F and type C fly ash were similarly tested at Kidd Creek mines. Type C fly ash was shown to have higher strength that type F fly ash at any mix proportion with OPC. For a 28 day curing time, both C and

F fly ash had lower strength than a 100% OPC mix. However, the strength of the 100% OPC mix was exceeded after 73 days of curing [6]. Stone (1993) adds that mixing PFA with OPC has many benefits such as reduced heat of hydration and increased fluidity. Also, most PFA and OPC compounds are stronger than equivalent weight of OPC alone [5]. At Thompson mine, the initial PFA to OPC ratio was 30:70. However it was increased to 50:50 as testing has shown that the mix delivers sufficient strength [8].

2.2.3 Water to cement ratio

The water to cement ratio of the cement affects the viscosity of the slurry and the workability of the fill [3]. At Kidd Creek mine, Farsangi notes that when there is too much water there is excess slurry volume as well as percolation bottom of the stope. Excess water will also reduce the cementation strength by washing off the cement coating of solids [4]. On the other hand, if there is too little water the slurry will be too dry and there can be incomplete hydration of the cement.

The required water to cement ratio to attain complete hydration is only about 0.22-0.25 [8]. For concrete, a typical water to cement ratio would be 0.4-0.5. For a longhole stope, the cement slurry needs to be wet and flowable. The ratio is there increased to 0.7-1.2. For a jam filled stope, there is no need for slurry flowability and the water to cement ratio is kept on the dry end [3]. Reschke recommends a water to cement ratio of 0.8 but only if the aggregate is relatively dry and the mixing thorough [9].

The interaction between moisture content and fines content on CRF strength was also quantified to be as strong as the interaction between fines content and cement content [7]. In essence, increasing fines content increases the surface area of the aggregate and consumes more cement. Increasing the slurry volume is required to obtain good mixing.

2.2.4 Aggregate moisture content

The main impact of aggregate moisture content is to increase the water to cement ratio of the CRF. For example, assuming a 5% binder content for the CRF with an initial water to cement ratio of 0.7, a 1% increase in moisture content of the aggregate will increase the water to cement ratio of the slurry to 1.0 or by about 40%. Close observation of the fill pile is therefore required to avoid an exceedingly high water to cement ratio.

2.2.5 Particle size distribution (PSD)

The primary purpose of properly grading aggregate is to minimize aggregate porosity, decreasing the wasted cement that pools in voids [1], and affecting the optimal cement content for maximum UCS of the fill [7]. Reduced contact area between particles was also observed to decrease strength in segregated fill with low fines [10].

A poorly graded aggregate will have a high void ratio, and a large amount of cement is wasted filling voids rather than binding particles together (see figure 1). A well graded aggregate will have both particles and cement filling the voids, reducing cement usage. On the other extreme, too many fines in the aggregate can be detrimental. The fines will consume more cement than an equal weight of coarse particles due to their high specific area per unit volume. The interaction between optimal binder content and particle size distribution is discussed in more detail in section 2.3. Excess fines will also reduce strength as the coarser particles are saturated in a sand-cement matrix [4].

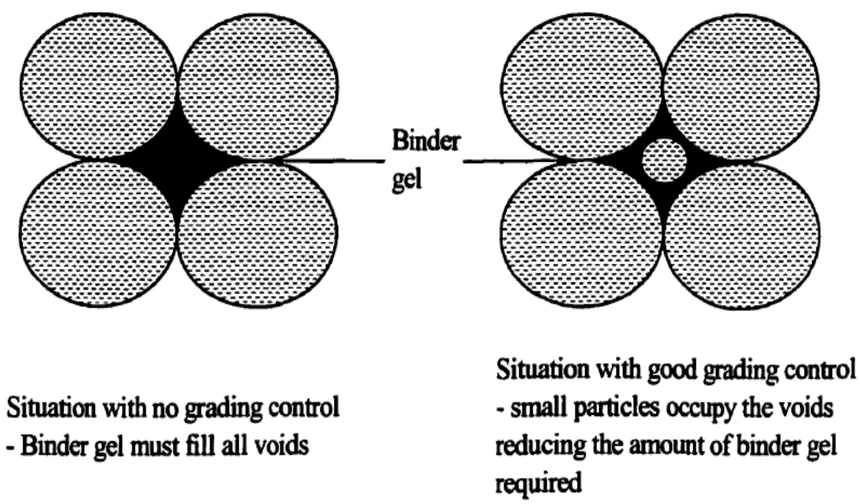

Figure 1: Demonstration of effect of particle size distribution on required binder content [1]

2.2.6 Aggregate Strength

Aggregate strength affects the quality of CRF through attrition rate in the fill raise; high attrition of the aggregate in the raise will produce excess fines. Multiple site specific rock attrition models have been proposed to predict the PSD of the aggregate at the draw point. Yu (1989) developed an empirical formula tailored for backfill at Kidd Creek mines:

$$\frac{d_{50}\,(surface)}{d_{50}\,(drawpoint)} = 1 + h/1100 \qquad (2\text{-}2)$$

where h is the depth in feet of the draw point where the aggregate is retired. Using this formula, the operators at Kidd Creek mines could adjust the particle size distribution at the surface to maintain an optimal fines content. At Thompson, a similar relationship was established for attrition: The relation is [8]:

$$Free - fall\ fines\ \% = 0.0152 * free - fall\ distance \qquad (2\text{-}3)$$

$$Full - raise\ fines\ \% = 0.00899 * full - raise\ distance \qquad (2\text{-}4)$$

The equation allows an estimation of the initial size distribution required on surface in order to produce an aggregate with a proper amount of fines at the stope level.

On the other hand a minimum aggregate strength of 70MPa is suggested to avoid excess attrition [3]. Durability of the aggregate is typically assessed using the Los Angeles abrasion test (LAA) [3].

2.2.7 Impact Damage

If impact occurs after the cemented rockfill has already cured, broken cement bonds in the rockfill due to the impact will most likely not re-cement unless cement slurry fill the crack. To avoid impact damage of the cemented rockfill, it is important that the falling cemented rockfill does not impact already cured rockfill. The shock will then be absorbed by a plastic state surface layer than prevents damage to the cured rockfill beneath [6]. Additives are therefore are to the cement slurry to retard cementation. This is common practice as described by Stone (2007) for Nevada mines and Farsangi (1996) for Kidd Creek.

2.2.8 Water Quality

Yu (1989) notes a decrease of sample UCS of 50% when recycled mine water was used as opposed to potable water. Contaminants causing a decrease in CRF strength at Kidd Creek are dissolved solids, oil and grease, and water treatment chemicals. Kidd Creek mines has subsequently made efforts to use recycled water by removing the oil and grease, coordinating the use of water treatment chemicals, increasing the water cycling time, and blending in potable water. For Nevada mines, Stone notes problems when using recycled water due to excess diesel fuel present in the water, as well as lubricants and nitrates [3]. Also, a study at Darlot gold mine determined that water quality would have a great impact on backfill strength. Nonetheless, Darlot mine water was still suitable for backfill [10]. At Namew mine, Sulphates in the mine water are known to reduce CRF strength. Observations made within 89 stopes indicated areas where the cement had not cured properly. Subsequent large scale tests using in-situ water obtained much poorer results than small scale laboratory tests with clean water [9].

2.2.9 Placement and Mixing

How well the aggregate and cement slurry is mixed and how the CRF is placed are the two main controllable factors govern the segregation of the aggregate and the distribution of the cement within a stope. Yu (1989) notes that within a same stope at Kidd creek Mines, a variation of 1.5MPa to 11MPa was observed due to segregation of the aggregate and unequal binder content across the stope. The control of segregation and the effects of mixing will be described in more detail in the section on design aspects of cemented rockfill.

2.3 Cemented Rockfill Optimization and Design

2.3.1 Aggregate Grading

Aggregate particle size distribution is the factor that has the largest effect on backfill strength [5, 11], controlling the void ratio and consequently the dry bulk density of the mix. In general, a poorly graded aggregate will have too many unfilled voids, consuming cement, decreasing strength, and decreasing the elastic modulus. One therefore wants a particle size distribution that maximizes the density of the fill. Maximizing fill density has two main effects:

- Decreasing the void ratio means a decrease in "wasted" cement that fills voids rather than bind aggregate particles.
- Decreasing void ratio increases contact area between aggregate particles, increasing strength.

Talbot [12] developed an ideal grading curve to maximize the density of fill for concrete. The grading curve is defined as follows:

$$P(u) = 100\left(\frac{u}{umax}\right)^k \tag{2-5}$$

where,

$P(u) = probability\ of\ particle\ being\ finer\ than\ sieve\ opening\ u$

$u =\ sieve\ opening\ size$

$u_{max} =\ maximum\ particle\ size$

$k =\ constant, 0.5\ for\ concrete$

This formula can be used to find the optimal grading based on the maximum particle size, albeit after having determined the optimal value for constant k. For concrete, optimal grading is obtained with a k value of 0.5, (maximum density). For rockfill however, the optimal k value depends on the placement method for the rockfill. Longhole drifts have been shown to perform better with excess fines, with a k value of 0.35 to 0.45 [3]. On the other hand, for drift and fill, a stiff fill is more desirable, with a optimal k value ranging from 0.55 to 0.65 [3].

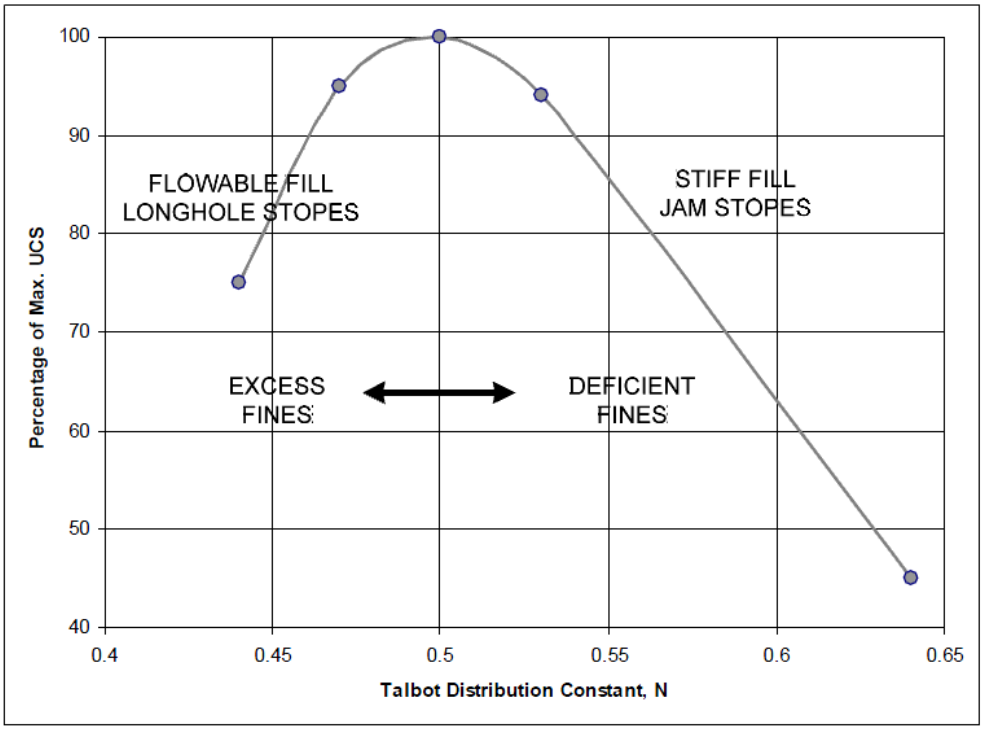

Figure 2: Optimal k value for talbot distribution based on stope type in Nevada mines [3]

In case grading the rock fill is too expensive, a viable alternative is to blend in sand with ungraded rockfill to attain comparable UCS values [5]. Yu (1989) points out that a 5% content of sand in the ungraded rockfill at Kidd creek increased the UCS of the rockfill by 40%. However, at 30% sand content by weight decreased UCS by up to 66%. In the former case, the contact area between aggregate particles is increased by the sand filling the voids, increasing strength. In the latter case, the aggregate is “saturated” in a sand cement matrix, reducing strength [4].

As will be shown in the cement content optimization below, particle size distribution is also closely linked to the optimal cement content for the cemented rockfill.

2.3.2 Cement content Optimization

Cement is the most expensive component of cemented rockfill, taking up 80-90% of backfilling costs [6]. It is therefore of prime importance to minimize the amount of cement used to attain the required backfill strength. This can be achieved using the Talbot-based design procedure proposed by Swan with the Binder number parameter [1]. The binder number assumes that there are 3 important parameters for the mix design: the cement content, the mean free distance between aggregate particles and the aggregates specific surface area:

$$BN = \frac{c_v}{d\alpha_p} \tag{2-6}$$

where,

$d = average\ interparticle\ distance$

$\alpha_v = specific\ aggregate\ surface\ area$

$c_v = \%\ cement\ content$

Swan plotted the binder number for 68 selected backfills and reported a very good correlation between binder number and compressive strength [1]. The relationship is [13]:

$$UCS = 0.283 * BN^{2.36}$$

where,

$BN = binder\ number$

Swan's binder number was also used by Bloss (1992) to formulate a relationship between cement content and UCS, and ultimately determine the cohesion of the fill. The empirical formula, based on Mount Isa Mines data and derived by Bloss, is:

$$c = 0.085 + 0.069\left(\frac{c_v}{(d\alpha_p)^{1.5}}\right)^{1.4} \tag{2-7}$$

While this formula is based on a data set specific to Mount Isa Mines backfill, it still illustrates that a direct relationship between cement content and cohesion is valid. Nonetheless, it is noted by Bloss that the while Swan's binder number is valid for any mixture of composite materials containing cement [1], the binder number is not well defined for cemented rockfill [13]. More specifically, the optimization of cement content requires the knowledge of the proportion of the aggregate which is part of the cement-aggregate matrix. This proportion goes between 2 extremes; For CHF, 100% of the aggregate is part of the cement-aggregate matrix. On the other hand, for CRF, the larger particles are not part of the matrix, and the proportion of the particles that are part of the matrix needs to be estimated. Bloss proposes 100%

of the fines plus 60% of the coarse particles [13]. However, more study is required to determine an exact proportion.

Optimal cement content can also be directly related to fines content in the rockfill. In a study by Peterson, Szymanski et al. (1998) at INCO Thompson, 5 factors were varied in a testing program to determine their effects on the UCS of the cemented rockfill. These factors were aggregate fines % (varied from 20% to 40%), aggregate moisture, total binder content, PFA content, and cement dispersant content. The percentage of fines in the aggregate was determined to have the largest effect, with a 50% increase in strength of cemented rockfill UCS at 40% fines. More importantly, the two-way interaction between fines content and cement content on specimen UCS was studied by evaluating the maximum difference. Fines content was determined to have a large impact on the effect of all other parameters on strength, with the strongest two-way interaction being with cement content (2.878MPa "maximum difference") [7]. Increasing the binder content from 4% to 5% at a fines content of 40% yields 2.878MPa more of strength than the same increase in binder content at 20% fines. The relationships developed between these 5 parameters and UCS were practically used to determined the most cost effective combination for a target UCS [7].

2.4 Segregation

2.4.1 Segregation Phenomenon

Segregation is a phenomenon that affects both particle size distribution and cement content within a stope. The mechanism is described in detail by Farsangi (1996) and Yu (1989) at Kidd Creek Mines. In general, larger particles with more momentum tend to settle further away from the fill cone after impact than the finer particles. The result is a segregated fill with a finer particle distribution near the fill cone and a coarser particle distribution near the edge of the stope. For CRF at Kidd creek mines, a variation of CRF strengths from 1.5MPa to 11MPa was observed within a single stope due to segregation [4]. In the zone with the coarser particles, the increased void and small contact area reduces strength [10].

Farsangi (1996) has assigned zones within a stope at Kidd Creek Mines depending on the type of particle size and cement content observed due to segregation. The zones are:

- Zone A: Wall on which collision occurs of incoming fill occurred. The zone has high in situ strength. The zone extends 5-10 meters from the fill peak and has a high binder content. The aggregate is small (90% minus 8cm)

- Zone B: Medium binder content, good particle size blend, and occurs 10-25 meters away from fill peak. 80% of aggregate mass is coated with slurry.
- Zone C: Stope boundaries, highly segregated fill, low binder content, low strength due to lack of fines.
- Zone D: Highly segregated zones. Rich in binder content but low in fines. Slurry runs to these zones.

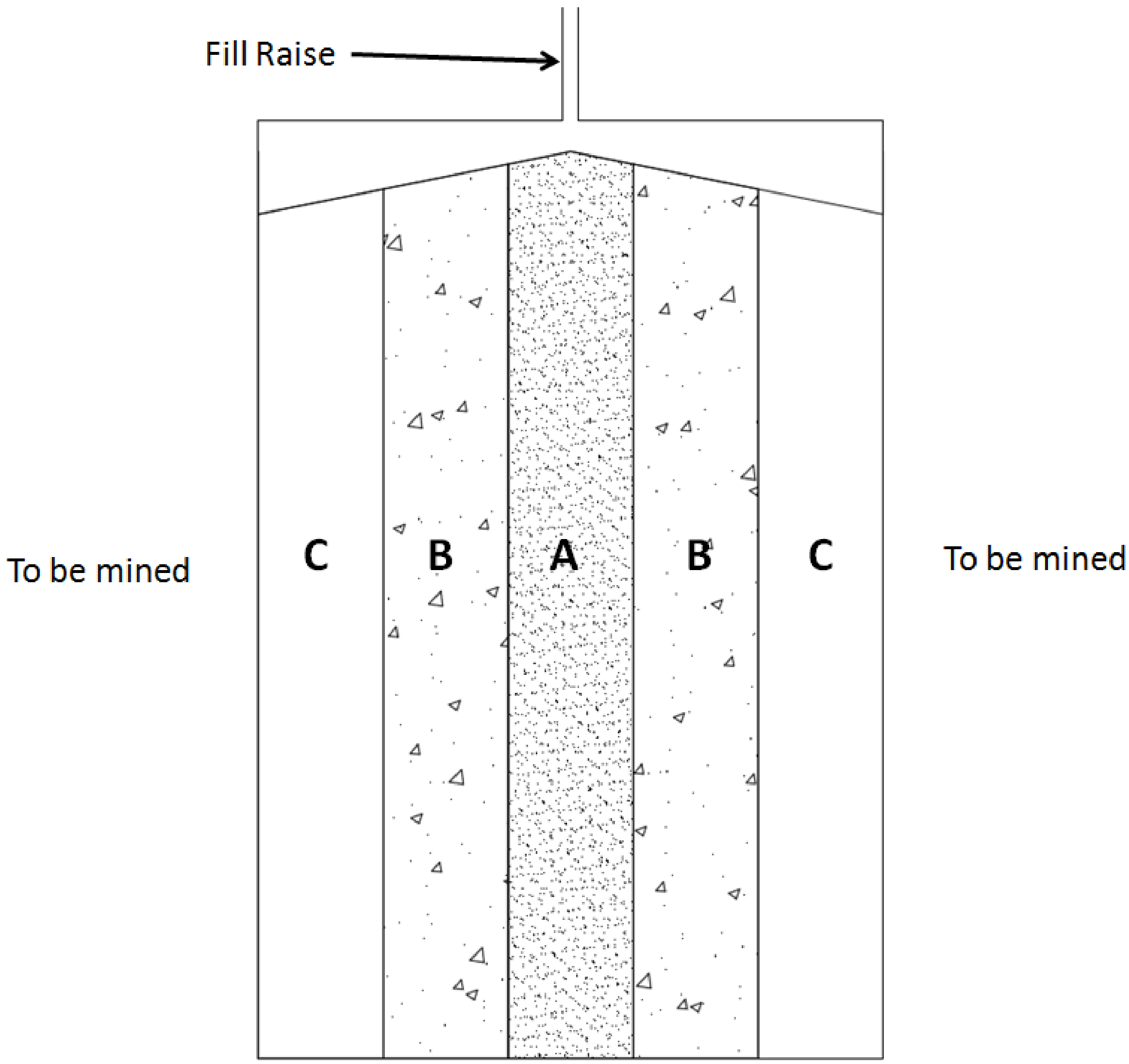

Figure 3: Segregation pattern for CRF dumped from straight fill raise at Kidd Creek Mines, modified from Farsangi [6]

Similar behavior was observed by Bloss [11] when modeling the segregated distribution of the fill at Mount Isa mines. However, Mount Isa mines employs CHF in conjunction with CRF, hence the different observation and classification. The model for the fill cone is nonetheless similar.

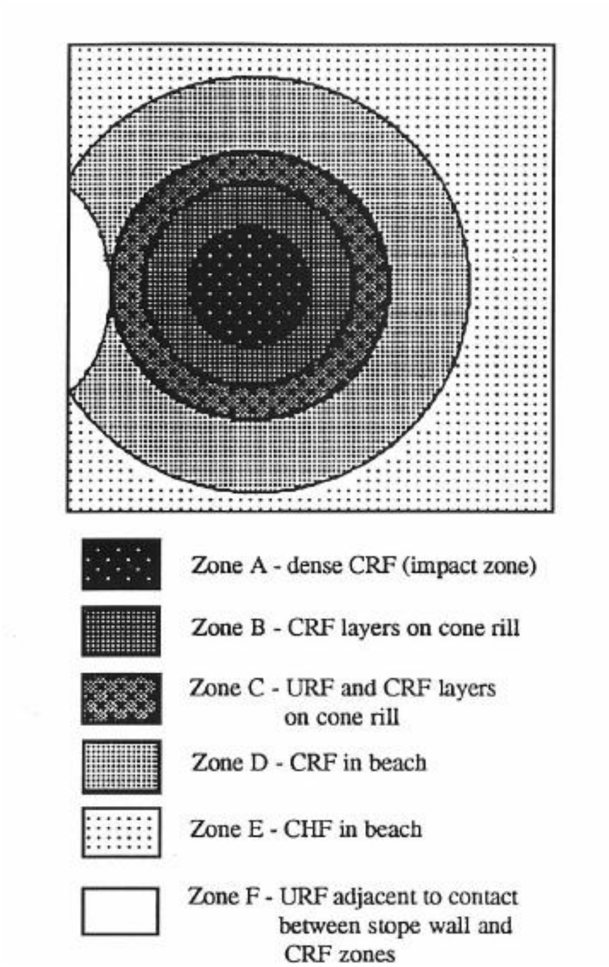

Figure 4: Plan view of segregation model for Mount Isa backfill [11]

2.4.2 Segregation Control

Segregation is unavoidable. However, it is desirable to control the segregation such that certain zones in the stope are well cemented with high strength; for instance, inducing "zone A" material at the faces that will be exposed in the future.

The extent of segregation depends mainly on 3 factors. These are the stope size, the stope geometry and the fill method. Stope size and geometry are fixed. Fill method is therefore he only factor that can be modified to control segregation. At Kidd Creek Mines, the fill method effect on segregation was studied in detail [4, 6] with large scale tests done at Thompson Mine [6, 8] as well as with test drifts [6]. Also, the mixing method for the aggregate and cement does have an effect on segregation insofar as the distribution of the cement with the stope is concerned. On the other hand, solutions proposed at Darlot gold mine to counteract segregation are increasing fill flowability by adding more water to the cement slurry and adding an extra 15% of fine material in the aggregate [10].

2.4.3 Filling Method: Fill Raise Position and Orientation

Filling method is only factor along with mixing that can be optimized in order to control segregation. At Kidd creek mines, stopes are filled with a backfill raise, which gives control on the position and number of impact cones within a stope. By properly orienting and positioning the fill raise, one can direct the strong, properly cemented fines towards the face that is to be exposed, causing the coarse particles forming the weak zone to roll away towards the center of the stope or the faces that are not to be exposed. Dumping from a backfill raise also has the added benefit of extra mixing of the rockfill with the cement slurry when it tumbles down the raise.

In case the mining level above is not yet developed or boring backfill raises is too costly or timely, dumping from the sill drive is an available option. Dumping from the sill drive however gives little control to the operator over segregation.

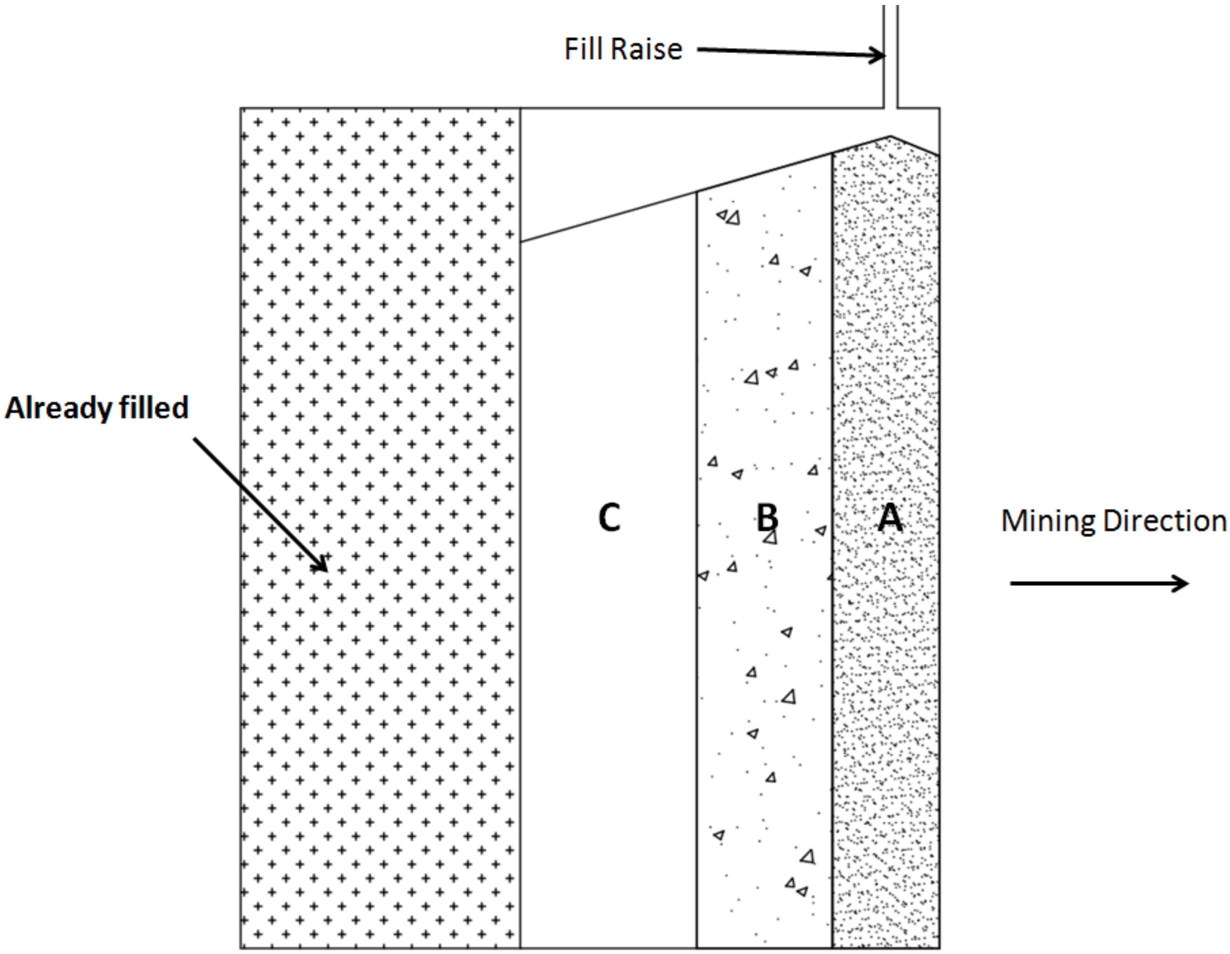

Figure 5: Positioning of fill raise to obtain strong CRF at future exposed at Kidd Creek Mines, modified from Farsangi [6]

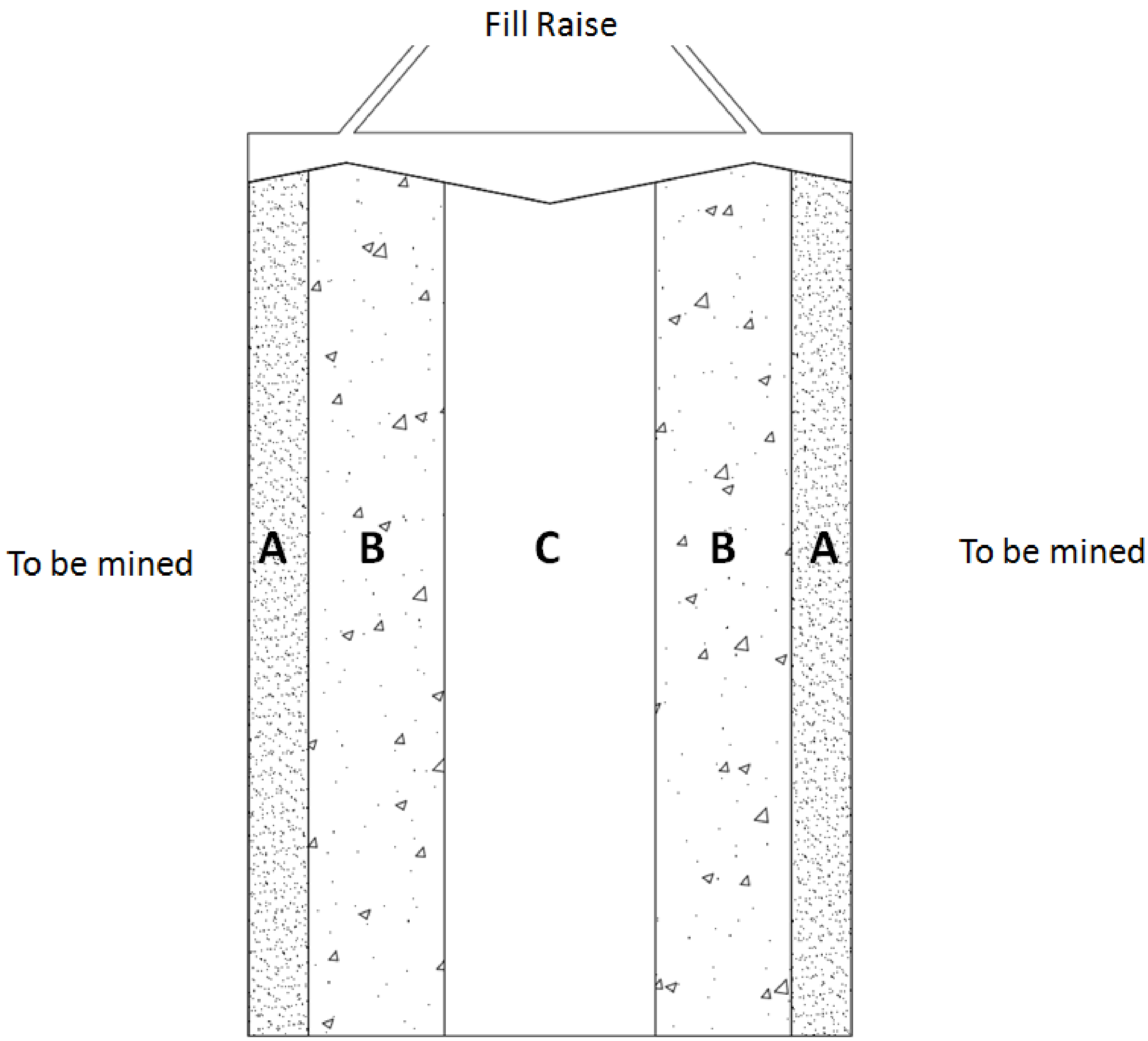

Figure 6: Position and orientation of 2 fill raises to obtain strong CRF at both future exposed faces, modified from Farsangi [6]

Fill raise position and orientation was studied in Thompson Mine [6, 8] as a way of controlling segregation. A 1:40 scale Plexiglas model of the stope was constructed to simulate the effect of the number of raises and their orientation on segregation.

The conclusions are that segregation is much more pronounced if the aggregate hit the footwall before impacting the fill cone; the coarse particles hitting the footwall bounce away, forming a coarse uncemented pile, while the fines and cement slump down the footwall, producing a strong highly cemented area [8]. This can be used to the advantage of the operator if the impacted wall is to be exposed by future mining. Other observation were that a vertical raise is better that an angles raise. This is because the aggregate dropping down the angled raise picks up horizontal momentum, aggravating segregation similarly to when the aggregate is dumped from a conveyor from the sill drive. Also, multiple fill raises reduces the risk of failure along a single plan of weakness. Finally, it was observed that it is possible to configure the raise such that the impact cone is a the toe of the stope, where higher shear stress is observed and therefore higher CRF strength required [6].

2.4.4 Effect of Stope Size

Another observation is the effect of stope size. For small stopes, the slumping fill cone will extend to the outer edges of the stope, reducing the extent of segregation. For larger stopes however, the fill cone will not extend to the edge and only the large particles will have enough momentum to reach it. In this case, segregation is much more pronounced [6]. However, stope size is not a design factor that can be optimized for cemented rockfill. The best method to deal with segregation in large stopes is therefore to have multiple strategically placed drop points for the fill [6], as was the case for the 30.4m high, 40.5m long, 30.5m wide stopes at Kidd Creek mines. At Thompson mine however, the stopes are 30.5m wide, 9-15m long, and 30.5m high, and only one fill raise was deemed necessary [8].

2.4.5 Effect of Mixing

However, the research conducted at Thompson Mine both assumed properly mixed CRF being dumped in the stope. In this case, the 3 zones observed are well cemented fine zone in the impact cone, an intermediate well cemented zone around the impact cone, and finally a coarse poorly cemented zone at the perimeter. This behavior only observed if the aggregate is properly mixed in the slurry.

The key to produce a competent consolidated fill is to coat all the aggregate with the supplied amount of cement slurry in a short time. If the particle is not coated at the stage at which it is dumped in the stope, it may never be cemented as the flow of free slurry is not controlled. The flow of slurry in the stope is not uniform; low porosity fines will impede the flow of a thick slurry, while a high porosity coarse aggregate will not retain a thin slurry. The only way to remediate poor cement distribution is a stope is to add more cement, increasing cost. At Kidd Creek mines, 10m^3 of extra cement slurry is available to be poured is the stope in case poor mixing is observed [4].

Also, proper mixing, along with segregation, will affect how the cement is distributed along the stope. In brief, if the fill is properly mixed, the fill cone will be properly cemented (as seen in zone A), the coarse particles will carry cement along with them on their surface when they segregate, as observed in zone B, where about 80% of the aggregate particles were coated in cement [6]. However, if the fill is not properly mixed with cement a different phenomenon will occur; the compacted fines in the fill cone will not bear cement (as there was no mixing), and the cement will flow down the fill cone to fill the voids in the coarse particle zone. This resulting fill (cemented coarse particles) was observed at Kidd Creek mines zone is classified by Farsangi (1996) as zone D.

Mixing of the cement slurry with the backfill can be a laborious process that impedes the backfill rate if the equipment capacity is too low or the mixing time is too high. Mixing the cement and slurry can be a passive (baffled culvert, tumbling action down stope backfill raise, vibration in LHD bucket during travel) or an active process (drum mixer). An intensive study was done at Kidd Creek mines with full scale tests for a vibratory mixing conveyor, a slusher, a baffled mixing culvert, and a drum mixer [4]. In practice, two methods were used: In No. 1 mine, the backfill and slurry was mixed in a 1.2m diameter by 2m long steel baffled culvert before being dumped in the raise. In No. 2 mine, the slurry is mixed with the aggregate and dumped from the sill drive. Initially, the backfill was mixed at No. 2 mine with 2 5m^3 concrete mixers, producing up to 300tpd of well coated rockfill. However, the mixing method was discontinued due to a greater demand of fill [4].

2.4.6 Conclusion

In all, segregation is an unavoidable phenomenon for cemented aggregates that causes the formation of weak and strong zones within a stope. By properly planning the position, orientation, and number of fill raises for a stope, segregation can be controlled. However, if the backfill is placed in the stope from the sill drive, no control is possible. However, stope size does have an effect on the extent of segregation; Small stopes filled from the sill drive showed a smaller extent of segregation that larger stopes filled from fill raises at Kidd Creek mines [6]. When characterizing backfill, it is important to take into account this phenomenon and how it will affect the overall stability of the stope. Bloss (1992) developed such a fill distribution model for Mount Isa mines.

2.5 Characterization of CRF

2.5.1 Static Strength: Mohr-coulomb criterion

The static performance of cemented rockfill is controlled by shear strength. The Mohr-Coulomb criterion can be used to quantify the performance of soil like materials including cemented rockfill:

$$\tau = c + tan\phi \qquad (2\text{-}8)$$

where,

$\tau = shear\ stress$

$c = cohesion$

$\phi = friction\ angle$

To determine both the friction angle and the cohesion of the cemented rockfill, one must conduct a triaxial test under different states of confinement (σ_1 and σ_3). Another option is to use site specific empirical formulas to estimate these parameters [13]. However, if only UCS tests are conducted, assumptions need to be made to determine these parameters. The assumptions are:

- The friction angle is governed entirely by the aggregate properties. It can be estimated as the aggregate angle of repose.
- The cohesion is provided entirely by the cement. It can be determined with a UCS test using the equation $UCS = \frac{2c\cos\phi}{1+\sin\phi}$

A factor of safety is then applied to the static strength in order to account for uncertainty or heterogeneity in the fill. At Kidd Creek mines, even dynamic strength was taken into account though a high safety factor of 2.5 for the static strength [4].

2.5.2 Dynamic Strength

The parameters governing blast damage to consolidated fill are assumed at Kidd Creek mines to be related to the dynamic tensile strength of the fill [4, 6]. Farsangi assumes that the dynamic tensile strength of the CRF is 5% of the UCS. The dynamic strength can be related to the blast vibrations in terms of the peak particle velocity:

$$Fd = Dynamic\ Strength/Dynamic\ Loading = T/dPV \qquad (2\text{-}9)$$

where,

$T = \ Dynamic\ tensile\ strength$ (5% $of\ UCS$)

$V = Particle\ velocity\ at\ failure$

$P = \ Compression\ wave\ velocity$

$d = \ fill\ density$

The particle velocity, force, and particle displacement in the fill can be calculated based on the acoustic equations. For example, the force transmission coefficient and force reflection coefficients are found as a function of the acoustic impedance of the media [4]:

$$P_t/P_i = 2z_2/(z_2 + z_1) \quad (2\text{-}10)$$

$$P_r/P_i = (z_2 - z_1)/(z_2 + z_1) \quad (2\text{-}11)$$

where,

$z_1 = acoustic\ impedance\ of\ medium\ 1 = D_1 \times C_1$

$z_2 = acoustic\ impedance\ of\ medium\ 2 = D_2 \times C_2$

$D = density$

$C = compression\ wave\ velocity$

However, due to the heterogeneous nature of the rockfill, the boundary conditions between the fill and the rock vary so widely across the stope that it is very difficult to obtain a representative result with the above equations [4]. Blast vibration monitoring is therefore necessary to obtain results for practical application.

2.5.3 Modulus of Elasticity

The modulus of elasticity of a CRF specimen is taken as the slope of the stress-strain curve at 50% UCS. However, similarly to rock masses, there are alternative definitions that can be applied to the deformability of CRF. Some authors quote both the modulus of deformation and the modulus of elasticity to describe the deformation properties of a rock mass. The modulus of deformation is easier to determine and is often reported as a low estimate for the deformability of a rock mass [14].

Cemented backfills are similar in nature to sedimentary rocks such as sandstones, consisting of rock particles cemented together by a cementitious matrix [13]. Two processes control the load deformation characteristics of sandstones, which are the closure of voids and the deformation of the aggregate particles. However, with backfill, void closure is the dominant process as the cement matrix material is weak and fails before any significant aggregate deformation occurs. CRF void ratio therefore controls deformability as well as strength. CRF deformability is therefore expected to correlate with CRF strength.

2.5.4 Effect of sample size on specimen strength

The size of test samples is known to play an important role in the assessment of the behavior of geotechnical materials such as soil and rock. Hoek and Brown compiled data that relates the specimen's measured UCS to the UCS of a 50mm specimen depending on its size. The correlation is [15]:

$$\sigma_{cd} = \sigma_{c50}\left(\frac{50}{d}\right)^{0.18} \quad (2\text{-}12)$$

For cemented rockfill however, no investigation has been done on the effect of scale of the aggregate with respect to the scale of the sample on UCS. Results for large scale specimens are generally accepted as representative in-situ conditions [1, 5]. From a study conducted at Que river mine [16], the strength of the large scale specimens (45cm) was approximately 60% of the laboratory strength of scaled-down gravel. On the other hand, Stone proposes a factor of about 0.65 to convert standard-test results in-situ [5].

Chapter 3

Birchtree Mine

3.1 Overall Operation

Birchtree mine is an underground nickel mine located in Thompson, Manitoba. It was owned by the International Nickel Company (INCO) and began production in 1974. Since 2005, the mine is owned and operation by Vale Manitoba Operations. It is one of the three operating nickel mines in Thompson, the others being Thompson 1 (T1) and Thompson 3 (T3). Nickel ore produced at Birchtree is processed by the milling and smelting facilities at T1. Currently, the mine produces about 2300 tonnes of ore per day at an average grade of 1.5% nickel.

3.2 Geology

Birchtree Mine is located in the Thompson Nickel Belt (TNB). The Thompson Belt is a linear NE-trending belt of Archean and early Proterozoic rocks. It forms the boundary between the Archean Superior and early Proterozoic Churchill provinces. It consists of gneiss, meta-sediments, meta-volcanics, ultramafic rocks and flesic plutons [17]. The Ni sulphide ores that characterize the TNB are associated with ultramafic komatiitic sills that intrude a sequence of paleoprotozoic sedimentary cover rocks [18].

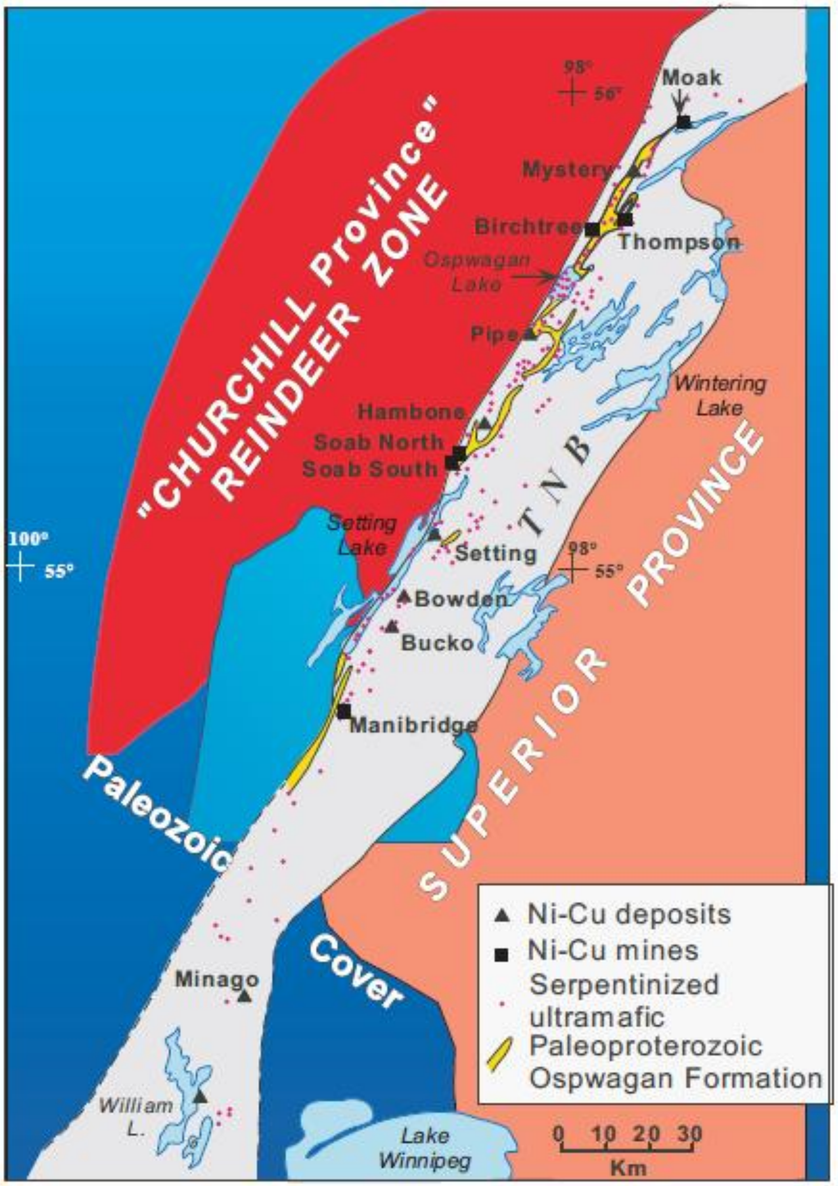

Figure 7: Thompson Nickel Belt regional geology [18]

The geology of the Birchtree orebody is described as brecciated ultramafic rock (peridotite) in a sulphide matrix. There are 3 categories of peridotite: core peridotite (0.20% nickel), mineralized peridotite (0.5% - 3.0% nickel), and barren peridotite (0.35% nickel). The mineralized peridotite is scattered with the presence of sulphide, with Pyrrhotite as the main constituent of the sulphides. The hanging wall consists mainly of schist, while metamorphic rock with biotite, plagioclase, pyrrhotite, and quartz are present in footwall.

3.3 Mining Method

The orebody is steeply dipping. The mine practices vertical block mining (VBM), which is a variation of the sub-level stoping method. The orebody is mined transversely. Sill drifts are developed at the top and bottom of the stope. The stopes are drilled and blasted from the top sill drift, and ore is extracted from the bottom sill drift. Stope production is done in 3 or 4 lifts.

A typical stope is 18m x 12m x 30m (length x width x height). There are generally three stopes over the thickness of the orebody. Stope production sizes are around 10000 tonnes. Once a stope is fully extracted, it is backfilled with CRF or URF.

On a vertical section, the stopes are extracted in a bottom-up pyramidal sequence. On a plan section, stopes are extracted in panels. A panel consists of a single row of stopes that span the width of the orebody. Panels alternate between primary and secondary panels, where primary panels are extracted first. All stopes in a panel are extracted before mining the adjacent (secondary) panels.

3.4 Current Backfill Practice Birchtree

3.4.1 Overall System

An average of 500 tonnes of backfill per day is placed. All extracted stopes with adjacent un-mined stopes are filled with CRF. On the other hand, un-cemented rockfill (URF) is employed for stopes with no adjacent un-mined stopes as the fill will never be exposed. Stopes in primary panels will be exposed from at least 2 sides. The target UCS for the CRF employed at the mine is therefore based on the static UCS failure model. The target strength is 0.6MPa with a factor of safety of 1.5.

3.4.2 Aggregate

The aggregate used at Birchtree mine is quarried biotite schist. It is crushed and screened to obtain a topsize of 8″ (20cm) and a minimum size of 3/8″ (1cm). It is conveyed to the mine by 50 tonne truck and dumped in a fill raise which is connected to the levels with finger raises. Attrition of the aggregate in the fill raise increases the fines content of the aggregate, with fines defined as particles passing a 3/8″ screen. The amount of fines depends on raise depth and aggregate free fall distance. A linear relationship is used to determine the fines content due to attrition [8]:

$$free\ fall\ fines\ \% = 0.0152 * free\ fall\ distance \tag{3-1}$$

$$full\ raise\ fines\ \% = 0.00899 * full\ raise\ distance \tag{3-2}$$

The raise is filled to the top during the summer but dropped 90m during the winter to avoid freezing of the aggregate. A maximum free fall distance of 150m is maintained. The target range for fines content is 25-40%.

3.4.3 Binder

Birchtree mine employs CRF with 4% binder. The binder consists of 70% type C fly ash and 30% type 10 Ordinary Portland cement. Binder is pumped pneumatically to an underground 20 ton binder silo through an 8″ (20cm) line in the shaft.

3.4.4 Binder Slurry

Water for cement slurry is taken from a nearby river. The slurry water to cement ratio is 0.54, set taking into account an estimated aggregate moisture content of 5%. The binder slurry is mixed underground with colloidal mixers. The binder slurry is then pumped with a Moyno pump through a slurry line to the slope. The slurry line is flushed every shift to prevent plugging.

3.4.5 Mixing and Placement

The binder slurry is mixed with the aggregate with an LHD. Two methods are used at Birchtree mine to mix the binder slurry with the aggregate. The first is the bucket method, where the binder slurry is sprayed on a bucket of aggregate and then dumped in the stope. This method relies on vibrations during truck travel and tumbling action when the CRF is dumped in the stope for mixing. The second is the sump method, where the aggregate is first dumped in a sump dug the end of the sill drift accessing the stope. The binder is sprayed over the sump. The LHD overturns the aggregate and binder slurry in the sump to mix the CRF. The CRF is then dumped in the stope from the sill drift. The CRF is allowed to cure for 28 days before mining adjacent stopes.

3.4.6 Issues with practice

Backfill practice at Birchtree mine has several issues [19] with respect to practice laid down in the literature.

1. Sump method and bucket method lead to poor mixing
2. Particle size distribution uncontrolled due to situational addition of un-sized developmental rock
3. Uncontrolled quantity of fines, 25%-40% is a wide target range as CRF strength is sensitive to fines content
4. Water for flushing slurry line ends in stope, and excess water reduces CRF strength
5. Material testing is not performed on a regular basis

6. Water to binder ratio is not regulated on the basis of moisture contents of aggregates
7. No quality control
8. Occasional large backfill failures have been observed

3.5 Summary

This chapter mainly presents the CRF practice at Birchtree mine. Main issues with the practice are presented, and the first 3 are assessed in the experimental program. The mixing and placement methods of the CRF described in this section are also simulated. The recipe described in this section serves as the base case of the experimental program with some modifications outlined in chapter 4.

Chapter 4

UCS Rig

4.1 Introduction

This chapter describes the design of a test rig to conduct uniaxial compression tests on large scale CRF specimens. The rationale behind the design is to keep the rig inexpensive and flexible. The rig is designed for use in an underground environment with a forklift for specimen handling. The rig is designed around a 10000PSI (68.95MPa) electric pump and a 200 ton (181.4 tonnes) hydraulic cylinder. All components of the rig were available during the design phase with the exception of the reaction plate, base plate and spherical seat which were fabricated on site.

The maximum specimen size is 15″ (37.5cm) in diameter by 30″ (75cm) in height. The maximum attainable load is 200 tons, which corresponds to the capacity of the hydraulic cylinder – the corresponding factor of safety is 2.32. Based on a maximum possible strength of CRF of 8 MPa, the anticipated working load is 102.5 tons (93 tonnes), which gives a factor of safety of 4.67. A stress analysis of the base and reaction plates show that the maximum stresses under the working load are well below the yield stress of the plate material.

4.2 UCS Rig Components

4.2.1 Component List

The test rig is composed of the following:

- 1 x base plate
- 1 x reaction plate
- 3 x threadbars
- 9 x Hex nuts
- 1 x hydraulic cylinder
- 3 x transfer plates (including one with brackets)
- 1 x Spherical Seat

The following components are placed in the rig along with the specimen and remain in the rig when testing takes place.

- 1 x specimen base plate

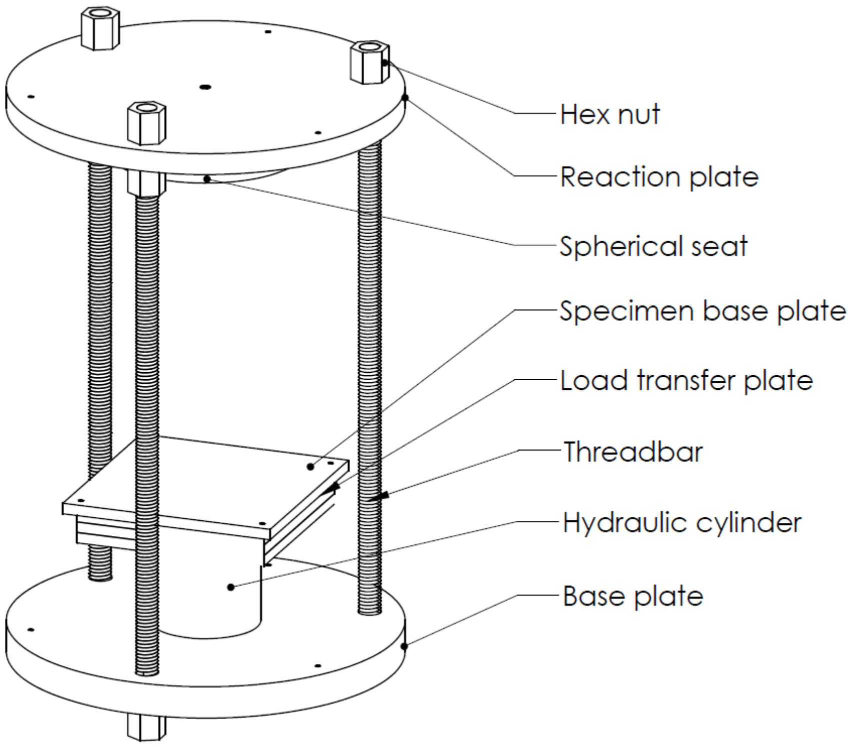

Figure 8: UCS rig components

Factor of safety calculations were done for 3 of the components of the test rig. These are the threadbar, the reaction plate, and the base plate.

4.2.2 Principal Components

- Hydraulic Cylinder: Simplex RLN 2002, maximum attainable load of 206.4 tons [20]
- Threadbar: DSI 1 ¾″ GR150, yield strength of 160 tons [21]
- Base Plate, and Reaction Plate: fabricated with 4340 Heat treated steel, minimum yield strength of 630MPa [22]

4.3 Safety Factors against Yielding for UCS Rig Components

4.3.1 Maximum Attainable Load, and Working Load

Maximum attainable load is calculated as the cylinder effective piston area times the pump pressure:

Effective Piston Area = 41.28in^2 [23]

Pump pressure = 10000PSI [23]

Maximum load = 206.4 tons

The sample size is Φ15″ x 30″. Working load is calculated as the assumed highest compressive strength of cemented rockfill times the sample area:

Sample area (15″ diameter) = 176.7in^2

Maximum backfill UCS = 8MPa = 1160.3PSI [3]

Working Load = 102.5 tons

In all, the rig components (base plate, reaction plate, threadbar) are selected or sized to resist the *working load* of 102.5 tons. The factor of safety will be based on this load. Since the maximum attainable load is larger than the working load, the rig will have the capacity to break rockfill samples with a UCS of 8MPa. The equation for the factor of safety for the threadbar is the following:

$$FS\ (working\ load) = \frac{Threadbar\ Capacity}{Working\ Load} \tag{4-1}$$

For the base plate and reaction plates, the factors of safety are:

$$FS\ (working\ load) = \frac{4340\ HT\ steel\ yield\ stress}{Maximum\ plate\ bending\ stress\ under\ working\ load} \tag{4-2}$$

Factors of safety will not be calculated for the maximum attainable load. The maximum attainable load of 206.4 tons cannot be attained with a typical CRF specimen. However, stress analysis will still be conducted for this load regardless of the specimen strength.

4.3.2 Threadbar Stress Analysis

The threadbar has a yield load of 160 tons [2]. There are 3 threadbars. Assuming equal distribution of the axial load, each bar will be subjected to a maximum tensile load of 68.8 tons when the maximum attainable load is applied, or a tensile load of 34.2 tons when the working load is applied. The corresponding factors of safety are 2.32 for the maximum attainable load and 4.67 for the working load.

4.3.3 Reaction Plate and Base Plate Stress Analysis

Two scenarios were analyzed to estimate the maximum bending stress in the reaction plate and base plate due to the load acting on the specimen.

- Circular plate with load in center
- Cantilever beam with point load

For each method, the maximum stress in the plate was plotted with respect to the thickness.

4.3.4 Circular plate with point load

The radius of the plate is the distance between the center of the base plate or reaction plate and the threadbar. The load on plate is assumed to be the load on the specimen. The circular plate is simply supported on the edge. The load is distributed over the specimen section area. The maximum bending stress is at the center of the plate, expressed as:

$$\sigma_{max} = \frac{6P}{4\pi t^2}\left((1+v)ln\left(\frac{r}{e\prime}\right)+1\right) \qquad (4\text{-}3)$$

where,

$P = single\ concentrated\ force$

$r = radius\ of\ circular\ plate$

$t = thickness\ of\ plate$

$v = poisson\ ratio$

$e = loaded\ area$

4.3.5 Cantilever beam with point load

The plate is simplified as a beam clamped at one end and with a point load at the other end. The point load is equal to the load in a single threadbar. The length of the beam is the distance between the edge of the sample and the threadbar. The maximum stress in the beam is found as:

$$\sigma = \frac{M_{max}y}{I_x} \qquad (4\text{-}4)$$

where,

$M_{max} = maximum\ bending\ moment\ (at\ clamped\ end)$

$P = single\ concentrated\ force$

$L = beam\ length$

$y = perpendicular\ distance\ to\ neutral\ axis$

$I_x = second\ moment\ of\ area\ of\ beam\ section$

$t = beam\ thickness$

$w = beam\ width$

The table below summarizes the parameters input for the two scenarios. The distinction between the base plate stresses and reaction plate stresses is also shown. Stresses at maximum load and working load are analyzed.

Table 2: Reaction plate and base plate stress analysis parameters and equations

Beam		**Circular Plate**	
Base Plate	**Reaction Plate**	**Base Plate**	**Reaction Plate**
$P_{work} = 34.2$ tons $P_{max} = 68.8$ tons $L = 10''$ $w = 8.66''$	$P_{work} = 34.2$ tons $P_{max} = 68.8$ tons $L = 7.5''$ $w = 13''$	$P_{work} = 102.5$ tons $P_{max} = 206.4$ tons $r = 15''$ $v = 0.3$ $e = (10''/2 * \pi) = 78.5 in^2$	$P_{work} = 102.5$ tons $P_{max} = 206.4$ tons $r = 15''$ $v = 0.3$ $e = (15''/2 * \pi) = 176.7 in^2$
$I_x = \frac{wt^3}{12}$ $M_{max} = P * L$ $\sigma = \frac{M_{max} y}{I_x}$		$\sigma_{max} = \frac{6P}{4\pi t^2}\left((1+v)\ln\left(\frac{r}{e'}\right)+1\right)$	

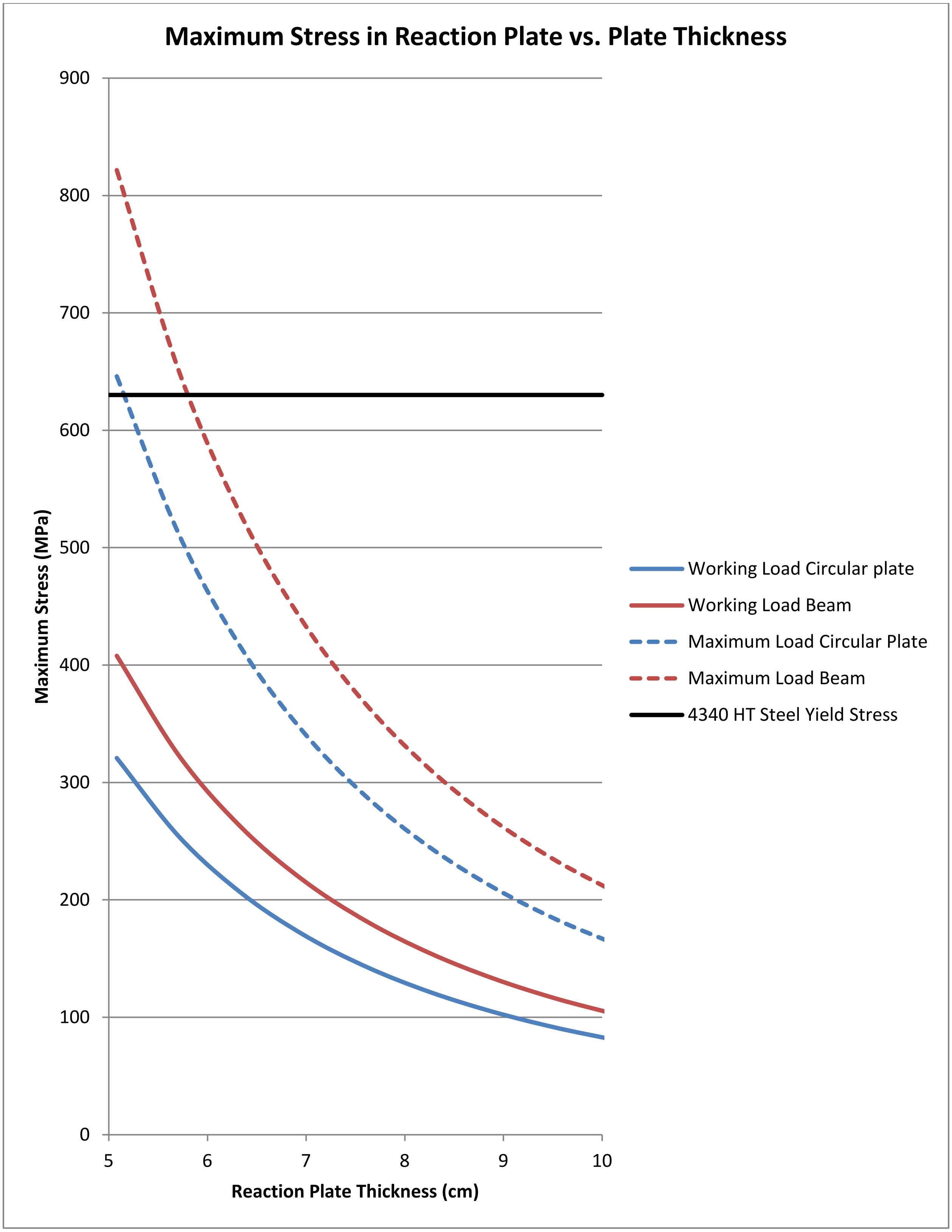

Figure 9: Reaction Plate Stresses

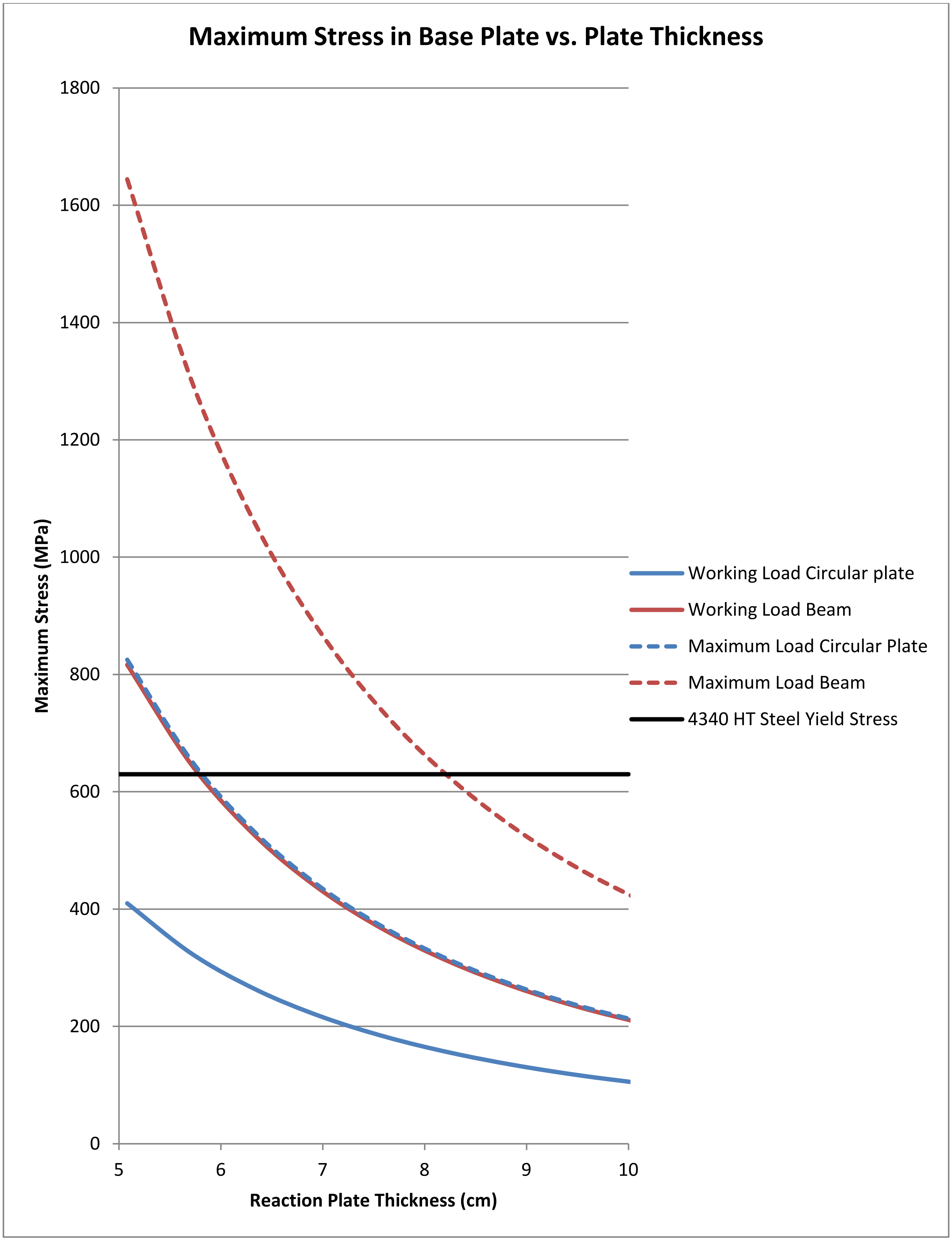

Figure 10: Base plate stresses

4.3.6 Stress Analysis Results

The beam model gives a very conservative estimate for the maximum stress in the beam. The plate model on the other hand gives a low estimate, as the threadbar is simplified to a simple support on the entire circumference of the plate rather than a point load. Nonetheless, the plate model is more representative than the beam model. The selected thickness for the reaction plate is 2″ (5cm). The selected thickness for the base plate is 2 ¾″ (7cm) at the point of maximum bending moment. The factor of safety for the base plate is 1.46. The factor of safety for the reaction plate is 1.54. All calculated factors of safety are presented below.

4.3.7 Safety Factors

Table 3: Factor of safety for analyzed rig components

		Plate Thickness (in)*	Factor of Safety under Working Load
Base plate	beam model	2.75	1.46
	plate model	2.75	2.91
Reaction plate	beam model	2	1.54
	plate model	2	1.88
Threadbar		N/A	4.67

* 1″ = 2.54cm

As can be seen from Table 2, the most critical component of the rig is the base plate. Assuming the conservative beam model, the minimum factor of safety is 1.46.

4.3.8 Maximum Attainable Load

The beam model indicates that the yield stress of the plate may be exceeded under maximum attainable load for the base plate and reaction plate (see figure 2 and 3). While this does not indicate that the UCS rig is unsafe, it does indicate that the rig must not be used for any specimen material other than cemented rockfill. The electric pump must be set to offer a maximum pressure of 8MPa (working load) on the sample.

4.4 Conclusion

The test rig design is safe for the implementation of the planned testing of cylindrical samples of 15" in diameter by 30" in height that are made from cemented rockfill. The main points revealed by the analysis are:

- Critical component is base plate.
- Working load (8MPa) factor of safety is 4.67 for the threadbars and 1.46 for the base plate.
- Rig should be used for cemented rockfill only

The electric pump is to be set to offer a maximum pressure of 8MPa on the specimen, attaining a safety factor of 4.67 for the threadbars and 1.46 for the bending of the base plate assuming the more conservative beam model.

Chapter 5

Experimental Procedure

5.1 Introduction

This chapter describes the experimental procedure of the UCS experiment conducted in the underground laboratory. The laboratory was placed underground to have quick access to CRF materials that can be used as-is. The laboratory is large enough such that all activities related to the experiment are undertaken in the lab. Specimen preparation and curing occur in in-situ conditions. Specimen handling is done with a forklift which is readily available. So far, 24 specimens were prepared and tested in the underground laboratory following the prescribed testing program. Another 3 specimens were prepared and tested to determine the long term strength of the CRF.

5.2 Experiment Overview

The purpose of the experiment is to investigate the effect on CRF strength of increased cement content, poorer water quality, mixing method, and controlled grading with respect to the cemented rockfill practice at Birchtree mine. The program involves 8 sets of 3 specimens, totalling 24 specimens. Another set of specimens (referred to as set 1b) were prepared to determine the long term strength of the CRF (4 months curing)

Table 4: Birchtree UCS testing program

Set	Binder	Grading	Mixing Method	Water Quality
1	4%	As practiced by Birchtree	Mechanical	River Water
2	4%	As practiced by Birchtree	Mechanical	Mine effluent water
3	4%	As practiced by Birchtree	Sump Method	River Water
4	4%	As practiced by Birchtree	Bucket Method	River Water
5	5%	As practiced by Birchtree	Mechanical	River Water
6	4%	Talbot grading 5″	Mechanical	River Water
7	4%	Talbot grading 3″	Mechanical	River Water
8	4%	Talbot grading 5″	Sump Method	River Water

5.3 Laboratory Location

The laboratory was placed in a tool storage drift located off the ramp on level 2750. The location of the lab was chosen based on its proximity to the materials required for the production of CRF such as the flash mixer for binder, aggregate fill raise, and level sump for mine effluent water. It was also of sufficient size to store curing CRF specimens, operate the UCS rig, and handle the CRF specimens with a forklift.

5.4 Equipment

To minimize costs, the experiment is designed to be conducted with minimal equipment. Main equipment required are:

- UCS rig
- Gilson screen shaker, with 5″, 3″, 3/2″, 3/4″, 3/8″ screens (12.7cm, 7.6cm, 3.8cm, 1.9cm, 1cm)
- 2000 lb scale
- 30 x specimens base plates
- 15″ diameter Sonotube, cut at 30″ length
- Modified digital caliper

Components of the UCS rig are discussed in more detail in chapter 4. The 30 specimen base plates were fabricated on site along with the components of the UCS rig. Additional lab equipment was collected from the yard on surface or from underground tool storage:

- Drum mixer
- Wheelbarrow
- Shovels
- Pelican pick
- Plastic containers (to store graded aggregate or waste CRF and waste slurry for disposal)
- pails

5.5 Acquiring CRF Material

5.5.1 Aggregate

A 7yd^3 bucket of aggregate was drawn from the fill raise on level 2750 and dumped at the lab. The aggregate material for all specimens is drawn from this pile.

5.5.2 Water

The lab has a water line. Water for the cement slurry of sets 1, 3-8, are from the mine water line. Set 2 uses mine effluent water. The mine effluent water is retrieved from a sump on level 2750.

5.5.3 Binder

Dry binder is obtained from the flash mixer on level 2750 or the binder silo on surface.

5.6 Specimen Preparation

5.6.1 Aggregate Sampling

The specimens with grading as practiced by Birchtree (sets 1 to 5) are prepared by shoveling equally across the 7yd^3 (5.3m^3) aggregate pile. Only two faces of the pile were exposed so preparation of the pile was required before sampling. Approximately 1 ton of segregated material was discarded before sampling the pile. Oversized particles (which could not be handled with a shovel) are manually removed in the sampling process. The density of the aggregate (weight of specimen) is used as a control to determine if the specimens are properly sampled. Between 4 and 5 full pails of aggregate are required to complete a specimen.

For the specimens with Talbot curve grading, the aggregate is split with a Gilson TS2 screen shaker with 5″, 3″, 3/2″, 3/4″, and 3/8″ screens. One 600lb (270kg) pile of 5″ Talbot curve material or 3″ Talbot curve material per specimen is assembled. The Talbot curve is corrected to account for the fact that the aggregate is wet when screened. Five 100lb (45kg) pails of aggregate are retrieved from the pile to prepare a specimen. The remaining 100lb of aggregate is screened to obtain the particle size distribution of the specimen.

Table 5: Graded aggregate piles and their %weight for 3″ Talbot, 5″Talbot and ungraded specimens

	**Oversize** 3″ Talbot → 0% 5″ Talbot → 0% Ungraded → 12% (estimated average)

	**5″ Passing** 3″ Talbot → 0% 5″ Talbot → 22% Ungraded → 18% (estimated average)
	**3″ Passing** 3″ Talbot → 30% 5″ Talbot → 23% Ungraded → 20% (estimated average)
	**3/2″ Passing** 3″ Talbot → 21% 5″ Talbot → 16% Ungraded → 18% (estimated average)
	**3/4″ Passing** 3″ Talbot → 15% 5″ Talbot → 12% Ungraded → 13% (estimated average)

	**3/8″ Passing (fines)** 3″ Talbot → 35% 5″ Talbot → 27% Ungraded → 19% (estimated average)

Figure 11: 600lb 5″ Talbot curve graded aggregate pile for specimen 6a

5.6.2 Correction for wet aggregate

The aggregate is wet when screened, leading to fine particles (<3/8″) coagulating and being retained by the 3/8″ and larger screens. A 10lb (4.5kg) sample batch of 3/8″ to 3/4″ of aggregate is dried and the retained fines measured. The fines retained by the 3/8″ screen are measured at 15% of the retained weight. The fines retained by the 3/4″ screen are measured at 0.6%. Fines retained by larger particles are assumed negligible.

The % moisture of 5 x 10lb samples (fines, 3/8″, 3/4″, 3/2″, 3″) is also measured. The data is used to determine the actual dry aggregate weight from the wet aggregate weight of the sized batches. The wet batch weights are then adjusted such that the dry weights match the Talbot grading curve.

The required dry batch weights to obtain a 5″ or 3″ Talbot curve are displayed below, along with the corresponding adjusted wet batch weights after correcting for fines content and moisture content. Moisture content results are discussed in chapter 6.

Table 6: 600lb Dry Weight 5″ Talbot Batch

Retained Screen*	Required Dry Weight (lb)**	% Moisture	% Fines	Adjusted Wet Batch Weight (lb)
5″	0	0%	0%	0
3″	135.2	0.2%	0%	135
3/2″	136.1	0.5%	0%	136
3/4″	95.9	1.5%	0.6%	95.5
3/8″	68.1	3.2%	15%	81
Pan	164.4	8.3%	100%	169

* 1″ = 2.54cm, **1lb = 0.454kg

Table 7: 600lb Dry Weight 3″ Talbot Batch

Retained Screen	Required Dry Weight (lb)	% Moisture	% Fines	Adjusted Wet Batch Weight (lb)
5″	0	0%	0%	0
3″	0	0.2%	0%	0
3/2″	175.7	0.5%	0%	176
3/4″	124.3	1.5%	0.6%	126
3/8″	87.9	3.2%	15%	103
Pan	212.1	8.3%	100%	206

5.6.3 Binder Slurry Preparation

Binder slurry is prepared at the lab. Water to cement ratio (w:c) of the cement slurry is adjusted depending on the moisture content and the fines content of the aggregate to obtain proper mixing. 50lb batches of cement slurry are prepared in a drum cement mixer during specimen preparation. The mixer is left to operate non-stop during specimen preparation.

5.6.4 Mixing

Manually mixed specimens are prepared by mixing binder slurry with the aggregate in 100lb batches. The batching is done in a wheelbarrow. The mixing is done manually with a grub hoe until all fines are coated with binder slurry. The mixing process takes 2-3 minutes per 100lb batch.

To simulate the bucket method, the specimen is prepared in ten 50lb (22kg) batches. Each batch is prepared in a pail. The binder slurry is poured on the aggregate in the pail. The pail is then shaken for 10 seconds, and then poured in the specimen tube.

To simulate the sump method, the specimen is prepared in ten 50lb batches. Each batch is prepared in a wheelbarrow. The binder slurry is poured on the aggregate in the wheelbarrow. The contents of the wheelbarrow are overturned once, and then shoveled into the specimen tube.

5.6.5 Specimen Filling

The specimens are prepared in a 15″ diameter cardboard Sonotube, cut at 30″ lengths. The specimen is filled with approximately 5 to 6 100lb batches of mixed CRF. The batch is shoveled from the wheelbarrow into the specimen tube. After each shovelful, the CRF in the tube is packed with the shovel. Large particles (close or exceeding 1/3 diameter) are packed by hand so that there is minimal void at the interface between the specimen tube and the CRF.

5.6.7 Curing and Testing Preparation

Specimens are left to cure for 14 days in the laboratory before testing. The Sonotube is removed before the specimen is placed in the rig. The top of the specimen is equalized with 10lb of fine aggregate mixed with 1lb of binder slurry one week before testing.

Figure 12: Set 6 and 8 ready for testing

5.6.8 Other factors

Other controlled and uncontrolled factors which are not explicitly stated in the testing program are: aggregate moisture content, water to cement ratio, particle size distribution for ungraded specimens, and specimen weight.

The particle size distribution of specimens 1-5 is determined with a 2000lb (900kg) sample using the bin sampling method. One in six shovels of aggregate material was retained during specimen preparation.

The moisture content of the graded aggregate is measured for two purposes:

1) Find the dry weights required to assemble the aggregate in a Talbot distribution.

2) Determine the water to cement ratios of the specimens taking into account aggregate moisture

First of all, the Talbot curved aggregate is blended with respect to the dry weight. Since the aggregate is not dried, the moisture content of each particle size is required to correct the wet batch weights to match a dry Talbot curve (see section 5.6.2).

Also, the overall water to cement ratios of the specimens cannot be directly measured as a representative sample, with respect to particle size distribution, is too difficult to acquire and to dry. Therefore, by determining the moisture content of smaller graded samples, and knowing the average particle size distribution of the aggregate in the ungraded specimens, the average moisture content of the ungraded specimens can be determined.

5.7 Moisture Content Data Acquisition

For sets 1-5, moisture content of the aggregate is estimated with a 50lb (22kg) sample and applied set 1-5. The bin sample method is used, where 2 shovels of aggregate per specimen prepared in one day (6 in total) are retained. The samples are dried and the moisture content measured. However, this acquisition method is unlikely to give a representative sample of all sets prepared. The result is not representative of the pile itself.

With the availability of a screen shaker, the moisture content of subsequent specimens (6-8) is instead estimated with four graded 10lb samples. The moisture retained by the 3″ and 5" retained portion was assumed negligible. The samples are dried and the moisture content measured. With the PSD of sets 6-8 known, the overall moisture content of the specimens is calculated by adding the moisture contained by each particle size.

$$wc_{total} = \sum P(u) * wc(u) \tag{5-1}$$

where,

$wc_{total} = moisture\ content\ of\ specimen$

$P(u) = dry\ proportion\ material\ retained\ by\ sieve\ of\ opening\ u$

$wc(u) = moisture\ content\ of\ material\ retained\ by\ sieve\ opening\ u$

Four more 10lb samples of 3/8″ passing and 3/4″ passing aggregate are taken to determine the rate at which the aggregate is drying after it is separated from the aggregate pile.

5.8 Specimen Testing

5.8.1 Stress vs. Strain Point Acquisition

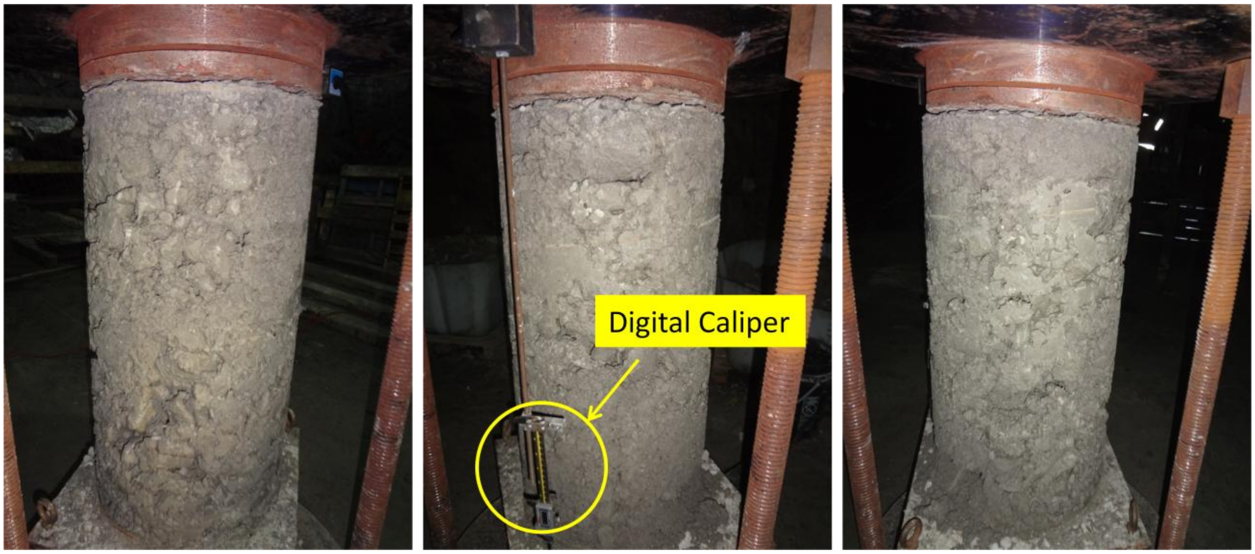

Figure 13: Specimen ready for testing. Digital caliper is placed between reaction plate and specimen base plate.

Two methods are used to acquire stress and strain data of a specimen during the course of the testing program. Sets 1-5 use the first method, while sets 6-8 use the second method.

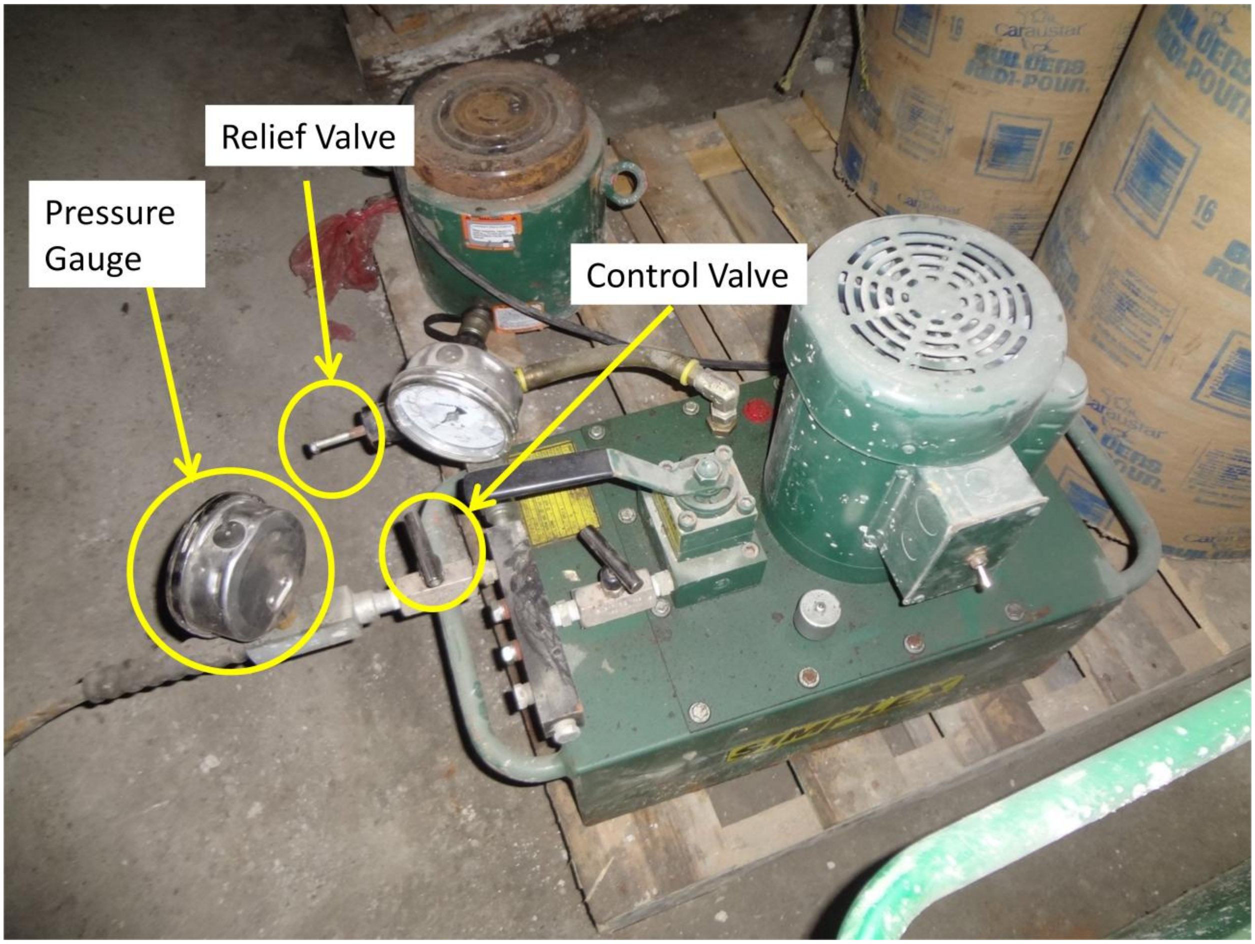

Figure 14: 10000PSI electric pump components

Method 1:

1. Set pump on advance for 5 seconds
2. Set pump on neutral to take displacement reading from LVDT
3. Repeat steps 1 and 2 until specimen has failed

This results in about 10-12 stress vs. strain points for stronger specimens and 3-5 stress vs. strain points for weaker specimens. Post-peak stress vs. strain values are also acquired with this method. The exact strain for the UCS has to be interpolated based on the acquired strain values. On the other hand, specimen sets 6-8 are tested with the following method.

Method 2:

1. Put pump on advance
2. Adjust relief valve for maximum of 500PSI (3440KPa) gauge at pump

3. Slowly open control valve until gauge pressure at hose reaches 100PSI
4. Close control valve
5. Take pressure and displacement reading
6. Repeat 3-5 until maximum set gauge pressure at pump reached
7. Adjust relief valve for additional 500PSI maximum pressure
8. Repeat 3-7 until failure of specimen

While method 1 is quicker, method 2 is preferable as the stress on the specimen is controlled, and stress increments can be reduced to obtain more stress-strain points for a specimen.

5.8.2 Result Correction

The load applied on the specimen is measured based on the gauge pressure measured at the hose. The pressure applied on the specimen is determined with the ratio between the cylinder effective piston area (EPA) and the specimen cross-sectional area, and then corrected by subtracting the weight of the specimen and transfer plates between the specimen and the hydraulic cylinder:

$$Stress\ Specimen\ (MPa) = \frac{[P_{hose} \times EPA\ ] - W_{specimen} - W_{plates}}{145 \times A_{specimen}} \quad (5\text{-}2)$$

where,

$P_{hose} = gauge\ pressure\ reading\ at\ hose\ (psi)$

$EPA = \ Effective\ Piston\ Area = 41.28in^2$

$W_{specimen} = weight\ of\ specimen\ (lb)$

$W_{plates} = weight\ of\ tranfer\ plates\ between\ specimen\ and\ cylinder = 120lb$

$A_{specimen} = Specimen\ surface\ area\ on\ which\ load\ is\ applied\ (in^2)$

5.8.3 UCS Determination

The maximum gauge pressure acquired for a specimen is recorded and corrected to determine the specimen UCS. The strain at the UCS is linearly interpolated between the two stress strain points bounding the acquired UCS.

5.8.4 Modified Curve for Modulus of Elasticity

The strain data of sets 1-5 is acquired by setting the pump to neutral, resulting in a gauge pressure loss each time data is acquired. Data points on the curve must be eliminated for the purpose of determining the tangent modulus of elasticity.

The modified curve is built by connecting data points based on the slope. The subsequent point in the curve is determined by sweeping all points and selecting the point that yields the highest slope. The process is repeated for all subsequent points until all data points have been processed.

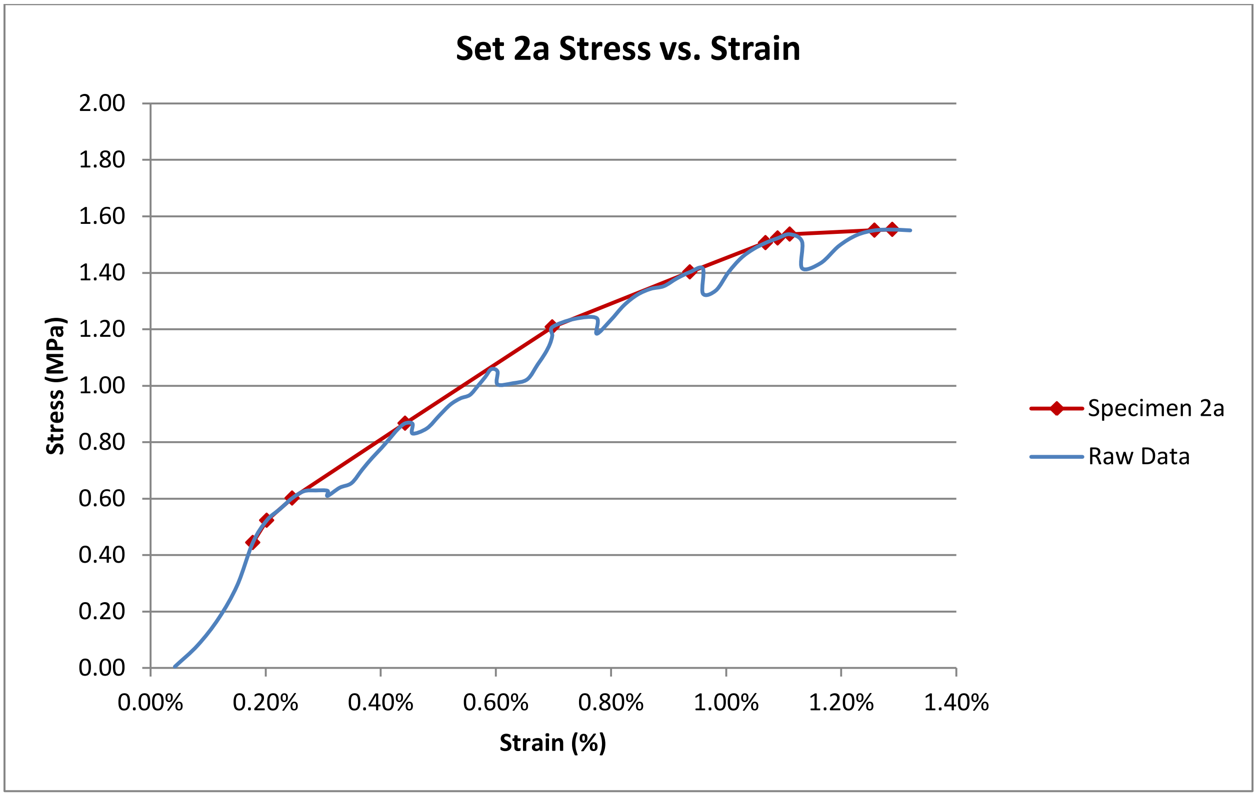

Figure 15: Modified curve for the purpose of determining the elastic tangent modulus

5.8.5 Modulus of Elasticity Determination

The elastic tangent modulus defined as the tangent of the stress strain curve at 50% of the UCS. The modulus of elasticity is determined graphically based on the two data points on the modified stress-strain curve bounding 50% of the UCS on the y axis.

$$E_{tangent} = \frac{d\sigma}{d\varepsilon} \quad (5\text{-}3)$$

$$\sigma = UCS/2$$

The modulus of deformation is defined as the UCS of the specimen over the strain at specimen UCS:

$$E_{def} = \frac{UCS}{\varepsilon_{UCS}} \tag{5-4}$$

Both tangent modulus of elasticity and modulus of deformability are acquired for all specimens. See below for a graphical example (set 2a).

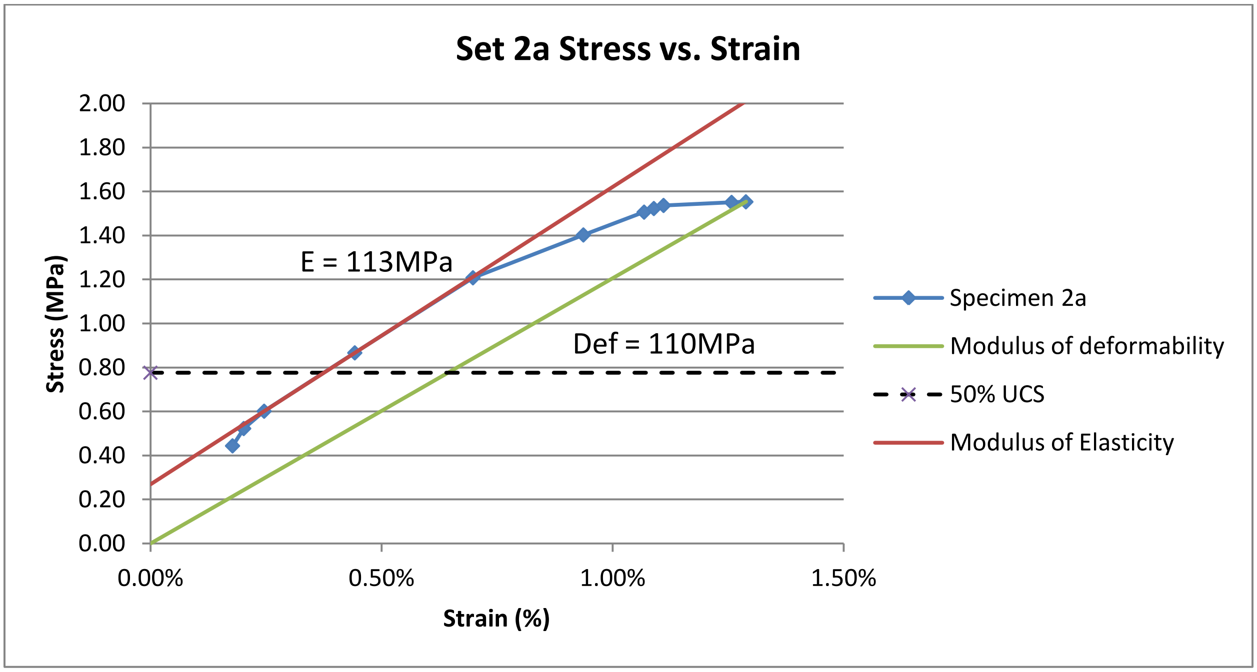

Figure 16: Modulus of deformability and tangent modulus of elasticity determination for set 2a

5.9 Obtained Specimens

5.9.1 Overall

Table 8: Actual specimen properties

Specimen	W (lb)	Density (t/m^3)	Binder Content	Aggregate Moisture	Slurry w:c	Specimen w:c
1a	521	2.4	4%	4.5%	0.7	2.4
1b	516	2.3	4%	4.5%	0.7	2.4
1c	460	2.3	4%	4.5%	0.7	2.4
1d	566	2.6	4%	4.5%	0.7	2.4
1e	546	2.4	4%	4.5%	0.7	2.4
1f	531	2.4	4%	4.5%	0.7	2.4
2a	618	2.6	4%	4.5%	0.7	2.4
2b	548	2.5	4%	4.5%	0.7	2.4
2c	588	2.6	4%	4.5%	0.7	2.4
3a	505	2.4	4%	4.5%	0.7	2.4
3b	556.5	2.4	4%	4.5%	0.7	2.4
3c	565	2.5	4%	4.5%	0.7	2.4
4a	546	2.4	4%	4.5%	0.7	2.4
4b	557	2.5	4%	4.5%	0.7	2.4
4c	506	2.4	4%	4.5%	0.7	2.4
5a	553	2.5	5%	4.5%	0.7	2.1
5b	581	2.5	5%	4.5%	0.7	2.1
5c	609	2.5	5%	4.5%	0.7	2.1
6a	504	2.4	4%	2.2%	0.7	1.6
6b	504	2.3	4%	2.2%	1.2	2.3
6c	520	2.3	4%	2.2%	1.2	2.3
7a	515	2.4	4%	2.5%	1.2	2.5
7b	528	2.4	4%	2.5%	1.5	3.0
7c	579	2.4	4%	2.3%	1.5	2.8
8a	533	2.4	4%	2.2%	1.2	2.3
8b	539	2.4	4%	2.2%	1.2	2.3
8c	529	2.3	4%	2.2%	1.2	2.3

5.9.2 Abnormal Specimens

Specimen 6a was prepared using a water to cement ratio of 0.7, but with lower aggregate moisture than specimens of sets 1-4. The overall water to cement ratio due to aggregate moisture is therefore 1.6 as opposed to 2.3-2.4 for specimens of sets 1-4. Due to the relatively low water to cement ratio of this specimen, and due to the added fines for the Talbot 6″ grading (total of 27.5% fines), the specimen is poorly mixed.

Specimen 7a is mixed with cement slurry with a water to cement ratio of 1.2. However, the 3″ Talbot graded curve requires 34% fines, increasing binder consumption due to high aggregate surface area, and leading to poor mixing for specimen 7a. The slurry water to cement ratio of remaining 3″ Talbot sets is therefore increased to 1.5 during the experiment to increase slurry volume for better mixing.

5.9.3 Particle Size Distribution

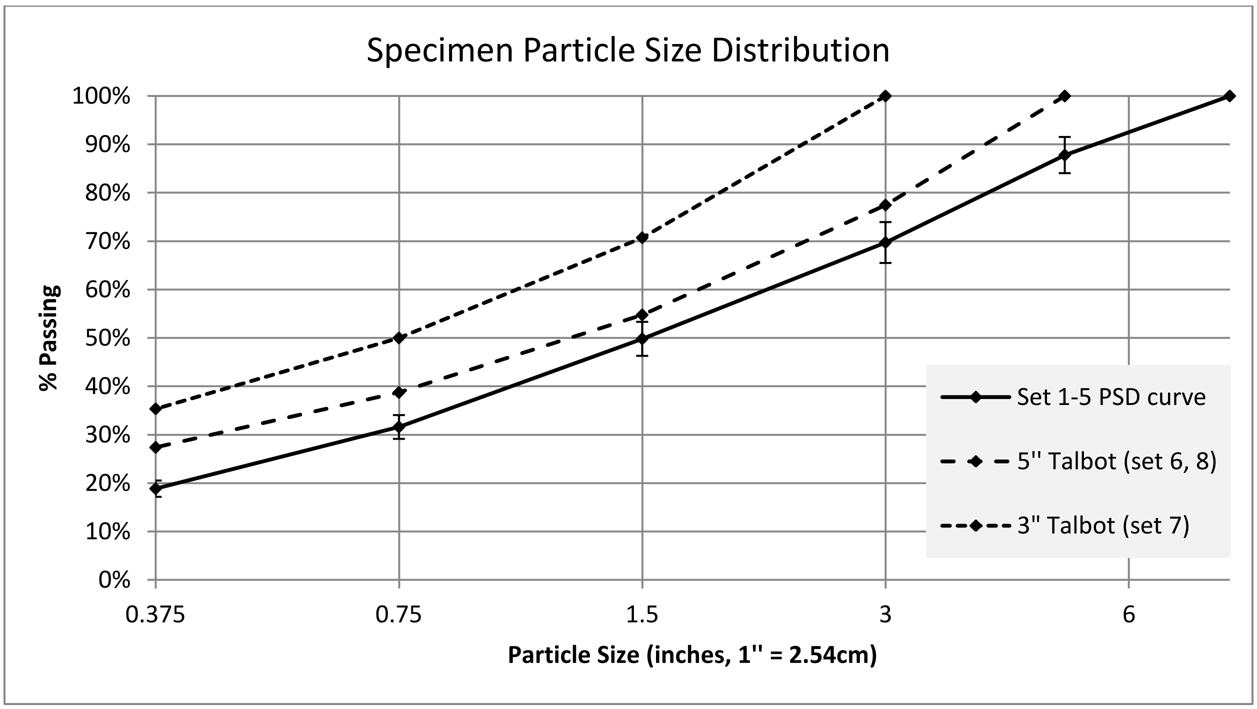

Figure 17: Particle size distribution of sets 1-5 (estimated with 2000lb of aggregate sampled during preparation), set 6 and 8 (graded to match 5″ Talbot curve) and set 7 (graded to match 3″ Talbot curve)

For the ungraded specimens, one ton of aggregate was sampled for PSD analysis during specimen preparation to obtain an average PSD for the ungraded specimens. Eighteen 100lb batches of aggregate were split in the screen shaker. The variation of PSD between 100lb batches was determined. However, this variation does not directly apply to the specimens as they consist of 5 to 6 batches.

The PSD of 10000 combinations of 5 random batches was calculated to yield an estimation of the variation of PSD between specimens. The most variable particle size is the 5″ to 8″ particle size range, which ranges from 6% to 17%. The fines content is estimated to range between 18% and 23%. This variation is problematic as CRF strength is sensitive to fines content. For example, a 5% addition of sand from 25% fines was observed to reduce CRF strength at Kidd Creek Mines by 66% [4].

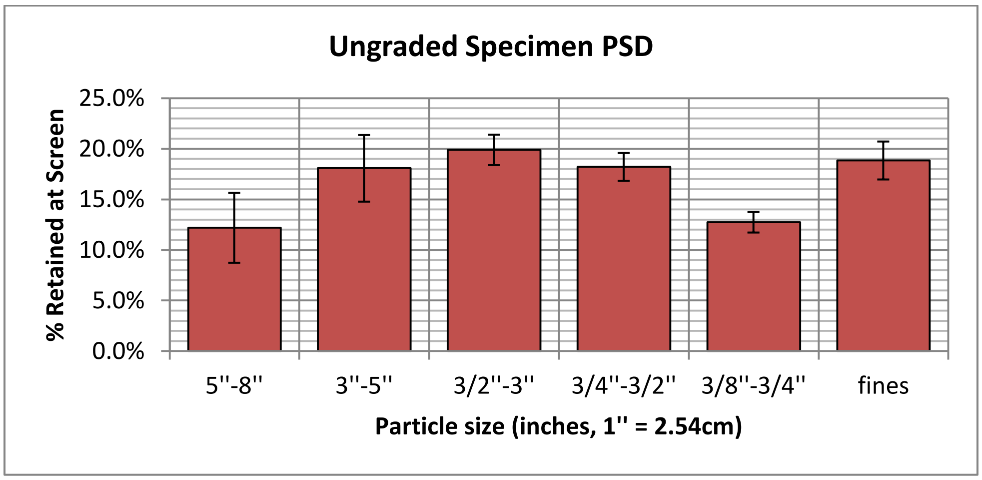

Figure 18: Average ungraded specimen PSD. Error bars are standard deviations of specimen PSD derived 10000 random combinations of 5 batches.

For the graded specimens, the particle size distribution of the remaining aggregate from the 600lb pile was determined to calculate de PSD of the aggregate in the specimens. The obtained PSD for sets 6 to 8 are shown below. Variation of PSD is smaller for the graded specimens.

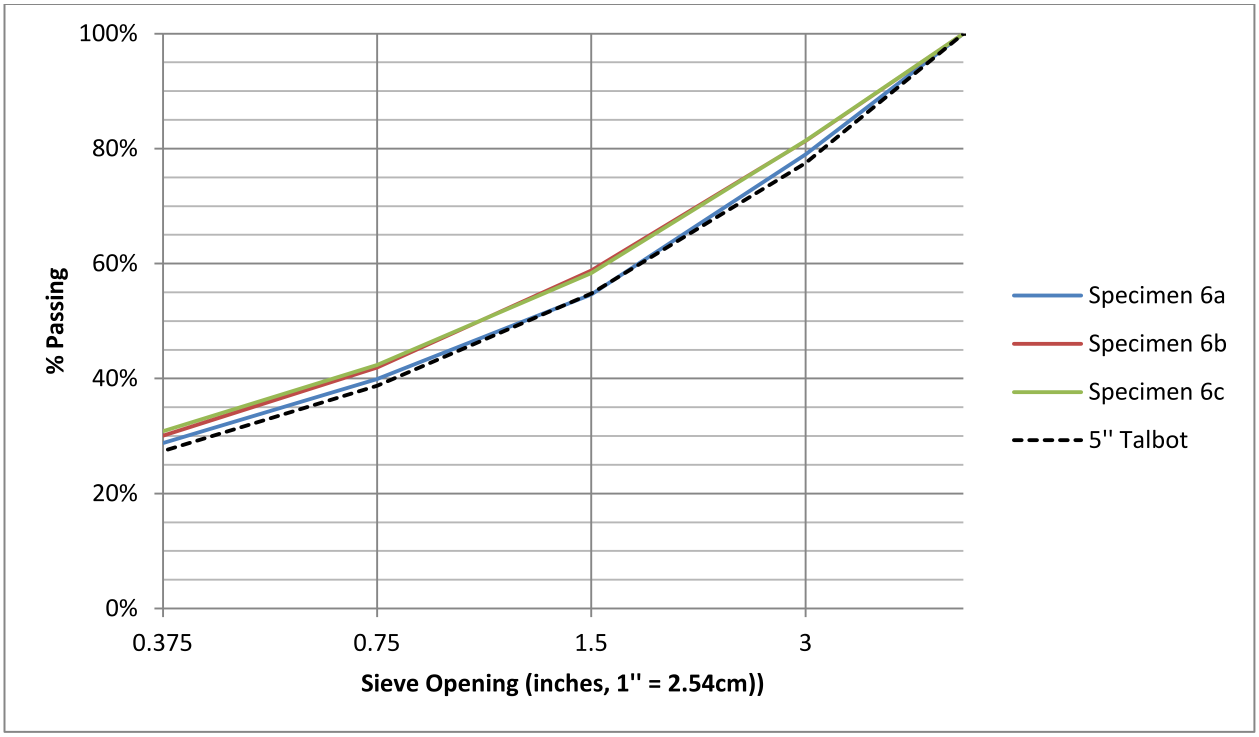

Figure 19: Obtained dry particle size distribution for set 6

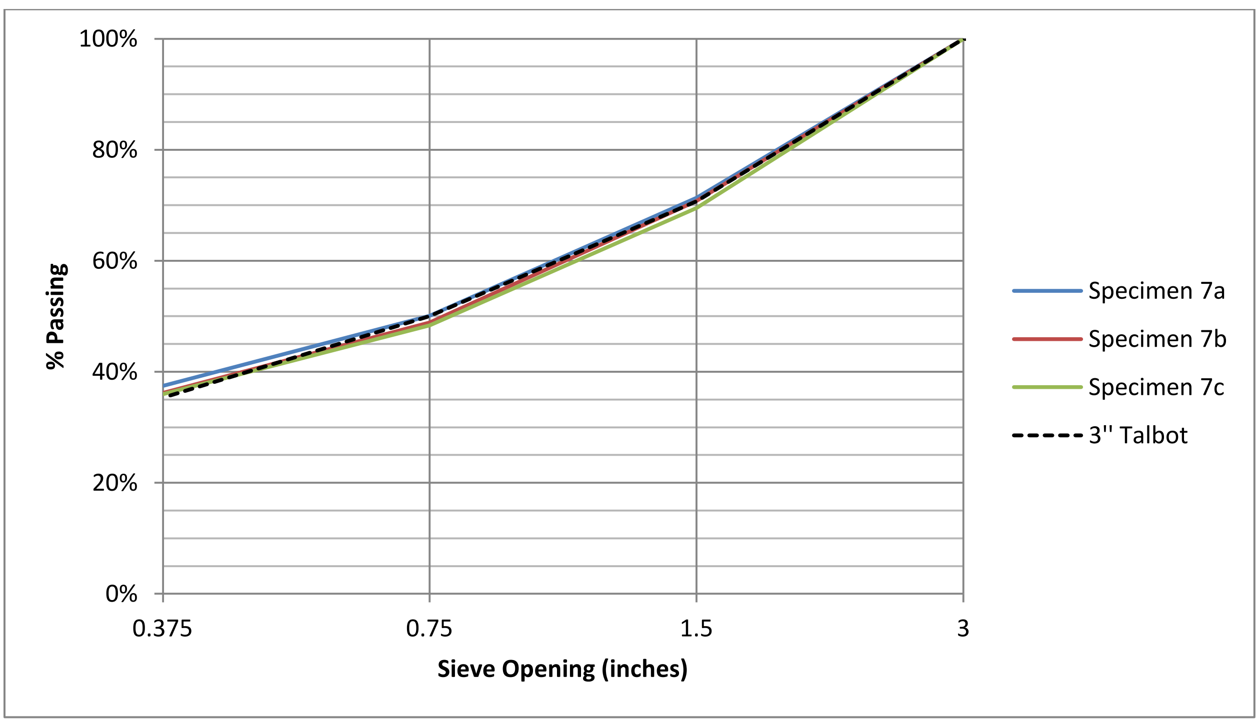

Figure 20: Obtained dry particle size distribution for set 7

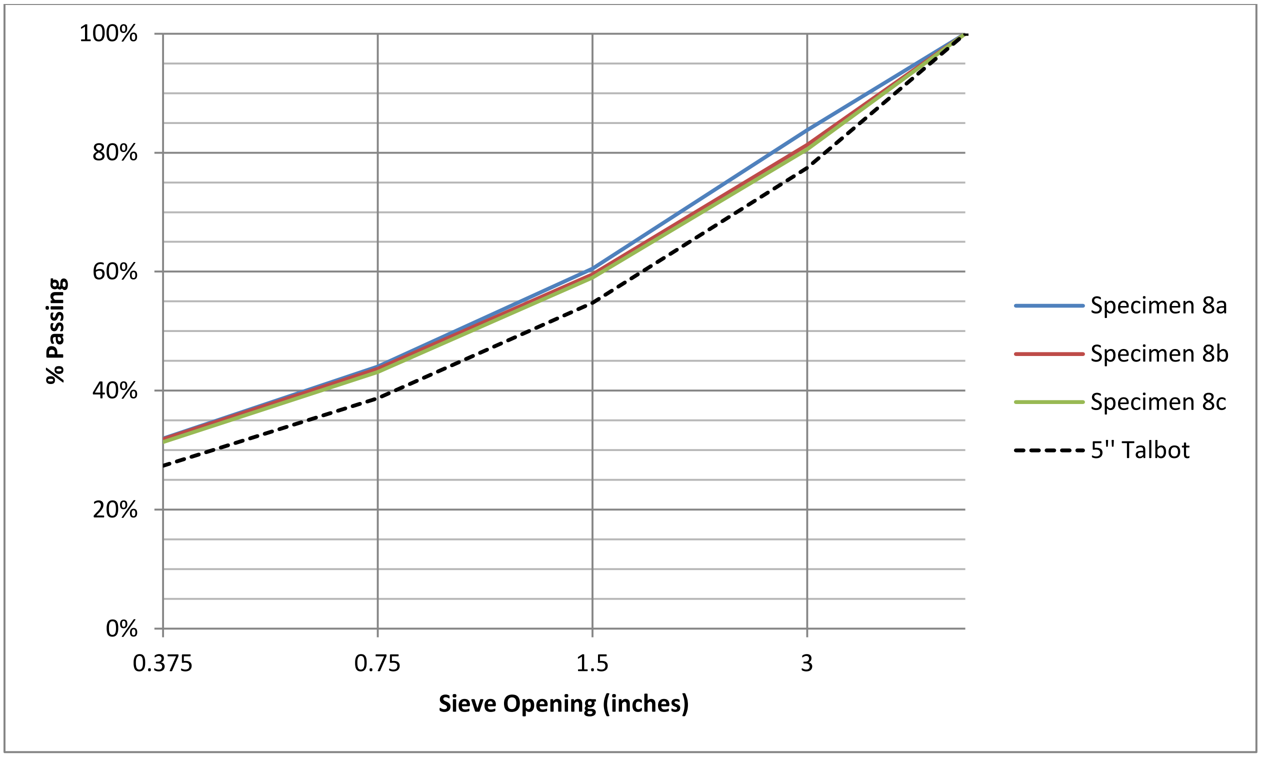

Figure 21: Obtained dry particle size distribution for set 8

5.9.4 Aggregate Moisture

For sets 1-5, moisture content of the aggregate is estimated with a 6 x 10lb samples taken during the preparation of the specimens. The average moisture content of the aggregate is 4.3%. This value was assumed for sets 1 to 5. Using the moisture content of the graded aggregate, the moisture content for the PSD of sets 1-5 is calculated as 2.4%. This value is not applicable to sets 1-5, but indicates that the pile has dried from 4.3% moisture to 2.4% moisture between the preparation of sets 1-5, the grading of the aggregate, and the acquisition of the graded samples. Monitoring of the moisture content of the aggregate is therefore crucial to control the amount of water in the specimens.

For sets 6-8, the moisture content of the aggregate calculated based on samples of graded aggregate and the specimen PSD. The moisture content of the graded aggregate is calculated as 2.2% for sets 6 and 8 (5″ Talbot), and 2.5% for set 7 (3″ Talbot).

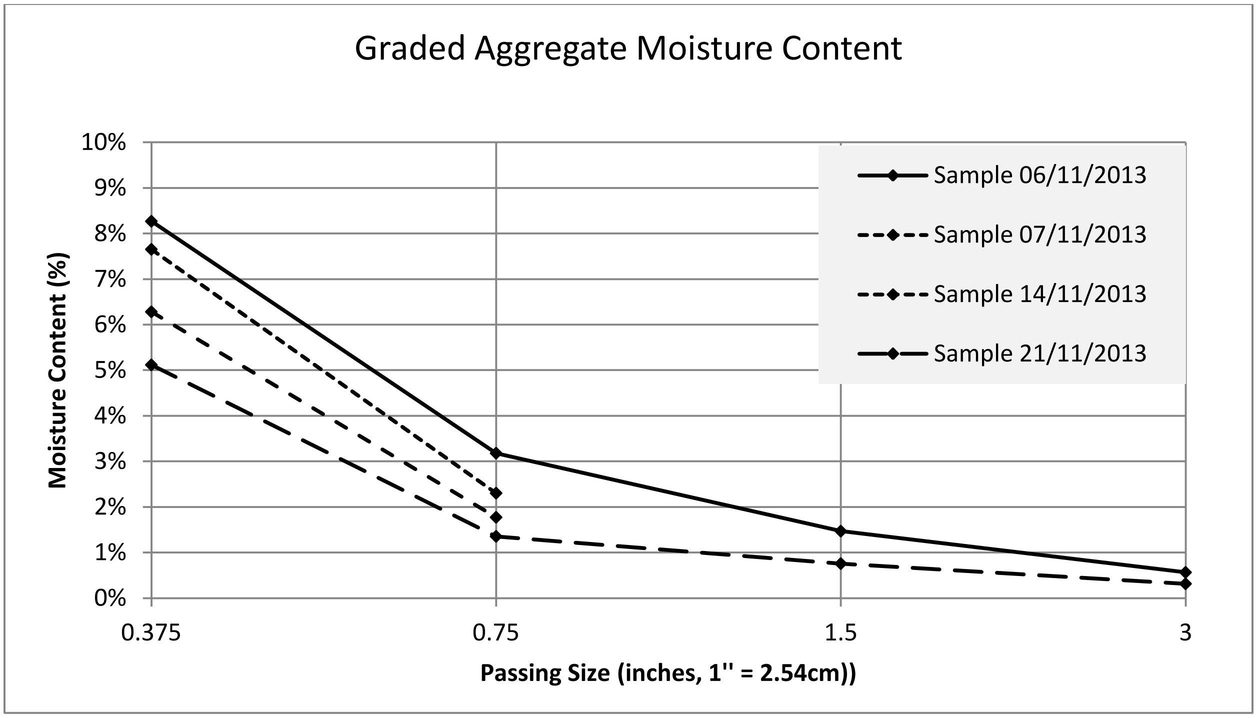

Figure 22: Moisture content of graded aggregate. Moisture content of specimens was calculated based on the PSD of the specimen and time of preparation.

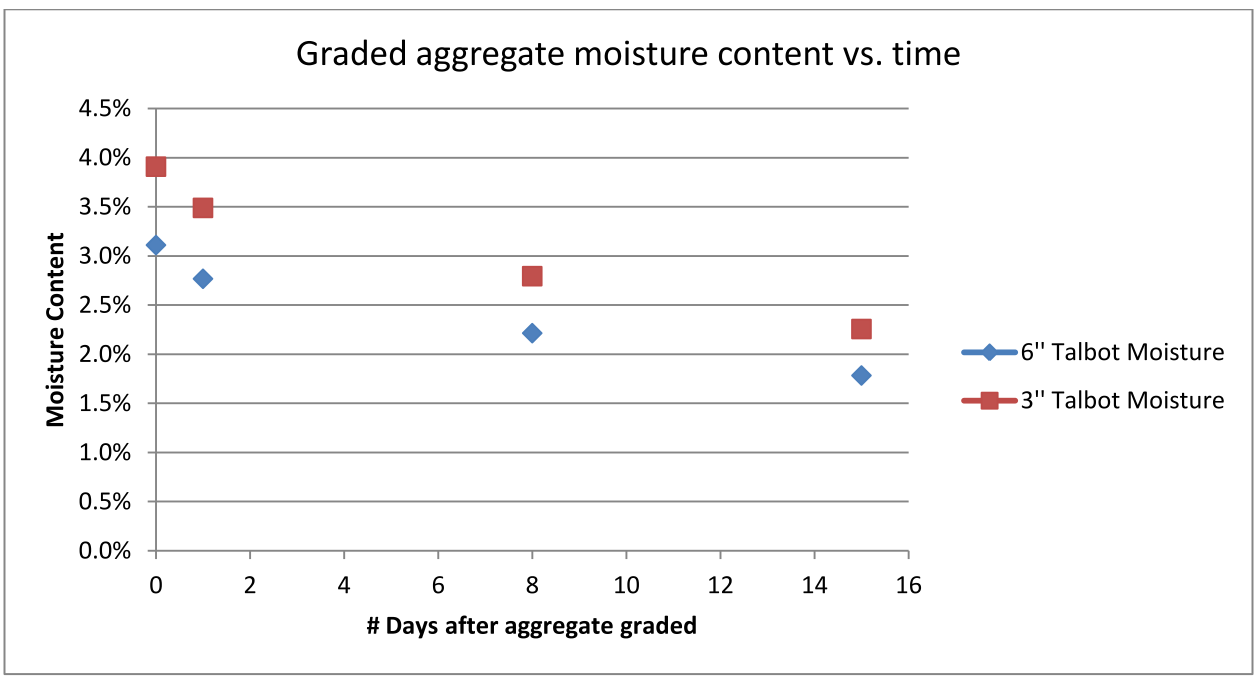

Figure 23: Graded aggregate moisture content over time

5.9.5 Specimen overall water to cement ratio

The water to cement ratio of the cement slurry prepared at Birchtree mine is 0.5, selected by taking into account assumed aggregate moisture content of 5%. This yields a CRF water to cement ratio of 2.2. The exact moisture content of the aggregate is unknown. This value is therefore a ballpark figure.

On the other hand, overall water to cement ratio ranges between 2.1 and 3 for the specimens prepared in the experiment. The variation of water to cement ratio is due to changes in slurry water to cement ratio, aggregate moisture, and cement content (slurry volume).

5.9.6 Discarded Specimens

Stress vs. strain results and UCS for Set 1c are discarded as the specimen was not properly centered in the UCS rig during the test. Specimen 6a is discarded due to poor mixing. Abnormal specimens 6a and 7a were also discarded.

Chapter 6

Test Results

6.1 Results overview

UCS, strain, modulus of elasticity, and deformation modulus were determined for all specimens. Exceptions are set 1 where no strain data was acquired, and set 6a which recorded a UCS of 0.

Table 9: Experiment Results

Specimen	UCS (MPa)	Strain @ UCS (%)	Modulus of Deformability (MPa)	Tangent Modulus of Elasticity (MPa)
1a	1.07	NA	NA	NA
1b	1.24	NA	NA	NA
1c	0.71	NA	NA	NA
1d	2.42	1.34%	181	197
1e	1.57	0.59%	265	360
1f	1.54	1.48%	104	76
2a	1.46	1.33%	110	113
2b	1.34	0.80%	168	196
2c	1.37	1.28%	107	110
3a	0.54	1.38%	39	71
3b	0.58	1.02%	56	93
3c	0.45	0.46%	97	118
4a	0.27	1.79%	15	24
4b	0.41	0.89%	46	51
4c	0.33	0.75%	44	67
5a	1.83	1.92%	96	109
5b	2.27	1.64%	139	205
5c	2.46	0.99%	249	295
6a	0.00	0.00%	0	0
6b	0.61	1.08%	56	60
6c	0.67	1.16%	58	60
7a	0.64	0.37%	171	354
7b	0.62	1.57%	39	64
7c	0.19	1.07%	18	21
8a	0.49	0.66%	74	79
8b	0.65	1.61%	40	57
8c	0.56	0.68%	82	91

6.2 Stress-Strain Curves

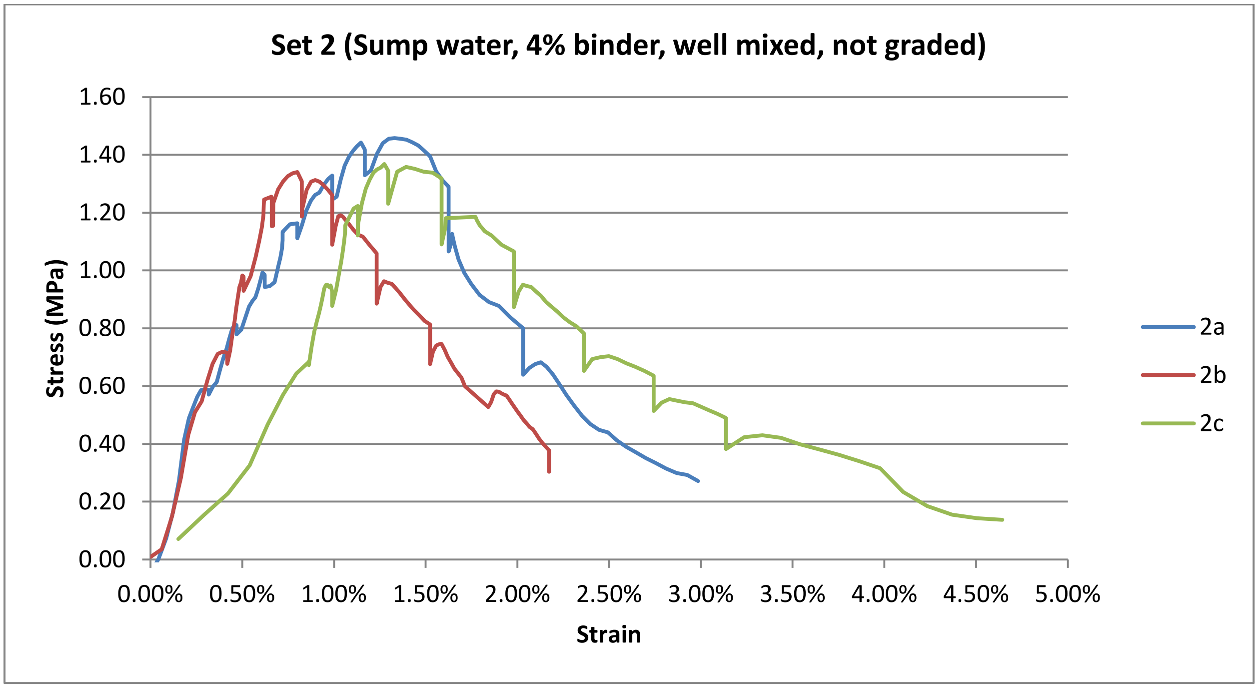

Figure 24: Set 2 stress vs. strain curves

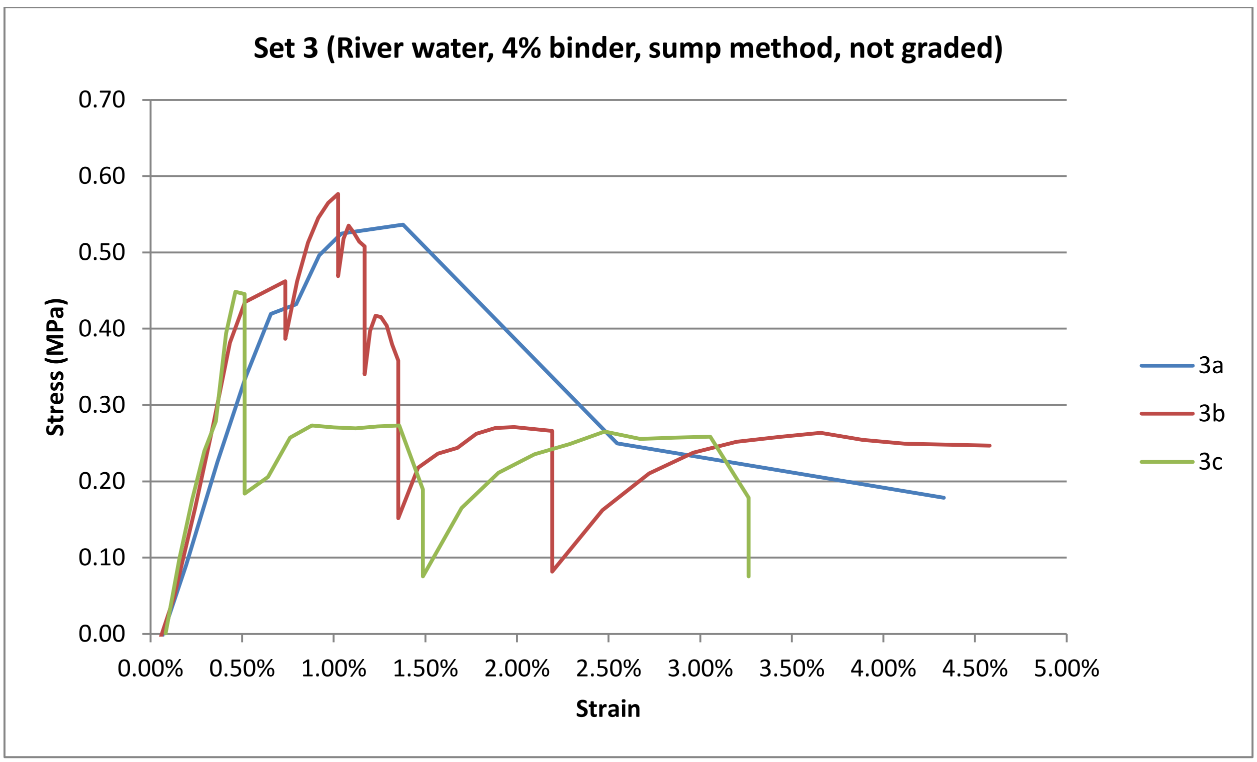

Figure 25: Set 3 stress vs. strain curves

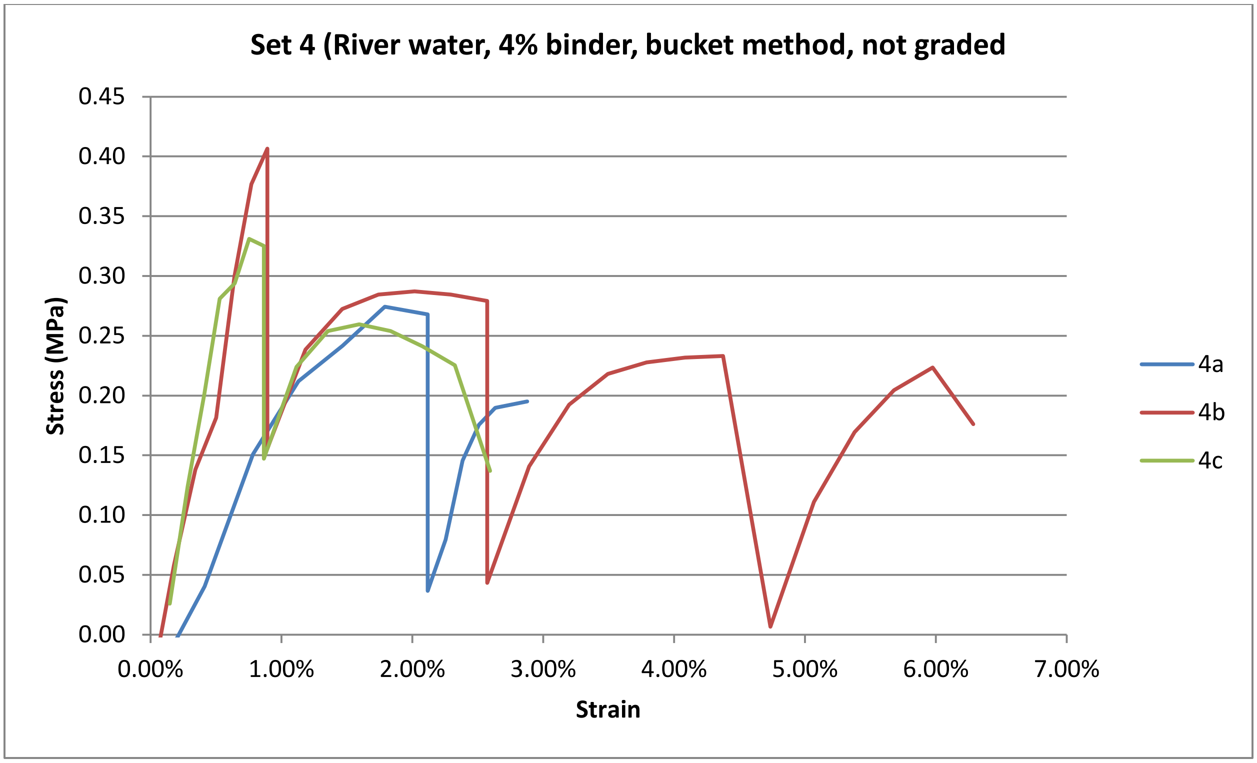

Figure 26: Set 4 stress vs. strain curves

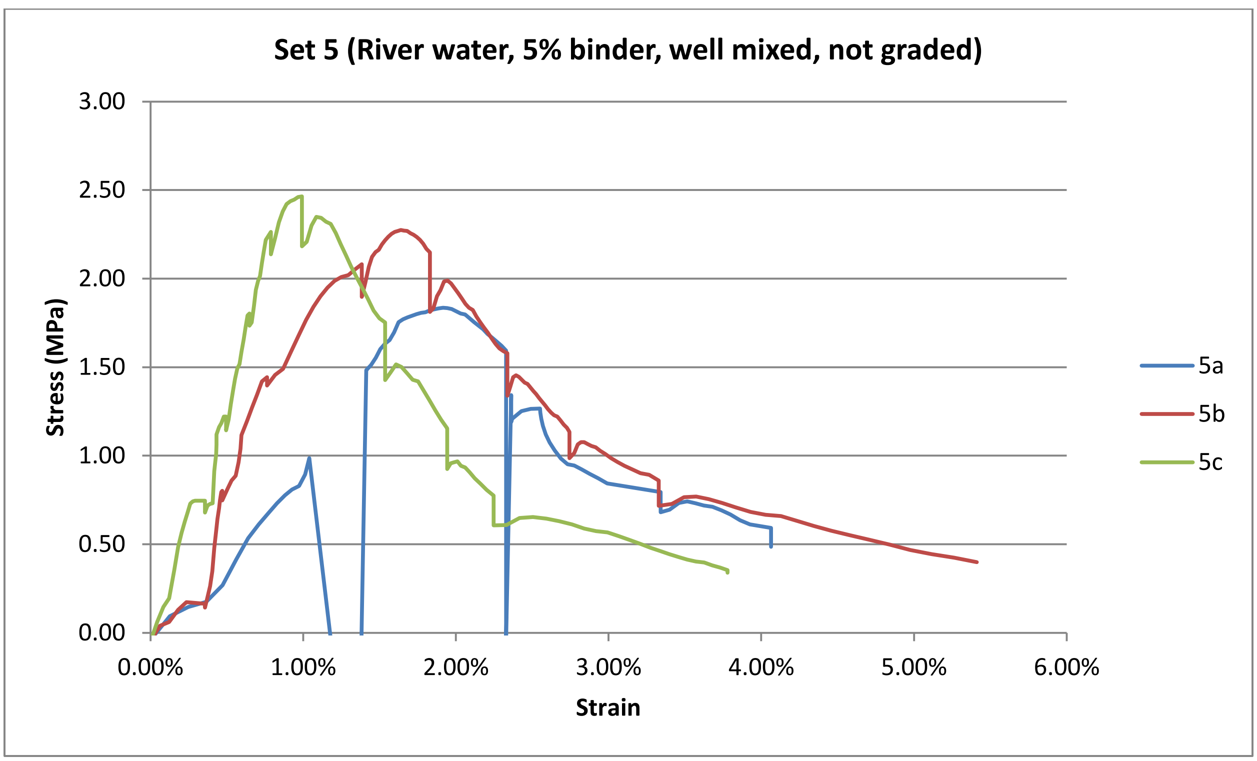

Figure 27: Set 5 stress vs. strain curve

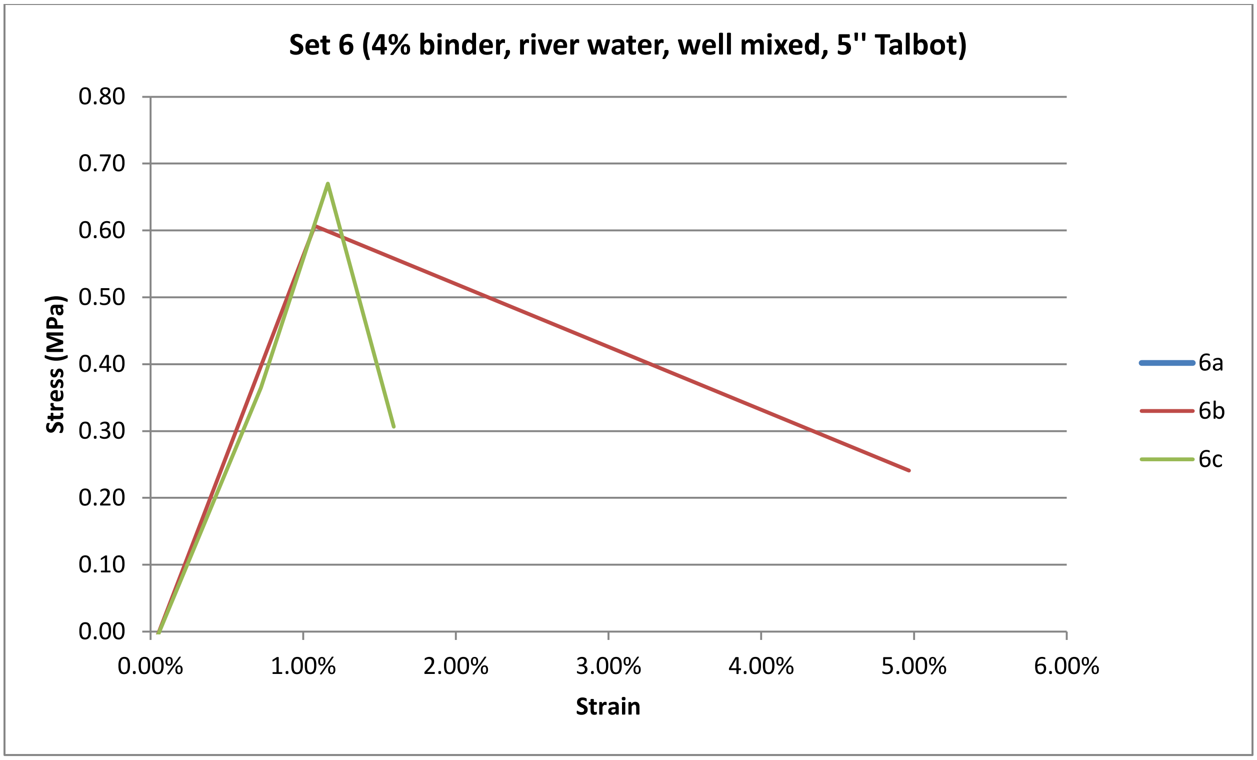

Figure 28: Set 6 Stress vs. strain curve

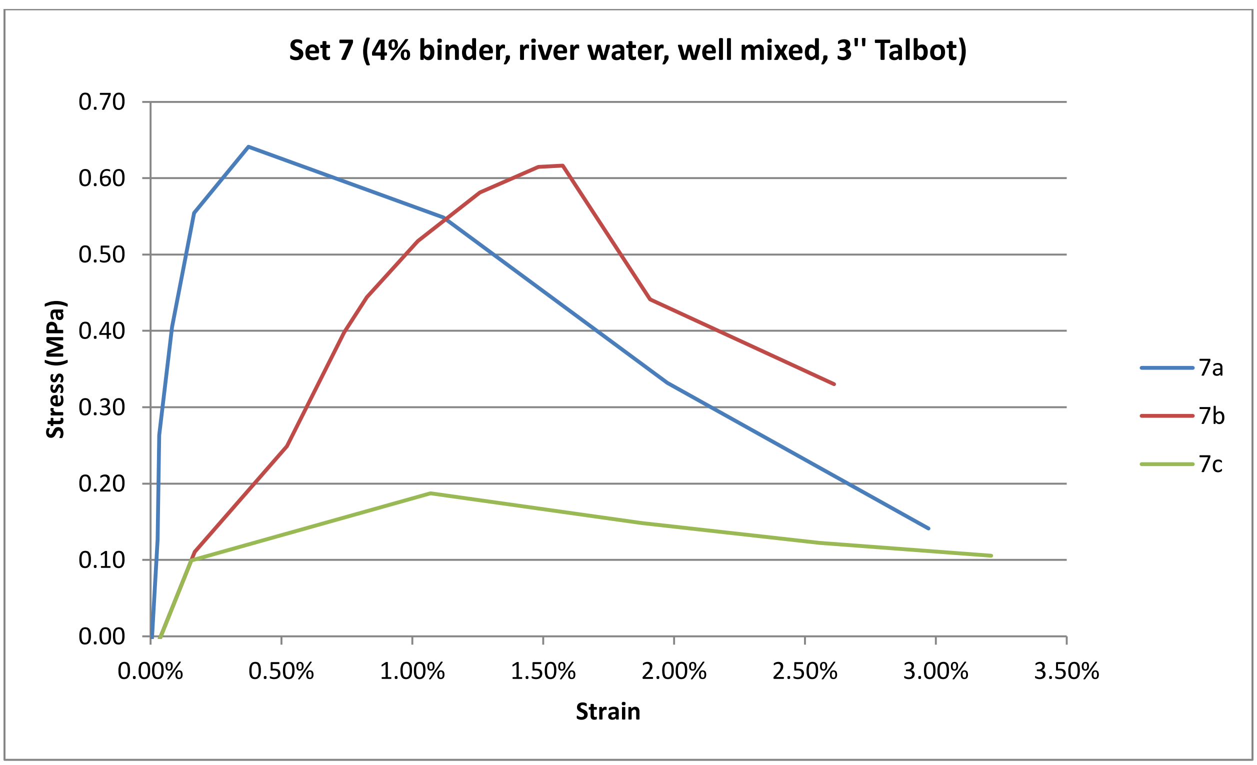

Figure 29: Set 7 Stress vs. strain curve

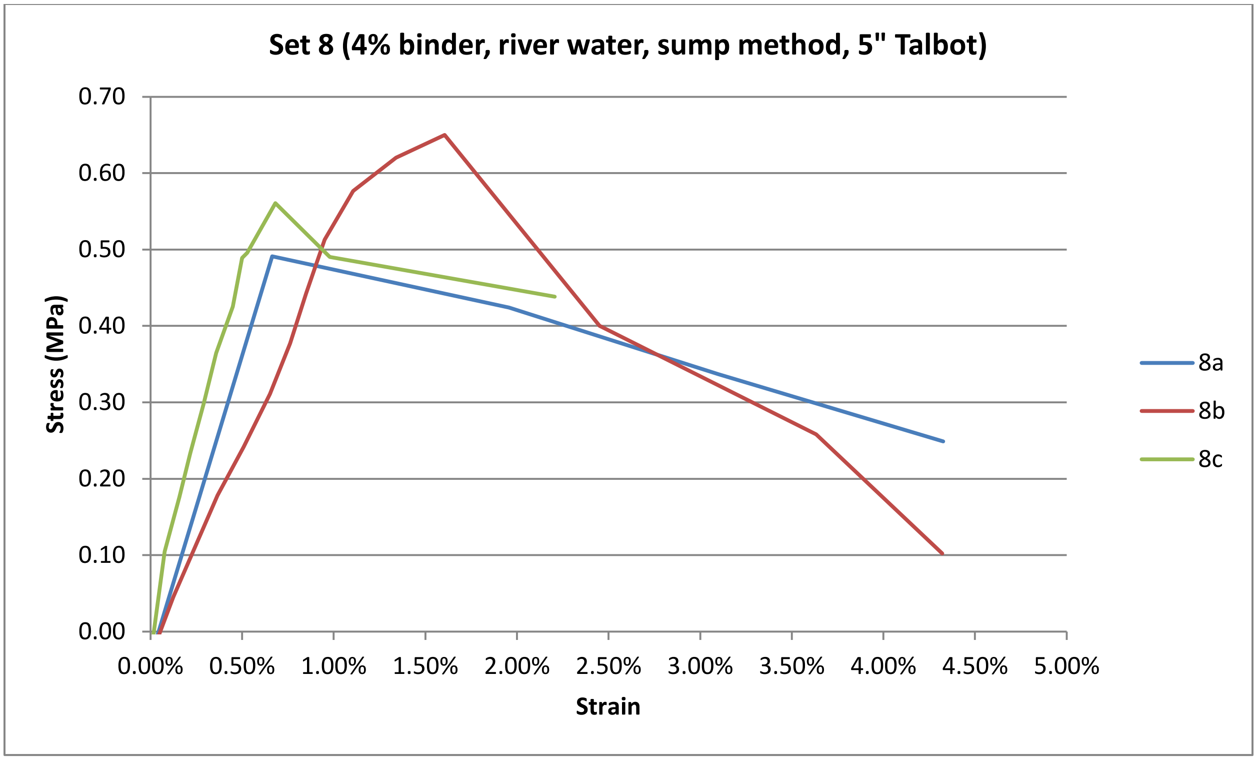

Figure 30: Set 8 Stress vs. strain curve

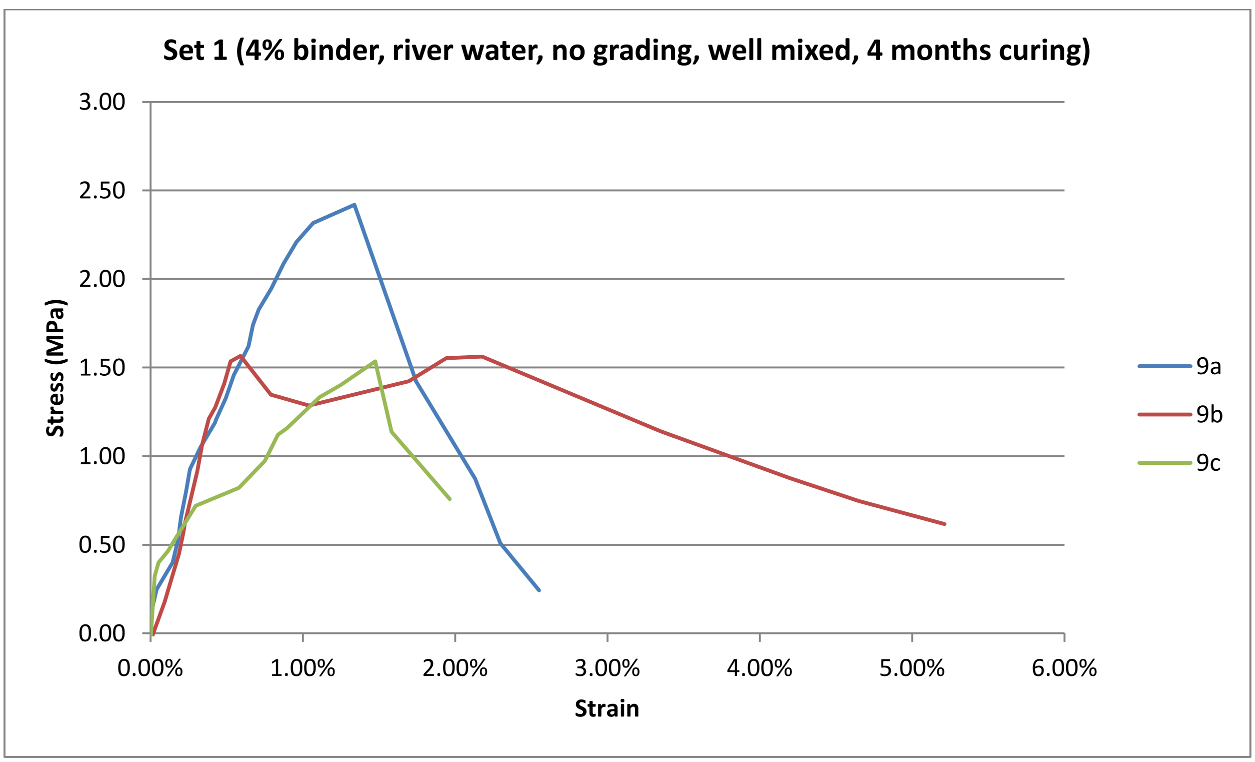

Figure 31: Set 1 Stress vs. strain curve, 4 months curing

6.3 Modulus of Elasticity

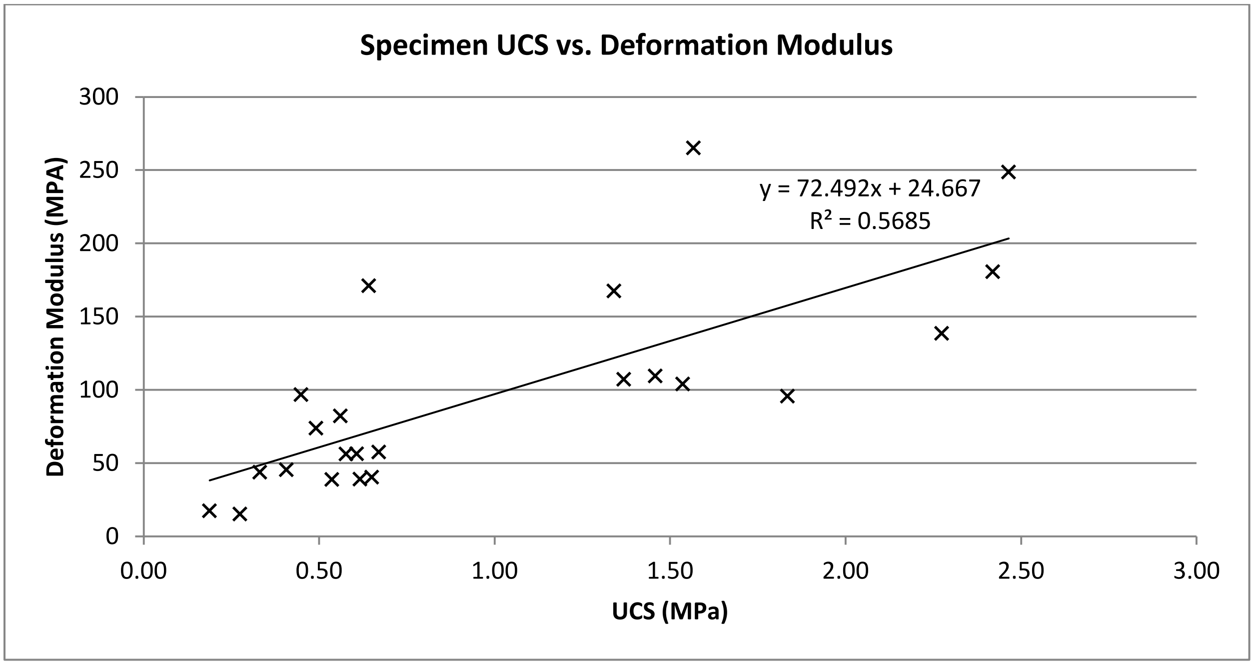

Figure 32: Specimen UCS vs. Deformation Modulus

The modulus of elasticity and the deformation modulus were determined for all specimens. Overall, specimen deformation modulus is weakly correlated with specimen strength (R^2 = 0.57). The correlation between modulus of elasticity and specimen strength is weaker (R^2 = 0.35). Modulus of elasticity and deformation modulus are well correlated (R^2 = 0.87), with the modulus of elasticity on average 30% higher than the deformation modulus.

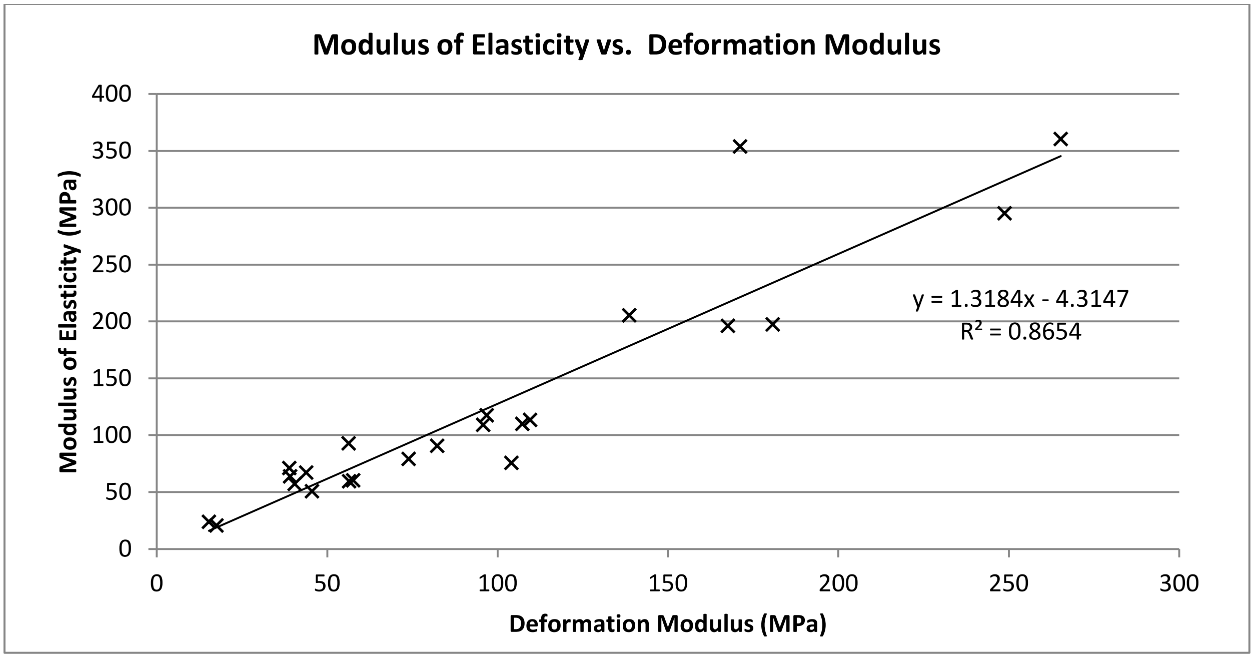

Figure 33: Modulus of Elasticity vs. Deformation Modulus

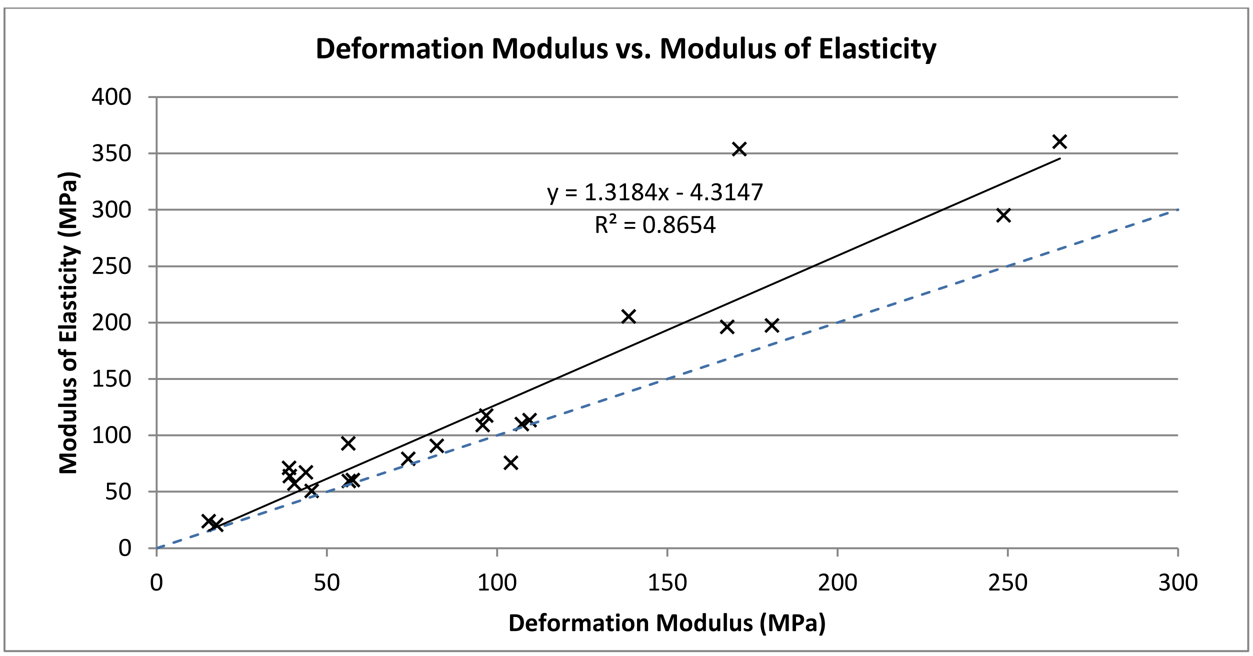

Figure 34: Deformation Modulus vs. Modulus of Elasticity

6.4 Discussion of Results

6.4.1 Specimen Uniformity

Specimen uniformity was not achieved with respect to specimen density and PSD. Specimen density varies between 2.3 and 2.6 t/m^3. The fines content is estimated to range between 18% and 23%. The most variable particle size is the 5″ to 8″ particle size range, which ranges from 6% to 17%.. This limits the conclusions of the experiment to direct comparisons between sets. Also, there are too few specimens to establish any statistical relationships between density and strength.

Uniformity was achieved with respect to the total amount of water in the specimens. Aggregate moisture was monitored and the water to cement ratio of the slurry adjusted. The exception is set 7 which required more water to obtain good mixing of the aggregate and cement slurry. All specimens were left to cure for 14 days under in-situ conditions. All abnormal sets with respect to mixing quality, curing time, and water content were discarded.

6.4.2 Curing Time

The target curing time for all specimens is two weeks. However, full specimen strength not attained after two weeks. High specimen curing time is due to multiple factors such as flyash in the binder and a high water to cement ratio. The effect of flyash is described in a study from Kidd creek mine[4]. The results obtained at Kidd creek mine are as follows:

- 100% OPC mix attains full strength in 28 days
- 50:50 mix of OPC:PFA attains full strength in 73 days

In this experiment, the average UCS obtained after 14 days of curing is 1.26MPa. After 132 days, the average specimen UCS for specimens of comparable weight is 1.60MPa. However, with only 2 data points, it is not possible to determine at which time full strength is attained.

6.4.3 Specimen Density

Specimen weight is obtained for all specimens. Specimen weight variation has two causes

1. Quality of tight fill at the CRF/tube interface
2. Density of the fill

The density of the fill is affected primarily by the particle size distribution of the aggregate. To evaluate the obtained density, the specimens prepared are sorted in two categories: graded (3″ Talbot and 5″ Talbot) and ungraded. In general, the obtained densities for graded specimens are lower than for the ungraded specimens. Also, the ungraded specimens have more density variation due to an uncontrolled particle size. Nonetheless, the number of specimens is too small to draw a significant conclusion on the effect of particle size on the specimen density.

Specimen UCS is theoretically linearly proportional to specimen density. The specimen UCS is plot against the specimen density below. However, due to the small number of specimens per set, it is not possible to draw any conclusions on the effect of density on the specimen UCS.

The quality of tight fill does not affect the density of the CRF but rather the cross-sectional area of the specimen. The quality of the tight fill at the CRF-tube interface is not monitored quantitatively in the experiment. The effect of the density of the fill and the effect of the quality of the tight filling on the specimen weight are therefore indistinguishable.

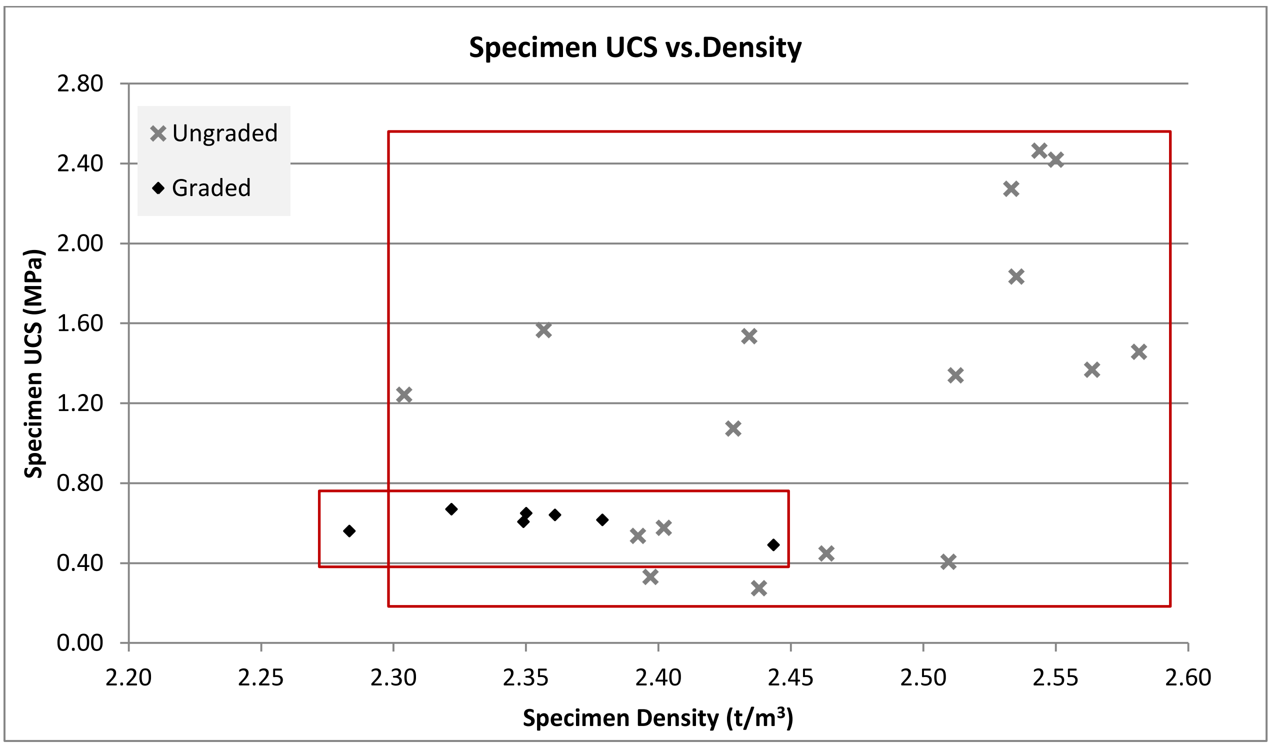

Figure 35: Specimen weight vs. UCS for all specimens

6.4.4 Grading

Good grading increases CRF strength in two ways:

1. Increases contact area between particles
2. Decreases voids, decreasing the wasted cement that pools in voids.

The experiment compares the results obtained with 3″ Talbot graded aggregate, 5″ Talbot graded aggregate, and ungraded aggregate. The ungraded specimens have a grading that ranges between 5″ Talbot grading and 8″ Talbot grading. Overall, the 3″ Talbot graded specimens and 5″ Talbot graded specimens obtained lower strength than the ungraded specimens.

Again, due to the small number of specimens per set, and due to the wide variation of specimen densities, it is not possible to conclude that the low UCS of the graded specimens is due to low specimen density as opposed to the ungraded specimens.

However, it is documented that aggregate fines content has a large effect on CRF strength [7]. From the same study, the optimal fines content set at Birchtree mine is 25-40%. The ungraded specimens contained on average 19% fines as opposed to the 5″ Talbot specimens which contained 27% fines and the 3″ Talbot specimens which contained 35% fines.

High fines reduces strength in two ways: directly as a consequence of the coarser particles being saturated in a sand-cement matrix, and indirectly due to the requirement of a higher w:c ratio in the slurry to obtain good mixing. The second phenomenon was directly observed during the preparation of specimens in set 7 where the overall water to cement ratio of the set was increased to 2.8-3.0 from 2.4. Also, the 5″ Talbot graded specimens are stronger than the 3″ Talbot graded specimens. 5″ Talbot graded specimens have a lower fines content, and consequently a lower w:c to obtain good mixing.

Finally, set 8 obtained close results to set 6. Both of these sets had a 5″ Talbot grading, while set 8 was mixed with the sump method and set 6 with the bucket method. Probable explanations for this are again high fines content leading to high w:c as well as low cement content in the fines. The cementation strength obtained with set 6 is much too low and not optimal.

6.4.5 Water to cement ratio

Two factors affect specimen w:c. These are slurry w:c, which is a controlled factor, and aggregate moisture, which needs to be monitored. In this experiment, the slurry w:c was adjusted to obtain complete coating of the aggregate for the well mixed specimens. With the added moisture from the aggregate, the specimen water to cement ratio obtained for most specimens ranges between 2.1 and 2.4. These values are relatively high with respect to industry standards as seen in Nevada mines for example [3]. While good mixing is obtained, high water to cement ratio lead to lower cementation strength [3]. Overall, poor UCS values obtained by all specimens with respect to other studies [3, 7] are in part due to high specimen w:c.

Specimens with abnormal water to cement ratios are specimens from set 5 and specimen 6a. Specimens from set 5 have a lower overall water to cement ratio due to higher binder content. In this case, the moisture in the aggregate had less effect on the specimen w:c. Specimen 6a, with a specimen w:c of 1.6, was prepared with a lower slurry w:c than set 6b and 6c. This specimen obtained poor mixing and consequently a low UCS.

The optimal value for w:c, which balances mixing and cementation strength, is not determined by this experiment. To determine optimal water content, the aggregate PSD and aggregate moisture content need to be controlled. However, an upper bound for specimen w:c is determined to be at 2.4.

6.4.6 Water quality

Using sump water as opposed to river water is expected to reduce strength due to the presence of dissolved solids, oil, grease, water treatment chemicals, diesel fuel, and nitrates in the water [3, 4]. However, the results for set 2 are inconclusive with respect to set 1 due to specimen weight as a muddling factor. However, even with conclusive results, assuming a reduced strength, it is difficult to determine the cause of the reduced strength without controlling the quality of the sump water during the tests. Testing of the water prior to addition in the CRF specimens is required.

6.4.7 Specimen size

Results for large scale specimens are generally accepted as representative in-situ conditions [5]. All specimens in the testing program were of the same dimensions (Φ 15.75″- 16.5″, h 30″) and therefore assumed representative of in situ conditions.

However, this assumption is not verified within the experiment.. From the literature, various scaling factors have been proposed for converting laboratory results to in-situ properties for intact rock [15]. However, very little work has been done on scaling effects in regards to mine backfills. From a study conducted at Que river mine [16], the strength of the large scale specimens (45cm) was approximately 60% of the laboratory strength of scaled-down gravel. On the other hand, Stone proposes a factor of about 0.65 to convert standard-test results of small scale specimens to in-situ [5].

6.4.8 Mixing

Specimens prepared with sump method have higher strength than specimens prepared with the bucket method. Both of these mixing methods obtained lower results than the well mixed specimens by a factor of 2. Sump method and bucket method specimens both showed poor distribution of cement during placement in the cylinder, leading to uncemented fines and therefore low specimen strength.

Poor mixing due to high fines (27%) was observed with set 6. The water to cement ratio was therefore adjusted for specimens 6b and 6c. For set 7, high fines content (35%) also led to poor mixing, and the water to cement ratio was again adjusted for specimens 7b and 7c. These two sets were well mixed. However, some fines remained uncoated even with a very high slurry volume.

Set 8 was mixed with the sump method and obtained similar results to set 6, which was well mixed. In this case, due to a high fines content (27%), good mixing required a slurry w:c of 1.2. The comparison between these two sets raises multiple points with regards to the specimens. First off, the slurry volume is equal in both sets, yet properly mixing the slurry with the aggregate did not noticeably increase strength. This indicates that the specimen formula used for specimen 7 and 8 is poor, due to a combination of excess fines and excess water. Another possibility is that while set 6 was “well mixed”, there remained uncoated fines which may have reduced the plane of weakness of the specimens to the same strength as the poorly mixed specimens.

6.4.9 Binder Content

Specimen strength is doubled with the addition of 1% binder content. However, the strongest two way interaction for CRF strength is between fines content and binder content [7]; an incremental addition of cement has a higher effect on UCS if fines content is high rather than low. Fines content therefore needs to be a controlled parameter when examining effect of binder content for the purpose of cement binder content optimization. Swan’s Binder number can also be applied for cement content optimization if the PSD of the specimen is controlled [13].

6.4.10 Slurry Mixing

A drum mixer was used to mix the binder slurry. Binder and water were left to mix for at least 5 minutes before being added into the specimens. However, Birchtree mine employs colloidal mixers which produce a more consistent and uniform product than paddle mixers [24]. Also, grout samples mixed with a colloidal mixer have an average strength increase of 10MPa over a paddle mixer depending on grout density [24]. Practical benefits which apply to CRF strength are less slurry bleed when stationary, uniform slurry permeation in pores, and an immiscible slurry leading to less washout from groundwater [24].

Initially, use of slurry as-is from the flash mixer on level 2750 was planned. However, obtaining dry binder and storing it at the lab was simpler. Nonetheless, the exercise should be done for at least 1 set as binder settlement was observed in the drum mixer during set preparation. The effect of binder slurry mixing quality could then be taken into account.

6.5 Experiment Conclusions

Overall, low specimen UCS was obtained for all specimens relative to the literature. However, all specimens were larger scale and with high water to cement ratio, both factors reducing specimen UCS. Conclusions for each set are as follows:

- Set 1: High long term strength (4 months) over 14 days strength (causes: flyash, high water content)
- Set 2: Mine water test results are inconclusive
- Set 3 and 4: Sump method significantly increases strength over bucket method
- Set 5: 90% strength increase with increase in binder from 4% to 5%.
- Set 6 and 7: 5″ Talbot obtained better results than 3″ Talbot. Poor strength for both sets.
- Set 8: 5″ Talbot sump method obtained similar results than well mixed 5″ Talbot, suggesting excess fines in 5″ Talbot, causing poor mixing as well as poor cohesion

6.6 Evaluation of Experiment

Specimen uniformity was not achieved with respect to specimen density and PSD. One ton of aggregate was sampled for PSD analysis during specimen preparation to obtain an average PSD for the ungraded specimens. A random Monte-Carlo analysis was conducted to estimate the PSD variation of the specimens based on the PSD variation of the 100lb batches. The fines content is estimated to range between 18% and 23%. The most variable particle size is the 5″ to 8″ particle size range, which ranges from 6% to 17%. This variation is problematic as CRF strength is sensitive to fines content. For example, a 5% addition of sand from 25% fines was observed to reduce CRF strength by 66% [4].

Due to specimen density and PSD as muddling factors, the investigation on water quality is inconclusive. This can be remedied with more rigorous sampling of the aggregate pile. However, specimen preparation is already time consuming and the rehandling required would have been impossible with the available equipment. A partial solution is to completely eliminate aggregate over 5″ in the specimens, as this was the particle with the most variation between specimens.

Scale effect for the specimens mixed with the sump method and the bucket method also need to be examined. Conclusive results were obtained from the poorly mixed sets with respect to the base case specimens. However, there are no recent in-situ observations of the actual mixing quality at the stope itself. Comparison between the mixing quality of the specimens and the actual mixing quality at the stope is crucial. Also, segregation of the fill was not simulated.

Specimen uniformity was achieved with respect total water content in the specimens. However, the water to cement ratio of the binder slurry was adjusted with respect to the mine practice to obtain good mixing. Since the exact aggregate moisture content at the time of sampling and its variation over time is unknown (estimated at 5%), total water content for the mine practice can only be estimated at this stage. However, small samples of aggregate taken from the sampled aggregate pile agree with the estimate.

Chapter 7

Conclusion

7.1 Laboratory Setup

A permanent laboratory was set up in a cross drift off the ramp on level 2750. The laboratory is suitable for the conduct of custom tests.

7.2 Experiment Results

So far, 27 specimens were prepared. The following conclusions were drawn from the results:

- Birchtree CRF has a long curing time to attain full strength. CRF with 4 months curing has a 60% increase in strength over CRF with 2 weeks curing.
- Sump method and bucket method for mixing the slurry and CRF both reduce strength. However, the sump method produces stronger CRF than the bucket method.
- Increasing binder content from 4% to 5% increases CRF strength by 90%
- Excess fines were observed for the specimens graded to match 3″ and 5″ Talbot curves (27% and 33% fines). These specimens have greatly reduced strength.
- Poor mixing did not reduce strength for specimens with excess fines.

However, the water quality tests were inconclusive due to varying specimen density.

7.3 Recommendations for Mine Practice

From the tests results, it is recommended that the sump method be used to mix the aggregate over the bucket method, as there is a significant increase in CRF strength. However, both methods still greatly reduce CRF strength compared to the manually mixed specimens. Based on the tests, completely mixing the CRF, with for example a drum mixer, can up to double the strength of the in-situ CRF. However, since the fill strength requirements are met, the expense is not necessary. Alternate solutions to obtain better mixing are the use of a baffled plate.

In addition, it is recommended that aggregate moisture be monitored as it was observed during the experiment that mixing quality is extremely sensitive to aggregate moisture, especially when the specimen had high fines. It was observed the mine practice (a water to cement ratio of 0.56) yielded poor mixing due to insufficient slurry volume and was adjusted to 0.7 for the experiment. Since the aggregate moisture at the raise during the time of sampling is unknown, no other conclusion can be drawn.

Finally, it is recommended that the optimal fines content be determined based on large scale specimens to compare with previous studies. A previous study at Birchtree set the target fines to 25-40%. However, from the large scale experiment, a 5% increase in fines content from the as-is aggregate (19% fines) greatly reduced strength. Based on the experiment results, a fines content of 40% is excessive. The fines content added in the CRF should also be controlled.

7.4 Experiment Shortcomings

Specimen density was monitored but not controlled. A cause for density variation is uncontrolled PSD for the ungraded specimens. However, graded specimens also showed density variation which means that packing of the aggregate also varied between specimens. In addition, voids at the CRF/Sonotube interface were also observed leading to non quantified variation in specimen volume. The variation of PSD can be tackled in two ways. The first is quarter the aggregate pile to create uniform batches. However, this is very time consuming to achieve manually due to the amount of aggregate to be handled. The second solution is to combine graded aggregate, as done for the 3″ Talbot and 5″ Talbot specimens. However, this solution is also time consuming, and amounts to rehandling aggregate which could have served to prepare more specimens.

7.5 Recommendations for Future Testing

The following recommendations were given for future testing at Birchtree Mine:

- Test 8″ Talbot
- Optimise fines content
- Optimise w:c ratio
- Examine effect of scale (5″, 10″, 15″)
- Test Curing time (7 days, 14 days, 28 days, 56 days)
- Test slurry mixing quality

7.6 Recommendations for Future Experimental Procedure

The procedure had shortcomings which can be addressed:

- More controlled parameters specimens using mine effluent water. For example, controlling PSD by combining graded aggregate)
- Sample mine effluent water used for tests to determine concentration of substances that can reduce CRF strength, as the quality of the mine effluent water may not be uniform over time and over the mine levels.
- Sets of 4 in order to reduce impact of outliers on available data, and reduce impact of variation of specimen density
- If possible, sample aggregate for ungraded specimens with quartering.
- Use binder slurry as-is from the mine level.

7.7 Statement of Contribution

This study simulates in-situ CRF through the use of large scale specimens, the use of aggregate, binder, and mine water as-is from the mine level, and through specimen preparation and curing in the underground environment.

References

1. Annor, A.B., *A Study of the Characteristics and Behaviour of Composite Backfill Material*, in *Department of Mining and Metallugical Engineering*1999, McGill University: Montreal.

2. Aitchison, G.D., M. Kurzeme, and D.R. Willoughb. *Geomechanics considerations in optimising the use of mine fill, Part A: The investigation of the response of fill as a structural component*. in *Jubiliee Symposium on Mine Filling*. 1973. Mount Isa: The Australasian Institute of Mining and Metallurgy: North West Queensland Branch.

3. Stone, D.M.R., *Factors that Affect Cemented Rockfill Quality in Nevada Mines*, in *Minefill 2007*2007: Montreal.

4. Yu, T.R., *Some factors relating to the stability of consolidated rockfill at Kidd Creek*, in *Innovations in Mining Backfill Technology*, F.P. Hassani, M.J. Scoble, and T.R. Yu, Editors. 1989, Baklema: Rotterdam.

5. Stone, D.M.R., *The Optimization of Mix Designs for Cemented Rockfill*, in *Minefill '93*1993, SAIMM: Johannesburg.

6. Farsangi, P.N., *Improving Cemented Rockfill Design in Open Stoping*, in *Department of Mining and Metallurgical Engineering*1996, McGill University: Montreal.

7. Peterson, S., J. Szymanski, and S. Planeta, *A Statisitcal Model for Strength Estimation of Cemented Rockfill in Vertical Block Mining*, in *Minefill '98*1998, The Australasian Institute of Mining and Metallurgy: Brisbane.

8. Peterson, S., J. Szymanski, and S. Planeta, *Cemented Rockfill Optimisation - The Rock Attrition Model and Fill Raise Orientation Effect*, in *Minefill '98*1998, The Australasian Institute of Mining and Metallurgy: Brisbane.

9. Reschke, A.E. *The use of cemented rockfill at Namew Lake Mine, Manitoba, Canada*. in *Minefill '93*. 1993. Johannesburg: SAIMM.

10. Chen, D., M.l. Messurier, and B. Mitchell. *Application of Cemented Fill at Barrick's Darlot Gold Mine*. in *The 8th International Symposium on Mining with Backfill*. 2004. Beijing: The Nonferrous Metal Society of China.

11. Bloss, M.L., R. Cowling, and J.L. Meek, *A Procedure for the Design of Stable Cemented Fill Exposures*, in *Minefill '93*1993, SAIMM: Johannesburg.

12. Talbot, A.N. and E.D. Richart, *The Strength of Concrete and its Relation to the Cement, Aggregate, and Water*, in *University of Illinois. Engineering Experiment Station. Bulletin ; no. 137* 1923.

13. Bloss, M.L., *Prediction of Cemented Rock Fill Stability - Design Procedures and Modelling Techniques*, in *Department of Mining and Metallurgical Engineering*1992, University of Queensland: Brisbane.

14. Hoek, E. and M.S. Diederichs, *Empirical estimation of rock mass modulus.* International Journal of Rock Mechanics and Mining Sciences, 2005. **43**: p. 203-215.

15. Hoek, E. and E.T. Brown, *Underground Excavations in Rock*, ed. I.M. Metall.1980, London: Chapman & Hall.

16. Barrett, J.R., J.E. Stewart, and J.G. Brock, *Cemented gravel fill for a small underground mine*, in *International Symposium on Mining with Backfill*1983: Lulea.

17. Peredery, W.V., *Thompson Ni-Sulphides, Manitoba*, in *Precambrian Sulphide Deposits*, R.W. Hutchison, C.D. Spence, and J.M. Franklin, Editors. 1982, The Geological Association of Canada. p. 165-209.

18. Eckstrand, O.R. and L.J. Hulbert, *Mineral deposits of Canada: a synthesis of major deposit-types, district metallogeny, the evolution of geological provinces, and exploration methods*, W.D. Goodfellow, Editor 2007, Geological Association of Canada, Mineral Deposits Division St. John's, NL, Canada. p. 205-222.

19. Emad, M.Z., et al. *Backfill practices for sublevel stoping system*. in *Mine Planning and Equipment Selection*. 2013. Dresden: Springer International Publishing, Switzerland.

20. Simplex. *Steel Cylinders*. 2013 14/05/2013]; Available from: http://www.tksimplex.com/customfiles/RLN30_1000.pdf.

21. DSI. *DYWIDAG Threadbar Technical Data*. 2011 14/05/2013]; Available from: http://www.dsicanada.ca/uploads/media/DSI-Canada_DYWIDAG-THREADBAR-Imperial-Units_ca_01.pdf.

22. BUAU. *4340 High Tensile Steel*. 2013 14/05/2013]; Available from: http://www.buau.com.au/media/4340.pdf.

23. Simplex. *RLR2002*. 2008 14/05/2013]; Available from: http://www.tksimplex.com/html/product_detail.php?pid=246&catname=Hydraulic Steel Cylinders&scatname=Load Return (RLR Series).

24. Reschke, A.E. *The development of colloidal mixer based CRF systems*. in *Minefill '98*. 1998. Brisbane: The Australian Institute of Mining and Metallurgy.

Appendix I – UCS Rig Components

DYWIDAG THREADBAR® - TECHNICAL DATA [IMPERIAL UNITS]

May 16, 2011

Steel Grade f_y / f_u ksi	Nominal Bar Diameter in	in	Steel Area A_s in²	Yield Load $P_y = f_yA_s$ kips	Ult. Load $P_u = f_uA_s$ kips	Nominal Wt. lbs/ft	Max. Bar Ø Across Ribs in	Mill length ft	Direction of Thread L or R
130/160 ksi Hot-Rolled THREADBAR®	5/8	5/8"	0.27	35.7	**43.6**	0.99	0.693	19.3	R
Form-Ties, Post-Tensioning, Ground Anchors	3/4	3/4"	0.49	63.4	**77.5**	1.74	0.900	39	R
120/150 ksi **ASTM A722** except 3" Ø	1	1"	0.85	102.0	**127.5**	3.01	1.201	60	R
	1 1/4	1 1/4"	1.25	150.0	**187.5**	4.39	1.457	60	R
Hot-Rolled THREADBAR®	1 3/8	1 3/8"	1.58	189.6	**237.0**	5.56	1.630	60	R
PT Ground Anchors	*1 3/4	1 3/4"	2.58	320.0	**400.0**	9.22	2.009	45	R
Post-Tensioning	*2 1/2	2 1/2"	5.16	619.2	**774.0**	18.20	2.790	45	R
*Cold-Rolled THREADBAR®	*3	3"	6.85	822.0	**1027.0**	24.10	3.150	45	R
75/100 ksi **CSA G30.18** **ASTM A615** except #20, #24, #28	3/4	#6	0.44	**33.0**	44.0	1.50	0.862	48	L
	7/8	#7	0.60	**45.0**	60.0	2.04	0.996	60	L
	1	#8	0.79	**59.3**	79.0	2.67	1.122	60	L
Hot-Rolled THREADBAR®	1 1/8	#9	1.00	**75.0**	100.0	3.40	1.268	60	L
Tie Rods, Hanging Rods	1 1/4	#10	1.27	**95.3**	127.0	4.30	1.433	60	L
Micropiles (*GEWI*® Piles), Anchor Bolts	1 3/8	#11	1.56	**117.0**	156.0	5.31	1.614	60	L
Concrete Reinforcing, Seismic Anchors	1 3/4	#14	2.25	**168.8**	225.0	7.65	1.862	60	R
Rock Bolts, Ground Anchors	2 1/4	#18	4.00	**300.0**	400.0	13.60	2.504	60	R
Soil Nailing, Precast Connections	** 2 1/2	#20	4.91	**393.0**	520.0	16.70	2.717	60	L
****80/106 ksi**	*3	#24	7.06	**529.5**	706.0	24.09	3.181	45	L
***Cold-Rolled THREADBAR®**	*3 1/2	#28	9.62	**721.5**	962.0	32.79	3.681	45	L
DYWI® Drill Hollow Bar **CSA G30.18**	**R25N**	13mm Ave core	0.45	**34**	45	1.56	1.00	9.8	L
73 ksi min. Yield Stress **ASTM A615**	**R32N**	18mm Ave core	0.67	**52**	63	2.28	1.25	9.8	L
Soil Nails	**T30/11**	11mm Ave core	0.73	**58**	72	2.48	1.18	9.8	L
Micropiles, Ground Anchors	**R32S**	11mm Ave core	0.81	**63**	81	2.76	1.25	9.8	L
Bars & hardware available in Hot Dip Galvanized or Metalized	**R38N**	17mm Ave core	1.19	**90**	112	4.1	1.50	9.8	L
Temporary Drill Casing not required	**R51L**	35mm Ave core	1.38	**101**	124	4.70	2.00	9.8	L
	T40/16	16mm Ave core	1.41	**118**	148	4.77	1.58	9.8	L
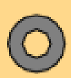	**R51N**	28mm Ave core	1.66	**142**	180	5.64	2.00	9.8	L
R = Rope Threads	**T76N**	45mm Ave core	3.29	**270**	360	11.20	3.00	9.8	L
T = Trapezoidal Threads	**T76S**	35mm Ave core	4.26	**337**	427	14.80	3.00	9.8	L

Approximate Modulus of Elasticity: E=29,700 ksi

Double Corrosion Protection (DCP) recommended for post-tensioned permanent ground anchors

Figure 36: 1 3/4″ threadbar properties [21]

Model	Cap. (tons)	Stroke (in)	Oil Cap. Required (cu.in.)	Ram Bore Diameter (in)	Effect Area (sq.in.)	Pressure @ Cap. (psi)	A Minimum Height (in)	B Extended Height (in)	C Body O.D. (in)	D Piston O.D. (in)	E Base to Port C/L (in)	Wgt. (lbs)
RLN302	30	2	13	2.87	6.49	9,240	6.38	8.38	4	2.44	.75	21
RLN306	30	6	38.9	2.87	6.49	9,240	10.38	16.38	4	2.44	.75	35
RLN502	50	2	22.1	3.75	11.05	9,054	6.75	8.75	5	3.19	.78	38
RLN506	50	6	66.2	3.75	11.05	9,054	10.75	16.75	5	3.19	.78	63
RLN5010	50	10	133	3.75	11.05	9,054	14.75	24.75	5	3.19	.78	100
RLN1002	100	2	40	5	19.63	10,200	8	10	6.38	4.31	1.25	87
RLN1006	100	6	118	5	19.63	10,200	12	18	6.38	4.31	1.25	132
RLN10010	100	10	196	5	19.63	10,200	16	26	6.38	4.31	1.25	202
RLN1502	150	2	66.4	6.25	30.68	9,780	8	10	8.5	5.56	1.93	149
RLN1506	150	6	199	6.25	30.68	9,780	12.25	18	8.5	5.56	1.93	221
RLN15012	150	12	398	6.25	30.68	9,780	18	30	8.5	5.56	1.93	311
RLN2002	200	2	88.4	7.25	41.28	9,054	9.5	11.5	10	6.56	2.06	233
RLN2006	200	6	265	7.25	41.28	9,054	13.5	19.5	10	6.56	2.06	332
RLN20012	200	12	530	7.25	41.28	9,054	19.5	31.5	10	6.56	2.06	479
RLN3002	300	2	120	8.75	60.13	9,978	11.5	13.5	12	7.81	2.44	357
RLN3006	300	6	361	8.75	60.13	9,978	15.5	21.5	12	7.81	2.44	485
RLN30012	300	12	722	8.75	60.13	9,978	21.5	33.5	12	7.81	2.44	677
RLN4002	400	2	174	10.5	86.59	9,238	13.81	15.81	14	9.31	3	520
RLN4006	400	6	520	10.5	86.59	9,238	17.81	23.81	14	9.31	3	675
RLN40012	400	12	1040	10.5	86.59	9,238	23.81	25.81	14	9.31	3	905
RLN5002	500	2	208	11.5	103.87	9,628	14.75	16.75	16	10.31	3.19	927
RLN5006	500	6	623	11.5	103.87	9,628	18.75	24.75	16	10.31	3.19	1041
RLN50012	500	12	1246	11.5	103.87	9,628	24.75	36.75	16	10.31	3.19	1383
RLN6002	600	2	246	12.5	122.79	9,778	15.62	17.62	17.5	11.31	3.5	985
RLN6006	600	6	738	12.5	122.79	9,778	19.62	25.62	17.5	11.31	3.5	1232
RLN60012	600	12	1476	12.5	122.79	9,778	27.62	39.62	17.5	11.31	3.5	1603
RLN8002	800	2	330	14.5	165.13	9,690	16.93	18.93	18	13.31	4.13	1148
RLN8006	800	6	991	14.5	165.13	9,690	21.93	27.93	18	13.31	4.13	1407
RLN80012	800	12	1982	14.5	165.13	9,690	27.93	39.93	18	13.31	4.13	1795
RLN10002	1000	2	402	16	201.06	9,950	19.62	21.62	21	14.81	4.25	1818
RLN10006	1000	6	1206	16	201.06	9,950	23.62	29.62	21	14.81	4.25	2178
RLN100012	1000	12	2412	16	201.06	9,950	29.62	41.62	21	14.81	4.25	2718

Figure 37: Hydraulic cylinder specifications [20]

Appendix II – Specimen Moisture and PSD

Table 10: Specimen 1-5 PSD Data

Batch	Screen	Weight Total (lb)*	Weight Sieve (lb)	Weight Aggregate retained (lb)	Batch Weight (lb)	Batch% retained
1	10	9	0	9	114	7.9%
1	5	25	15	10	114	8.8%
1	3	39	15	24	114	21.1%
1	1.5	44	16	28	114	24.6%
1	0.75	34	15.5	18.5	114	16.2%
1	0.375	38	13.5	24.5	114	21.5%
2	10	39	0	39	195	20.0%
2	5	40	15	25	195	12.8%
2	3	46	15	31	195	15.9%
2	1.5	55	16	39	195	20.0%
2	0.75	41	15.5	25.5	195	13.1%
2	0.375	49	13.5	35.5	195	18.2%
3	10	39	0	39	190	20.5%
3	5	32	15	17	190	8.9%
3	3	57	15	42	190	22.1%
3	1.5	50	16	34	190	17.9%
3	0.75	40	15.5	24.5	190	12.9%
3	0.375	47	13.5	33.5	190	17.6%
4	10	0	0	0	51	0.0%
4	5	0	15	0	51	0.0%
4	3	28	15	13	51	25.5%
4	1.5	27	16	11	51	21.6%
4	0.75	25	15.5	9.5	51	18.6%
4	0.375	31	13.5	17.5	51	34.3%
5	10	9	0	9	137	6.6%
5	5	52	15	37	137	27.0%
5	3	33	15	18	137	13.1%
5	1.5	40	16	24	137	17.5%
5	0.75	32	15.5	16.5	137	12.0%
5	0.375	46	13.5	32.5	137	23.7%

*1lb = 0.454kg

Batch	Screen	Weight Total (lb)*	Weight Sieve (lb)	Weight Aggregate retained (lb)	Batch Weight (lb)	Batch% retained
6	10	8	0	8	84	9.5%
6	5	29	15	14	84	16.7%
6	3	32	15	17	84	20.2%
6	1.5	34	16	18	84	21.4%
6	0.75	25	15.5	9.5	84	11.3%
6	0.375	31	13.5	17.5	84	20.8%
7	10	12	0	12	119	10.1%
7	5	37	15	22	119	18.5%
7	3	43	15	28	119	23.5%
7	1.5	37	16	21	119	17.6%
7	0.75	29	15.5	13.5	119	11.3%
7	0.375	36	13.5	22.5	119	18.9%
8	10	0	0	0	113	0.0%
8	5	34	15	19	113	16.8%
8	3	42	15	27	113	23.9%
8	1.5	43	16	27	113	23.9%
8	0.75	31	15.5	15.5	113	13.7%
8	0.375	38	13.5	24.5	113	21.7%
9	10	18	0	18	107	16.8%
9	5	35	15	20	107	18.7%
9	3	36	15	21	107	19.6%
9	1.5	34	16	18	107	16.8%
9	0.75	27	15.5	11.5	107	10.7%
9	0.375	32	13.5	18.5	107	17.3%
10	10	22	0	22	100	22.0%
10	5	41	15	26	100	26.0%
10	3	33	15	18	100	18.0%
10	1.5	28	16	12	100	12.0%
10	0.75	24	15.5	8.5	100	8.5%
10	0.375	27	13.5	13.5	100	13.5%
11	10	0	0	0	98	0.0%
11	5	46	15	31	98	31.6%
11	3	39	15	24	98	24.5%
11	1.5	32	16	16	98	16.3%
11	0.75	26	15.5	10.5	98	10.7%
11	0.375	30	13.5	16.5	98	16.8%

*1lb = 0.454kg

Batch	Screen	Weight Total (lb)	Weight Sieve (lb)	Weight Aggregate retained (lb)	Batch Weight (lb)	Batch% retained
12	10	22	0	22	128	17.2%
12	5	34	15	19	128	14.8%
12	3	40	15	25	128	19.5%
12	1.5	41	16	25	128	19.5%
12	0.75	31	15.5	15.5	128	12.1%
12	0.375	35	13.5	21.5	128	16.8%
13	10	22	0	22	120	18.3%
13	5	37	15	22	120	18.3%
13	3	38	15	23	120	19.2%
13	1.5	36	16	20	120	16.7%
13	0.75	29	15.5	13.5	120	11.3%
13	0.375	33	13.5	19.5	120	16.3%
14	10	0	0	0	100	0.0%
14	5	41	15	26	100	26.0%
14	3	35	15	20	100	20.0%
14	1.5	33	16	17	100	17.0%
14	0.75	32	15.5	16.5	100	16.5%
14	0.375	34	13.5	20.5	100	20.5%
15	10	28	0	28	158	17.7%
15	5	40	15	25	158	15.8%
15	3	44	15	29	158	18.4%
15	1.5	43	16	27	158	17.1%
15	0.75	36	15.5	20.5	158	13.0%
15	0.375	42	13.5	28.5	158	18.0%
16	10	8	0	8	133	6.0%
16	5	44	15	29	133	21.8%
16	3	48	15	33	133	24.8%
16	1.5	40	16	24	133	18.0%
16	0.75	32	15.5	16.5	133	12.4%
16	0.375	36	13.5	22.5	133	16.9%
17	10	10	0	10	124	8.1%
17	5	40	15	25	124	20.2%
17	3	41	15	26	124	21.0%
17	1.5	38	16	22	124	17.7%
17	0.75	33	15.5	17.5	124	14.1%
17	0.375	37	13.5	23.5	124	19.0%

*1lb = 0.454kg

Batch	Screen	Weight Total (lb)*	Weight Sieve (lb)	Weight Aggregate retained (lb)	Batch Weight (lb)	Batch% retained
18	10	22	0	22	125	17.6%
18	5	45	15	30	125	24.0%
18	3	33	15	18	125	14.4%
18	1.5	33	16	17	125	13.6%
18	0.75	32	15.5	16.5	125	13.2%
18	0.375	35	13.5	21.5	125	17.2%

*1lb = 0.454kg

Table 11: Moisture content samples

Date	Sampled From	Size*	Pan (g)	Total (g)	w wet total (g)	Dry total (g)	w dry (g)	w Water (g)	% Water
6/11/2013	TOP	Pan	1652.8	3746.7	2093.9	3586.8	1934.0	159.9	8.27%
6/11/2013	TOP	3/8′′	840.0	4065.6	3225.6	3966.2	3126.2	99.4	3.18%
6/11/2013	TOP	3/4′′	774.3	2978.5	2204.2	2946.6	2172.3	31.9	1.47%
6/11/2013	TOP	3/2′′	1571.8	6027.0	4455.2	6002.0	4430.2	25.0	0.56%
7/11/2013	TOP	Pan	407.4	1632.8	1225.4	1545.7	1138.3	87.1	7.65%
7/11/2013	TOP	3/8′′	440.5	1697.9	1257.4	1669.6	1229.1	28.3	2.30%
7/11/2013	MIDDLE	Pan	439.5	2229.6	1790.1	2100.7	1661.2	128.9	7.76%
7/11/2013	MIDDLE	3/8′′	439.8	2348.7	1908.9	2305.7	1865.9	43.0	2.30%
14/11/2013	6A	Pan	1661.0	3240.6	1579.6	3148.2	1487.2	92.4	6.21%
14/11/2013	6B	Pan	438.1	1979.5	1541.4	1888.4	1450.3	91.1	6.28%
14/11/2013	6B	3/8′′	440.0	1709.2	1269.2	1687.1	1247.1	22.1	1.77%
21/11/2013	7C	Pan	1571.8	2705.8	1134.0	2650.6	1078.8	55.2	5.12%
21/11/2013	7C	3/8′′	926.2	2490.8	1564.6	2469.9	1543.7	20.9	1.35%
21/11/2013	7C	3/4′′	840.3	3010.4	2170.1	2994.1	2153.8	16.3	0.76%
21/11/2013	7C	3/2′′	774.5	5891.0	5116.5	5875.0	5100.5	16.0	0.31%

*1′′ = 2.54cm

Table 12: Specimen Density

Specimen	W (lb)*	H (in)**	D (in)	Density (t/m^3)
1a	521	29	16.15	2.4
1b	516	29	16.5	2.3
1c	460	29	15.75	2.3
1d	566	30	16.15	2.6
1e	546	30	16.5	2.4
1f	531	31	15.75	2.4
2a	618	31	16.5	2.6
2b	548	31	15.75	2.5
2c	588	31	16.15	2.6
3a	505	30	15.75	2.4
3b	556.5	30	16.5	2.4
3c	565	31	16.15	2.5
4a	546	29	16.5	2.4
4b	557	30	16.15	2.5
4c	506	30	15.75	2.4
5a	553	31	15.75	2.5
5b	581	31	16.15	2.5
5c	609	31	16.5	2.5
6a	504	30	15.75	2.4
6b	504	29	16.15	2.3
6c	520	29	16.5	2.3
7a	515	31	15.75	2.4
7b	528	30	16.15	2.4
7c	579	31	16.5	2.4
8a	533	31	15.75	2.4
8b	539	31	16.15	2.4
8c	529	30	16.5	2.3

*1lb = 0.454kg, ** 1″= 2.54cm

Appendix III - Experiment Results

Table 13: Set 2 Data

Specimen 2a		Specimen 2b		Specimen 2c	
Displacement (mm)	Pump Pressure (PSIG)*	Displacement (mm)	Pump Pressure (PSIG)	Displacement (mm)	Pump Pressure (PSIG)
0	0	0	0	0	0
2.5	479	3.3	527	6.8	530
2.5	466	3.3	500	6.8	522
3.7	651	4	711	7.8	709
3.7	626	4	677	7.8	673
4.9	785	5.2	897	8.9	928
4.9	752	5.2	834	8.9	853
6.3	922	6.5	943	10.2	1018
6.3	882	6.5	857	10.2	934
7.8	1049	7.8	909	12.5	998
7.8	985	7.8	789	12.5	830
9.2	1118	9.7	768	15.6	795
9.2	1050	9.7	646	15.6	670
12.8	1019	12	595	18.6	603
12.8	847	12	499	18.6	507
16	642	13.5	445	21.6	495
16	519	14.5	395	21.6	405
23.5	236	17.1	290		
		17.1	238		

* 1PSI = 6.895KPa

Table 14: Set 3 Data

Specimen 3a		Specimen 3b		Specimen 3c	
Displacement (mm)	Pump Pressure (PSIG)	Displacement (mm)	Pump Pressure (PSIG)	Displacement (mm)	Pump Pressure (PSIG)
0	0	0	0	0	0
10.5	401	5.6	381	4.1	354
19.4	200	5.6	323	4.1	161
33.0	150	7.8	469	11.7	165
		7.8	386	11.7	81
		8.9	416	25.7	157
		8.9	287	25.7	81
		10.3	301		
		10.3	142		
		16.7	230		
		16.7	88		
		34.9	215		

Table 15: Set 4 Data

Specimen 4a		Specimen 4b		Specimen 4c	
Displacement (mm)	Pump Pressure (PSIG)	Displacement (mm)	Pump Pressure (PSIG)	Displacement (mm)	Pump Pressure (PSIG)
0	0	0	0	0	0
15.6	231	6.8	325	6.6	252
15.6	53	6.8	140	6.6	127
21.2	175	19.6	231	19.8	120
		19.6	57		
		33.3	197		
		33.3	30		
		47.9	155		

Table 16: Set 5 Data

Specimen 5a		Specimen 5b		Specimen 5c	
Displacement (mm)	Pump Pressure (PSIG)	Displacement (mm)	Pump Pressure (PSIG)	Displacement (mm)	Pump Pressure (PSIG)
0	0	0	0	0	0
18.6	966	2.8	146	2.8	601
18.6	860	2.8	131	2.8	549
26.3	582	3.7	617	3.9	967
26.3	503	3.7	577	3.9	907
32.0	440	6.0	1090	5.1	1415
32.0	366	6.0	1055	5.1	1361
		10.9	1561	6.2	1769
		10.9	1425	6.2	1672
		14.4	1610	7.8	1924
		14.4	1362	7.8	1706
		18.4	1190	12.1	1375
		18.4	1013	12.1	1125
		21.6	862	15.3	915
		21.6	753	15.3	738
		26.2	659	17.7	623
		26.2	554	17.7	493
				17.7	287

Table 17: Set 6 Data

Specimen 6a		Specimen 6b		Specimen 6c	
Displacement (mm)	Pump Pressure (PSIG)	Displacement (mm)	Pump Pressure (PSIG)	Displacement (mm)	Pump Pressure (PSIG)
0.0	0	0.0	0	0.0	0
		7.9	472	5.3	305
		36.6	202	8.6	540
				11.7	260

Table 18: Set 7 Data

Specimen 7a		Specimen 7b		Specimen 7c	
Displacement (mm)	Pump Pressure (PSIG)	Displacement (mm)	Pump Pressure (PSIG)	Displacement (mm)	Pump Pressure (PSIG)
0.0	0	0.0	0	0.0	0
0.2	113	1.3	106	1.2	102
0.3	209	4.0	208	8.4	170
0.7	308	5.6	318	14.8	140
1.3	413	6.3	352	20.1	120
3.0	474	7.8	406	25.3	107
8.8	409	9.6	453		
15.6	257	11.3	478		
23.4	123	12.0	479		
		14.5	350		
		19.9	268		

Table 19: Set 8 Data

Specimen 8a		Specimen 8b		Specimen 8c	
Displacement (mm)	Pump Pressure (PSIG)	Displacement (mm)	Pump Pressure (PSIG)	Displacement (mm)	Pump Pressure (PSIG)
0.0	0	0.0	0	0.0	0
5.2	369	1.0	58	0.6	105
15.4	322	2.9	156	1.2	160
24.4	261	4.0	203	1.7	204
34.1	199	5.1	254	2.2	254
		6.0	303	2.7	305
		6.7	351	3.4	352
		7.5	403	3.8	401
		8.7	450	4.0	406
		10.6	482	5.2	456
		12.6	504	7.5	402
		19.3	320	16.8	362
		28.6	215		
		34.0	100		